INTERCOMPARISON OF PERFORMANCE CHARACTERISTICS OF OSLDs AND TLDs USED FOR INDIVIDUAL MONITORING

THIS THESIS IS SUBMITTED TO THE DEPARTMENT OF MEDICAL PHYSICS

SCHOOL OF NUCLEAR AND ALLIED SCIENCES

UNIVERSITY OF GHANA

PHILIPPE ONDO MEYE

(10542173)

IN PARTIAL FULFILMENT OF THE REQUIREMENTS FOR THE AWARD OF

MASTER OF PHILOSOPHY DEGREE

IN

NUCLEAR SCIENCE AND TECHNOLOGY

JULY, 2016

DECLARATION

I, Philippe ONDO MEYE, declare that this thesis, submitted in partial fulfilment of the requirements for the award of Master of Philosophy Degree in Nuclear Science and Technology in the Department of Medical Physics, School of Nuclear and Allied Sciences, University of Ghana, is wholly my own work undertaken under the supervision of Prof. C. SCHANDORF and Dr. J. K. AMOAKO. Except for the references to publications that have been duly cited, this document has not been submitted for qualifications elsewhere.

……... Date: …….

Philippe ONDO MEYE

(Student)

……... Date: ……

Prof. Cyril SCHANDORF

(Principal Supervisor)

…… Date: ……...

Dr. J. K. AMOAKO

(Co-supervisor)

ABSTRACT

This research work performed an intercomparison on some important performance characteristics of optically stimulated luminescence (OSL) and thermoluminescence (TL) dosimetry systems used by dosimetry services in Gabon and Ghana, respectively. The study verified the status of the selected performance indicators and propose ways to improve the performances of individual monitoring services of Ghana and Gabon if found necessary. The performance indicators assessed included the zero - dose, the minimum detectability and some important reader performance characteristics. These tests were performed using statistical and experimental methods. The overall uncertainty in measurement of the dosimetry systems of Ghana and Gabon for *Hp(10)* was determined using the IEC technical report TR 62461, and comparisons were carried out with IAEA 99, PTB 99, IEC 1066 and IEC1283 series performance standards. The IEC 62387 standard was used to assess the linearity dependence of the response and the coefficient of variation of the two dosimetry systems. For the Harshaw TLD 6600 system of the dosimetry service of Ghana, the Reference light QC test meets the requirement given in the user manual. For the OSL system microStar of the dosimetry system of Gabon, the three QC tests, DRK count, CAL count and LED count, meet the user manual requirements. However all these tests failed the statistical test that is part of counting statistics. This led to the conclusion that there may be some abnormalities in the counting system, and that the statistical abnormalities suspected have apparently no impact on the results of the reading. It was also concluded that since the DRK count and the CAL count failed the Chi - squared test by very small margin , a Gaussian distribution could still be considered as an approximation of the experimental data distributions of these two QC measurements. The zero dose for the Harshaw 6600 and the microStar system

were found to be ***0.026 mSv*** and ***0.08 mSv*** respectively. The monthly lower limit of detection for the TL and OSL systems were found to be ***0.08 mSv*** and ***0.05 mSv***, respectively. The quarterly recording levels that have been proposed from this work are ***0.25 mSv*** for the Harshaw 6600 system and ***0.15 mSv*** for the microStar system. In spite of some observed abnormal points, the linearity test obtained for the two systems showed that they are globally in accordance with the performance standards tested. The results for the coefficient of variation of the two systems do not meet the IEC 62387 requirement. The results for uncertainty analysis were globally in accordance with the requirements of all the performance standards tested.

DEDICATION

This work is dedicated to my beloved parents, François Xavier MEYE MBA and Bernadette NTSAME OBAME, who have joined my ancestors after they had done their best to raise and educate me and all my sisters and brothers. I hope that from where they are now they are proud of me.

ACKNOWLEDGEMENTS

First, I would like to gratefully acknowledge the government of Gabon through the General Director of the General Directorate of Nuclear Techniques (DGTN), M. Charles CHALEY, and Ms. Lily Esther NDOUNA DEPENAUD**,** National Liaison Officer for International Atomic Energy Agency (IAEA) programmes for Gabon, who facilitate the IAEA fellowship.

I would like also to sincerely thank The IAEA for the two year scholarship made available to enable me to undertake this programme in very good conditions.

My thanks go to Prof. Cyril SCHANDORF, my principal supervisor for his professionalism, his sense of concision, his friendship, and Dr. Joseph K. AMOAKO, my second supervisor, for his supervisory role in introducing me to the Dosimetry and the Secondary Standard Dosimetry Laboratories of the Radiation Protection Institute (RPI).

I will acknowledge the following staff of RPI who contributed to the successful completion of the work , Philip O. MANTEAW, Daniel N. ADJEI, Collins KAFUI AZAH, Prince M. APPIAH , Edith AMOAKIE, Eunice AGYEMANG, Manfred LARYEA, Ben Doe GBEKOR and Dr. John O. BANAHENE

TABLE OF CONTENTS

LIST OF FIGURES

LIST OF TABLES

LIST OF ABBREVIATIONS

BSS	(IAEA) Basic Safety Standards
CRNA	Nuclear Research Centre of Algiers
DGTN	General Directorate of Nuclear Techniques (Gabon)
GUM	Guide to the Expression of Uncertainty in Measurement
IAEA	International Atomic Energy Agency
IEC	International Electrotechnical Commission
ICRP	International Commission on Radiological Protection
ICRU	International Commission on Radiation Units and Measurements
ISO	International Organisation for Standardisation
LLD	Lower Limit of Detection
OSL	Optically Stimulated Luminescence
OSLD	Optically Stimulated Luminescent Detector or Dosimeter

PMMA	Polymethyl methacrylate
PMT	Photo-Multiplier Tube
PSDL	Primary Standard Dosimetry Laboratory
PTB	Physikalisch - Technische Bundesanstalt
QC	Quality Control
RCA	(IAEA) Regional Cooperative Agreement
RPI	Radiation Protection Institute (Ghana)
RPL	Radiophotoluminescence
SNAS	School of Nuclear and Allied Sciences (Ghana)
SSDL	Secondary Standard Dosimetry Laboratory
TC	(IAEA) Technical Cooperation

TL	Thermoluminescence
TLD	Thermoluminescent Detector or Dosimeter
TTP	Time Temperature Profile

CHAPTER ONE

INTRODUCTION

This chapter introduces the background, the statement of the problem ,the objectives, the relevance and justification and the scope and limitation, of the study .

1.1 BACKGROUND

Workers are occupationally exposed to radiation as a result of various human activities. These include work associated with the different stages of the nuclear fuel cycle, the use of radioactive sources and *X* ray machines in medicine, scientific research, education, agriculture and industry, and occupations that involve the handling of material containing enhanced concentration of naturally occurring radionuclides. In order to control this exposure, it is necessary to assess the magnitude of the doses involved [1,2,3].

According to the IAEA BSS [4], employers, including self-employed persons, registrants and licensees shall be responsible for making arrangements for assessment of the occupational exposure of workers, on the basis of individual monitoring where appropriate, and shall ensure that arrangements are made with authorized or approved dosimetry service providers that operate under a quality management system. One of the means for fulfilling this regulatory requirement is to ensure that workers are monitored by an individual dosimetry service, using passive dosimeters, such as thermoluminescent dosimeters (TLDs) and optically stimulated luminescent dosimeters (OSLDs), for external exposure.

I.2 STATEMENT OF THE PROBLEM

In the framework of the International Atomic Energy Agency (IAEA) Technical Cooperation (TC) Regional Project RAF/9/043: Strengthening the transfer of experience related to occupational radiation protection of nuclear industry and other application involving ionizing radiation, an intercomparison on measurements of the quantity personal dose equivalent *Hp (10)* in photon fields, in the African Region, was organized by the Algerian Second Standard Dosimetry Laboratory (SSDL) in 2013 [5]. This exercise revealed that several laboratories operated out of the required standards (Figure 1.1) and should take immediate steps to improve their internal procedures to be in accordance with their national regulatory body and the international basic safety standards. Furthermore, this exercise showed that the national laboratories which participated in this event should perform regularly the same type of exercise in order to maintain the reliability of their results. The present work was to perform an intercomparison studies on the performance characteristics of OSLDs and TLDs used for personal monitoring dosimetry services in Gabon and Ghana making use of the Secondary Standards Dosimetric Laboratory in Ghana.

1.3 OBJECTIVES

The main objective of the study was to verify and to improve the performances of individual monitoring services of Ghana and Gabon using several international performance standards taking into account the resources available in Ghana and Gabon .

The specific objectives of the study were:

- to assess the capabilities of the dosimetry services of Ghana and Gabon to estimate the personal dose equivalent *Hp (10)* in photon fields;
- to provide recommendations and guidelines for addressing deficiencies detected in order to upgrade the quality of the dosimetry services in Ghana and Gabon.

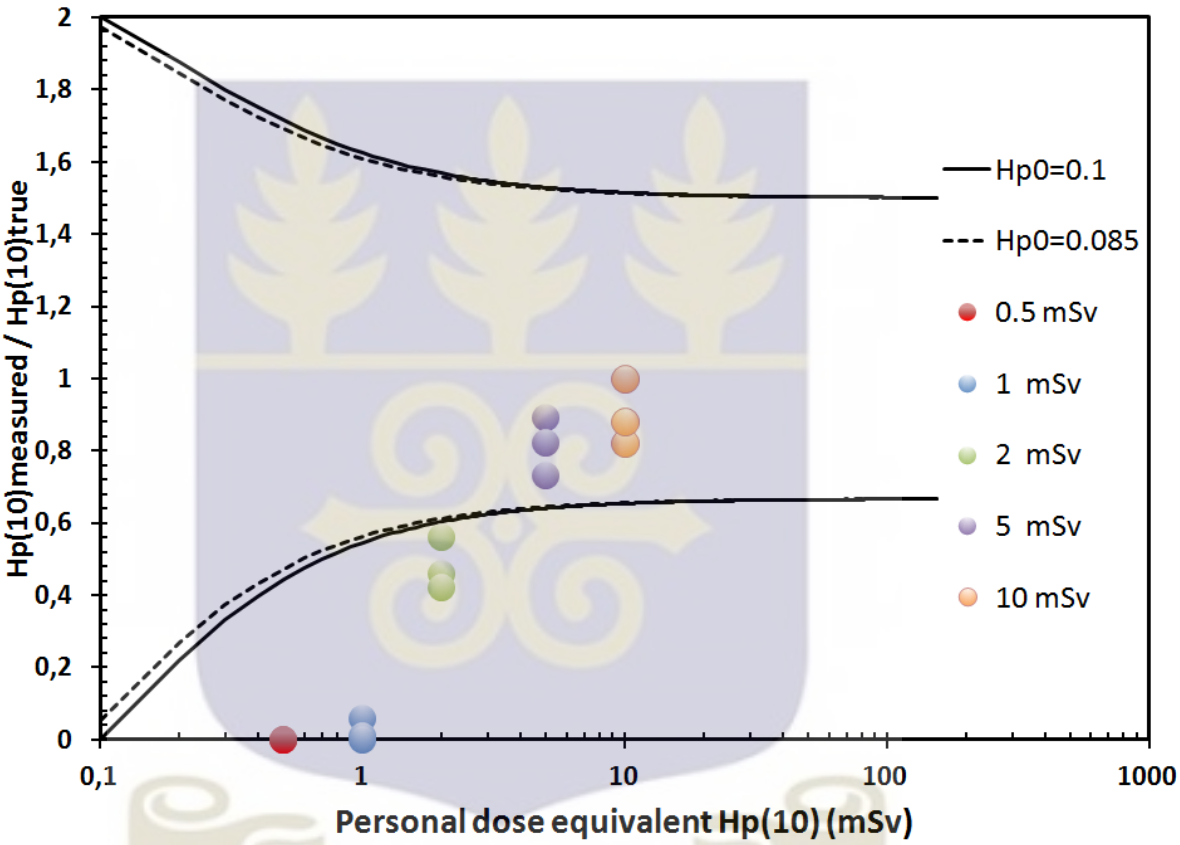

Figure 1.1: Linearity response test obtained by one laboratory which participated in the 2013 African Region intercomparison. It is obvious that this laboratory needs to improve its internal procedures.

1.4 RELEVANCE AND JUSTIFICATION

This work is in line with international requirements and expectation to engage in national , regional and inter-regional intercomparisons as a peer review mechanism for maintaining the credibility , reliability and accuracy of dosimetry services and adoption of the best practices where necessary [1, 6].

1.5 SCOPE AND LIMITATION

The study used relevant International assessment protocols to intercompare the performance of OSLDs and TLDs used for personal monitoring dosimetry services in Gabon and Ghana making use of the Secondary Standards Dosimetric Laboratory in Ghana.

The basic assessment parameters included the zero - dose, the minimum detectability and some important instrumental (reader) performance tests. These tests were performed using statistical and experimental methods. The overall uncertainty in measurement of the dosimetry systems of Ghana and Gabon for *Hp(10)* was determined using the International Electrotechnical Commission (IEC) technical report TR 62461 [7]. A comparison with other standards, such as IAEA 99, PTB 99, IEC 1066 and IEC1283 series [1, 8] was carried out. The IEC 62387 standard [9] was used to assess the linearity dependence of the response and the coefficient of variation of both dosimetry systems.

The study was limited to TLDs and OSLDs, and the quantity *Hp (10)* in photon (*X* and gamma rays) fields.

CHAPTER TWO

LITERATURE REVIEW

The chapter reviews literature relevant to intercomparison for individual monitoring of external exposure, highlighting the intercomparisons that have been performed in different regions of the world with the support of IAEA, the infrastructure required for intercomparisons, individual monitoring services and associated standard dosimetry laboratories, and the methodology for intercomparison including counting statistics

2.1 Introduction

In the early 1980s, the International Atomic Energy Agency (IAEA) started the organization of intercomparisons for different purposes in the occupational radiation protection area. While the first intercomparison was aimed at overcoming the technical difficulties associated with the introduction of the new set of operational quantities introduced in the International Commission on Radiation Units and Measurements (ICRU) Report 39 in 1985, later intercomparisons focussed on the performance of personal dosimetry services, mainly for photon fields [10].

More generally, intercomparisons are part of the activities of the IAEA Occupational Protection Programme, the objectives of which are to promote an internationally harmonized approach for optimizing occupational radiation protection through [11]:

- the development of guidelines for restricting radiation exposures in the workplace and for applying current occupational radiation protection techniques;
- the promotion of the application of these guidelines.

Several intercomparisons have been performed in different regions of the world with the support of IAEA. The following is a brief overview of some of them.

2.1.1 International intercomparison (1988 - 1992)

This international intercomparison was conducted in two phases with a total participation of twenty nine laboratories from twenty one Member States and three international organisations [12]. The first phase of the intercomparison focussed on the selection of a backscatter phantom for calibration, and identifying systematic differences in the quality of dosimetry. Based on the results from the first phase, a second phase was conducted addressing issues of phantom and angular dependence as well as energy dependence. This intercomparison demonstrated that:

- a certain number of dosimetry systems were capable of measuring the new ICRU quantities to an acceptable degree of accuracy;
- the performance of TLD systems was usually superior to film based systems; and
- dosimeters with simple designs performed as well as the more sophisticated ones.

2.1.2 IAEA / RCA Personal Dosimeter intercomparison (1990 - 1992)

The programme of the IAEA Regional Cooperative Agreement project (RCA) for strengthening and harmonizing the radiation protection infrastructure in the Asian and Pacific Region included a regional personal dosimetry intercomparison, which was conducted over the period 1990 - 1992 [11]. Seventeen organizations from all the fourteen Member States participated in this programme. During this period, very few regional dosimetry services calibrated their dosimeters on backscatter phantoms, so

that the intercomparisons were mainly conducted with the traditional physical quantity exposure, in units of Rontgen. It was concluded that this intercomparison contributed significantly to technical improvement of personal dosimetry and instrument calibration in the region of South East Asia.

2.1.3 IAEA / Eastern Europe intercomparison for individual monitoring of external exposure from photon radiation (1997 - 1998)

In 1997 an intercomparison for individual monitoring of external exposure from photon radiation was started [12]. This involved twenty three participating dosimetry services from Eastern Europe and the countries of the former Soviet Union, and focussed on personnel dosimetry services for nuclear power plants. This exercise was conducted in two phases. The phase I, referred to as the " type-test " intercomparison, provided the participants with data about the variation of energy and angular dependence of the response of their dosimeters with respect to the operational quantity personal dose equivalent. The phase II, referred to as the " simulated workplace field " intercomparison, enabled the participants to judge the performance of their dosimeters under realistic conditions arising in practice. It was concluded that the participating dosimetry services demonstrated a satisfactory proficiency to assess, in photon fields, the quantity personal dose equivalent *Hp (10)*, the quantity recommended by the IAEA to assess the occupational whole body exposure.

2.1.4 Intercomparison of measurements of personal dose equivalent *Hp (10)* in photon fields in the West Asia Region (2004)

This regional intercomparison was conducted in two phases with a total participation of twenty one laboratories from all the countries in West Asia Region [10]. In phase I,

namely the " performance testing " intercomparison, irradiation in selected monoenergetic radiation fields was performed to investigate energy and angular dependence and linearity. The phase II, called the " mixed photon qualities " intercomparison, was aimed at simulating real workplace conditions. This intercomparison showed the necessity for a support to the personal dosimetry service providers in the region. The participants emphasized the need for continuous locally organized intercomparisons, which could lead to a self-supporting regional testing arrangement with decreasing necessity of IAEA involvement.

2.1.5 Intercomparison on measurements of the personal dose equivalent *Hp (10)* in photon fields in the African Region (2013)

This intercomparison exercise was jointly organized by IAEA and the Nuclear Research Centre of Algiers (CRNA) through its Secondary Standard Dosimetry Laboratory (SSDL) [5]. The intercomparison was aimed at verifying the performance of the individual monitoring services of the participants in order to assess their capabilities to measure the quantity *Hp (10)* in photon fields and help them to comply with dose limitation requirements. Twenty four countries from the African Region and three countries from outside this region participated in this intercomparison exercise. The intercomparison was organized in two phases. The phase I was aimed at testing the dosimetry systems through linearity verification, energy dependence and angular dependence of their response. The phase II was a blind test for the dosimetry services, as the dosimeters were irradiated at doses known only by the SSDL. It was concluded that the intercomparison exercise was satisfactory since 87.7 % of the participants had their results within the acceptable limits.

Apart from the intercomparisons organized by IAEA addressed above, it is important to stress that a study entitled [13] " A comparative study between the performance characteristics of optically stimulated luminescent dosimeters and thermoluminescent dosimeters " was undertaken by a previous SNAS student. The performance parameters that were assessed for that study are globally different from the present research work, and international performance standards were not used as in this study.

2.2 Infrastructure for intercomparison for individual monitoring of external exposure and dose assessment

2.2.1 Individual monitoring services

Usually, a personal dosimetry laboratory requires a full dosimetry system, which, in general, consists of a reader, a personal computer, a software for dose assessment, a dose report printer, dosimeters, and sometimes a dosimeter annealer (Figure 2.1)

Generally, dosimetry systems encountered in intercomparison exercises for individual monitoring of external exposure are film, radiophotoluminescence (RPL), thermoluminescence (TL), and optically stimulated luminescence (OSL) based dosimetry systems. TL and OSL based dosimetry systems are the dosimetry systems commonly used in the African Region. In general, thermoluminescence dosimeters (TLDs) and optically stimulated luminescence dosimeters (OSLDs) are made of LiF : Mg : Ti and Al_2O_3 : C materials, respectively.

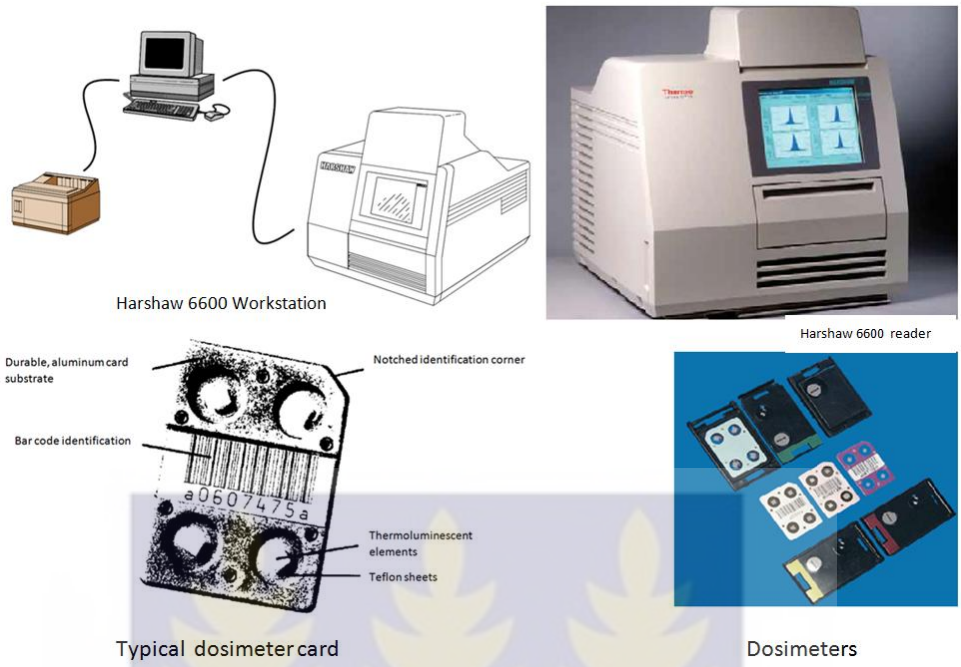

Figure 2.1: An example of a full dosimetry system composed of a reader, a personal computer, a dose report printer, and dosimeters (from Harshaw 6600 user manual [14] and Harshaw 6600 specification sheet available on www.thermofisher.com).

2.2.2 Irradiation facilities

Generally, irradiation facilities required for intercomparison exercises are either Secondary Standard Dosimetry Laboratories (SSDLs) or Primary Standard Dosimetry Laboratories (PSDLs) (figure 2.2). The irradiation laboratory shall have the following equipment:

- an ionization chamber, traceable to an authorized standard laboratory;
- an electrometer, traceable to an authorized standard laboratory;
- irradiation sources;
- phantoms (PMMA Slab phantom, ISO water slab phantom, ISO pillar phantom, ISO rod phantom);

– equipment for measurement of ambient temperature, pressure, and relative humidity;
– lasers for the alignment of the dosimeters with the central beam axis of the source, and for positioning the phantom at the right distance from the source.

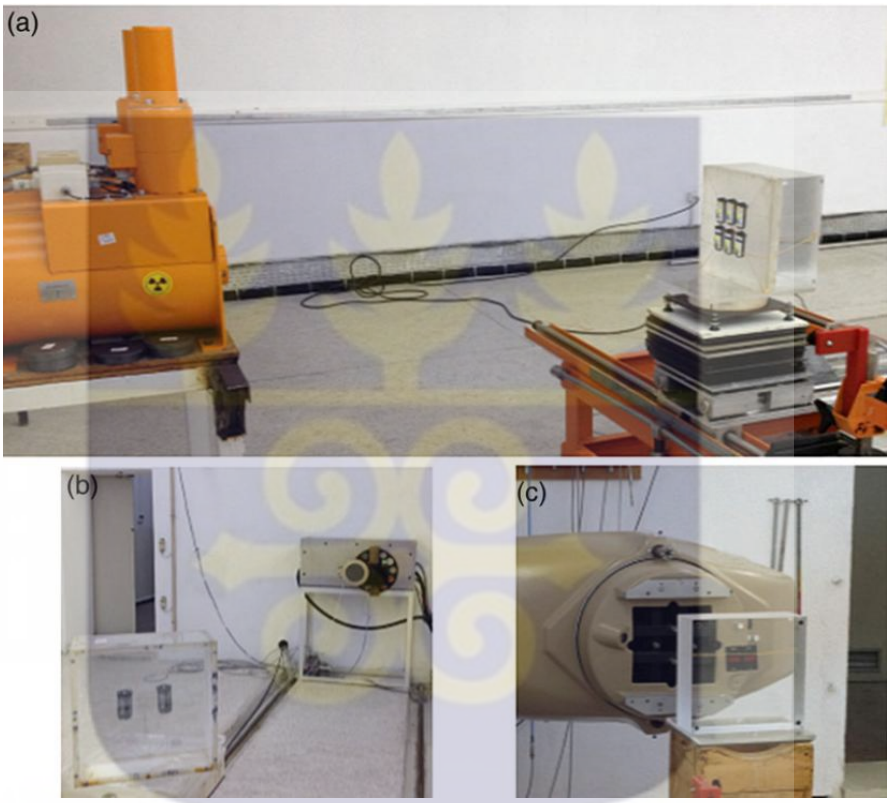

Figure 2.2: An example of an irradiation facility. Irradiation of dosimeters in ^{137}Cs (a), X rays (b) and ^{60}Co (c) qualities (from Arib et al. [5]).

2.3 Methodology for intercomparison for individual monitoring of external exposure and dose assessment

2.3.1 Dosimetric quantities and phantoms

The quantities in which the dose limits, given in the basic safety standards (BSS) [4], are expressed are the effective dose E and the equivalent dose H_T in tissue or organ T [3]. These quantities are called *protection quantities*. The quantity effective dose is generally considered to be an adequate indicator of the health detriment from radiation exposure at the levels experienced in normal operations. A limit on equivalent dose is needed for skin and the lens of the eye in order to ensure the avoidance of deterministic effects in these tissues.

The basic quantities for physical measurement of external radiation exposure include kerma K and absorbed dose D, which are also formally defined in the BSS. These quantities are called *physical quantities* and are used by national standards laboratories. The need for readily measurable quantities that can be related to effective dose and equivalent dose has led to the development of *operational quantities* for assessment of external exposure. The operational quantities provide an estimate of effective or equivalent dose that avoids underestimation and excessive overestimation in most radiation fields encountered in practice. The operational quantity for use in an individual monitoring is the personal dose equivalent $H_p\ (d)$ at the specific depth d *mm* in soft tissue. By using the operational quantity $H_p\ (10)$, one obtains an approximate value for the effective dose E. The operational quantity $H_p\ (0.07)$, is used to obtain an approximate value for the equivalent dose to the skin. Similarly, $H_p\ (3)$, may be used for an approximate assessment of the equivalent dose

to the lens of the eye. The present work only deals with the operational quantity $H_p\ (10)$.

$H_p\ (10)$ is defined primarily for the human body, but the definition is extended to calibration phantoms [15]. In this case, $H_p\ (10)$ is the dose equivalent at $10\ mm$ depth in a phantom used for calibration and composed of ICRU 4 - element tissue equivalent material. It is assumed that a personal dosimeter whose the response matches the energy and angle dependence of the response of $H_p\ (10)$ in the calibration phantom will determine adequately $H_p\ (10)$ in the human body when worn, and provide an estimate of the effective dose of sufficient accuracy. A phantom is usually required for the calibration of personal dosimeters in terms of $H_p\ (10)$ because the radiation field at the wearing position of the dosimeter on the body comprises an incident component and a backscattered component, whose characteristics depend on the energy and angle of incident photons, and also on the body itself, and where on the body the dosimeter is positioned. The response of a dosimeter will, in general, depend on both incident and backscattered components of the radiation field.

A solid material having the composition of the ICRU 4 - element tissue equivalent material has not yet been fabricated. Several tissue substitute materials are available among which are polymethyl methacrylate (PMMA), water and various types of specially fabricated plastics. The important property of tissue substitute materials is their ability to replicate the backscatter from tissue. The backscatter field, its magnitude and its energy and angle distribution, depend not only on the material but also on the shape of the phantom. The International Organization for standardization (ISO) and IAEA recommend the use of a calibration phantom which is a $30\ cm \times 30\ cm \times 15\ cm$ slab made of thin PMMA walls (front wall $2.5\ mm$ thick, other walls

10 mm thick) and filled with water [16, 17]. For a radiation with a mean energy equal to or above that of radionuclide ^{137}Cs, ISO recommends the use of a solid PMMA slab of the same outer dimensions [16].

2.3.2 Requirements for personal dosimeters

The basic requirements for personal dosimeters are to provide a reliable measurement of the appropriate quantities, that is $H_p\ (10)$ and $H_p\ (0.07)$, for almost all practical situations, independent of the type, energy and incident angle of the radiation, and with a prescribed overall accuracy [1,18]. Of particular importance to the measurement of $H_p\ (10)$ and $H_p\ (0.07)$ is the dependence of the dosimeter response on the energy and direction of the radiation.

2.3.3 Type testing of personal dosimeters

Type testing of a dosimetry system involves testing the performance characteristics of the system as a whole under a series of irradiation and storage conditions [1,18]. In particular, the main sources of uncertainty should be quantified. This largely concerns an investigation into the variation of dosimeter response with the energy and angle of incidence of the radiation beam. However, it also includes other dosimetric characteristics such as the linearity of the dosimeter response, the minimum and maximum measurable doses, the zero - dose variations, fading, dose build up, self irradiation, response to natural radiation, the ability of the system to perform satisfactorily over a reasonable range of temperature and humidity conditions, and the ability to respond properly in high dose rates and in pulsed radiation fields. Tests should also be made for these latter dosimetric characteristics in addition to the test of the dosimeter response to radiation energy an angle of incidence.

2.3.4 Reader performance tests

In addition to the type testing of a personal dosimetry system, in which the whole performance of the system is carefully analysed, it is necessary to demonstrate that this standard of performance is maintained continuously. Certain reader performance tests should be carried out regularly for this purpose. Among these, some will be addressed in the present work. These are:

- (reader) calibration;
- reader background noise test (PMT noise or Dark current for Harshaw 6600, and DRK count for microStar InLight);
- Photomultiplier tube consistency test (Reference light test for Harshaw 6600, and CAL count test for microStar InLight);
- Beam intensity test (LED count for microStar InLight only).

Calibration is a means by which the sensitivity, precision and accuracy are verified for a single radiation type and energy [1]. The purpose of calibration in individual monitoring is to test the accuracy and precision of the dosimetry system for measurement of doses at a single energy, usually that of the calibration source, e.g. ^{137}Cs or ^{60}Co gammas for photon dosimeters. The precision and accuracy should be tested at different dose levels. Calibration also serves to normalize the overall sensitivity of the system.

Reader background noise test measures the inherent electronic noise generated by the photomultiplier tube. This noise comes from light leaks (stimulation light leaks for microStar InLight) and dark counts or current. for Harshaw 6600, when this reading is taken, the gas is flowing but is not heated. For microStar InLight, the DRK count is taken with the shutter closed and the LEDs off [14, 19].

The photomultiplier tube consistency test measures the light output from - for Harshaw 6600 - two CaF_2 scintillation crystals doped with ^{14}C or - for microStar InLight - a small exempted ^{14}C radioactive source embedded in a plastic scintillator. The absolute value of the Reference Light readings or CAL counts is not significant, but consistency of the readings is important [14, 19].

The beam intensity test or LED count, for the system InLight microStar only, measures counts from the PMT with the filter shutter open and the LEDs on to indicate the beam intensity [19].

The four reader performance tests addressed above are part of the quality control procedures that require to be performed at regular intervals. Apart from the calibration of the reader, the other three performance tests require to be performed with no dosimeter under the PMT.

2.3.5 Intercomparison procedures

The practical aspect of intercomparison starts with the phase of preparation of dosimeters by the participating individual monitoring services. In this phase, the same dosimeters used to monitor occupationally exposed workers, commonly called field dosimeters, are annealed. More often, since the SSDL is not always in the same country than the participating dosimetry laboratories, additional dosimeters, usually called control dosimeters, which are used for transport and natural background radiation measurement, are prepared the same way than the field dosimeters. Then after the dosimeters are sent to the irradiation facility where they are irradiated.

The first step in irradiation of dosimeters is the determination, with the reference instrument (ionization chamber + electrometer), and at the appropriate distance from the radiation source, of free - in - air air kerma *Ka*. The radiation qualities commonly

used for irradiation are ISO *N*, *W* or *S* series [20]. The personal dose equivalent H_p *(10)* is then derived using appropriate conversion coefficients that can be taken from ISO 4037 - 3 [16]. Then, the reference instrument is removed and replaced, at the same position, by the dosimeters fixed on the surface of an appropriate phantom for irradiation.

Generally, a linearity verification together with an energy and angular dependence test are performed. The first consists of irradiating the dosimeters with a ^{137}Cs or ^{60}Co radiation source at various doses. The second consists of irradiating dosimeters with various radiations qualities at various incident angles, but at the same radiation dose.

After irradiation, the dosimeters are sent back to the dosimetry laboratories for evaluation. Generally, net doses are assessed by subtracting the mean dose measured with control dosimeters from the raw doses measured with field dosimeters.

2.3.6 Performance requirement for accuracy

The International Commission on Radiological Protection (ICRP) recommendations [6] indicate acceptable levels of uncertainty at two dose levels:

- in the region near the relevant dose limit, a factor of *1.5* in either direction is considered acceptable;
- In the region of the recording level, an acceptable uncertainty of ± *100 %* is implied.

This formulation of acceptable uncertainty leads to the allowable accuracy interval, commonly known as the trumpet curve (Figure 2.3), given by equations [1]:

$$\begin{cases} R_{Upper} = (\frac{H_m}{H_t})_{Upper} = 1{,}5\left(1 + \frac{H_0}{2H_0 + H_t}\right) \\ R_{Lower} = (\frac{H_m}{H_t})_{Lower} = \begin{cases} 0 & for\ H_t < H_0 \\ \frac{1}{1{,}5}\left(1 - \frac{2H_0}{H_0 + H_t}\right) & for\ H_t \geq H_0 \end{cases} \end{cases} \quad (2.1)$$

where the ratio H_m / H_t, the response of the dosimeter, is the quantity that should fall within the limits $R_{Upper} = (\frac{H_m}{H_t})_{Upper}$ and $R_{Lower} = (\frac{H_m}{H_t})_{Lower}$ which are the upper and the lower limits of the allowable accuracy interval, respectively. H_t is the conventional true value and H_0 is the lowest dose that needs to be measured (i.e. the recording level).

A value for the recording level has been prescribed by the *ICRP* , that is the dose above which recording of the doses should be required. For individual monitoring, this recording level should be derived from the duration of the monitoring period and an annual effective dose no lower than *1 mSv* or an annual equivalent dose of about *10%* of the relevant dose limit. Doses just below this recording level will not be included in assessment of a worker's dose. The recording level, H_0, is then given by:

$$H_0 = L\frac{Monitoring\ period\ in\ months}{12} \quad (2.2)$$

where L = *1 mSv or L = 10%* of the relevant annual equivalent dose limit. Applying Eq. 2.2 for monthly and quarterly monitoring periods and for the quantity individual dose equivalent *Hp (10)* we find $\boldsymbol{H_0 = 0.083\ mSv}$ and $\boldsymbol{H_0 = 0.25\ mSv}$ respectively.

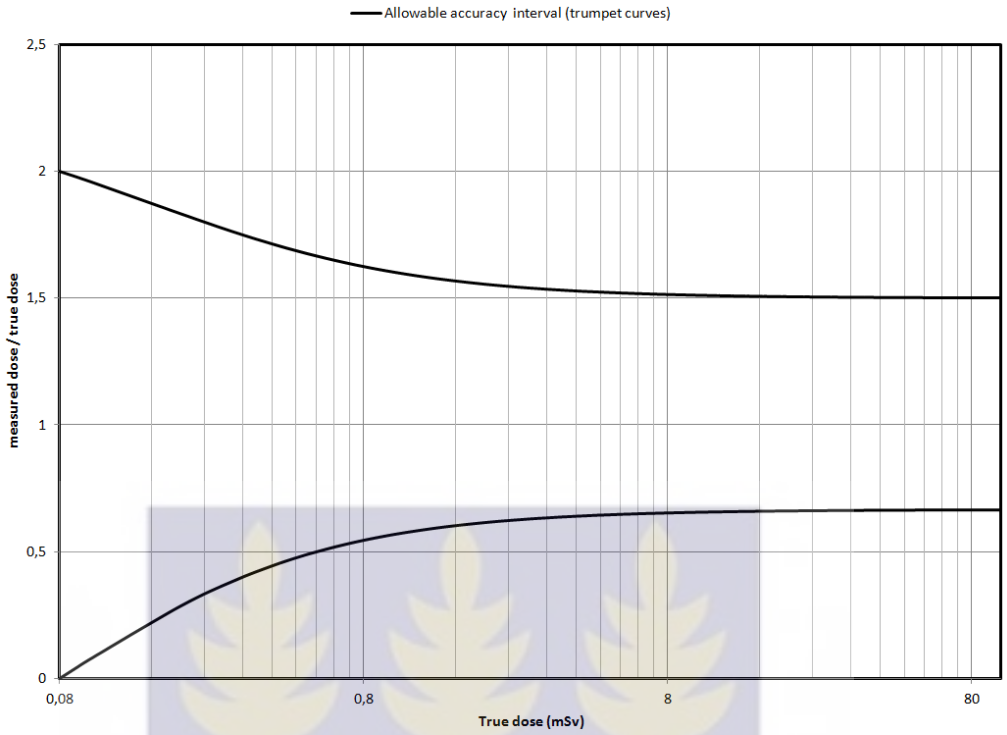

Figure 2.3: Acceptable upper and lower limits for the ratio measured dose / conventional true dose as a function of dose, and for a monthly recording level H_0 = 0.08 mSv. 95 % of all measurements must fall within the limits. The graph has been obtained using Eq. 2.1 and the software Microsoft Office Excel 2007.

2.4 Counting Statistics

2.4.1 Characterization of data

A collection of N independent measurements of the same physical quantity is considered:

$$x_1, x_2, x_3, \dots, x_i, \dots, x_N$$

The experimental mean, $\bar{x}$, is an elementary property of this data set:

$$\bar{x} = \frac{1}{N}\sum_{i=1}^{N} x_i \qquad (2.3)$$

The data set can be represented by a corresponding frequency distribution function *F(x)*, whose value is the relative frequency with which the number appears in the collection of data. By definition

$$F(x) = \frac{number\ of\ occurences\ of\ the\ value\ x}{number\ of\ measurements} \qquad (2.4)$$

The distribution is automatically normalized:

$$\sum_{x=0}^{\infty} F(x) = 1 \qquad (2.5)$$

The experimental mean can also be calculated by using the data distribution function:

$$\bar{x} = \sum_{x=0}^{\infty} xF(x) \qquad (2.6)$$

Another important property, dependent on the statistical model mean μ, is the sample standard deviation which serves to quantify the amount of internal fluctuation in the data:

$$s = \sqrt{\frac{1}{N-1}\sum_{i=1}^{N}(x_i - \mu)^2} \qquad (2.7)$$

The sample standard deviation can also be calculated directly from the data distribution function *F(x)*:

$$s = \sqrt{\sum_{x=0}^{\infty}(x-\mu)^2 F(x)} \qquad (2.8)$$

2.4.2 Statistical models

The distribution function, as defined by Eq. 2.4, and that will describe the results of many repetitions of a given measurement can be predicted. A measurement can be defined as counting the number of successes resulting from a given number of trials. Each trial is assumed to be a binary process in that only two results are possible. Either the trial is a success or it is a failure. The probability of success of one trial is identified as p. Three specific statistical models are generally addressed: The binomial distribution, the Poisson distribution and the Gaussian or normal distribution.

The binomial distribution is the most general model and widely applicable to all the processes in which the probability of success p is constant. Unfortunately, this statistical model is computationally cumbersome in nuclear counting applications where the number of trials is very large.

The Poisson distribution model is a direct mathematical simplification of the binomial distribution under conditions that the success probability p is small and constant for each individual trial. The Poisson probability density is given by

$$P(x) = \frac{\mu^x e^{-\mu}}{x!} \qquad (2.9)$$

where x is the number of successes. One of the important properties of the Poisson distribution is the fact that the standard deviation σ is the square root of the mean:

$$\sigma = \sqrt{\mu} \qquad (2.10)$$

The Poisson distribution is a mathematical simplification to the binomial distribution in the limit $p \ll 1$. If, in addition, the mean value of the distribution is large (greater

than *20* or *30*), additional simplifications can generally be carried out which lead to the Gaussian distribution

$$P(x) = \frac{1}{\sqrt{2\pi}\sigma} e^{-(x-\mu)^2/2\sigma^2} \qquad (2.11)$$

Now *x* is a continuous random variable with mean value μ, and Eq. 2.10 is still valid. The probability that the value of *x* lies between *x* and *x* + *dx* is [21]

$$P(x)dx \qquad (2.12)$$

The probability that *x* has a value between x_1 and x_2 is equal to the area under the curve *P(x)* between these values:

$$Pr(x_1 \leq x \leq x_2) = \frac{1}{\sqrt{2\pi}\sigma} \int_{x_1}^{x_2} e^{-(x-\mu)^2/2\sigma^2} dx \qquad (2.13)$$

For computational purposes, it is convenient to transform the normal distribution (given by Eq. 2.11), which depends on the two parameters μ and σ, into a simple, universal form. The standard normal distribution, having zero mean and unit standard deviation, is obtained by making the substitution

$$z = \frac{x - \mu}{\sigma} \qquad (2.14)$$

Eq. 2.13 becomes

$$Pr(z_1 \leq z \leq z_2) = \frac{1}{\sqrt{2\pi}} \int_{z_1}^{z_2} e^{-z^2/2} dz \qquad (2.15)$$

Tables in the literature list values of integral

$$Pr(z \leq z_0) = \frac{1}{\sqrt{2\pi}} \int_{-\infty}^{z_0} e^{-z^2/2} dz \qquad (2.16)$$

giving the probability that the normal random variable z has a value less or equal to z_0.

In the counting statistics approach followed here, a set of measurements is recorded under conditions in which all aspects of the experiment are held as constant as possible [22]. Because of the influence of statistical fluctuations, these measurements will not all be the same but will show some degree of internal variation. The extent of this fluctuation can be quantified and compared with predictions of statistical models. If the observed fluctuation is not consistent with predictions, one can conclude that some abnormality exists in the counting system. The Chi-square defined as

$$\chi^2 = \frac{1}{\bar{x}} \sum_{i=1}^{N} (x_i - \bar{x})^2 \qquad (2.17)$$

where the summation is taken over each individual data point x_i, is another property of the experimental data distribution which measures the significance of the difference between an observed distribution and an expected distribution. The Chi-square can also be written as a function of the sample variance:

$$\chi^2 = \frac{(N-1)s^2}{\bar{x}} \qquad (2.18)$$

The numerical value of chi-square depends on the number N of measurements that are made. In statistical language, it is said that the value of chi-square depends on the number of degrees of freedom, $v = N-1$. For the perfect agreement, $\chi^2(v) = 0.5$. This means that there is a *50 %* chance that we would get a wider distribution of counts, and a *50 %* chance that we would get a narrower distribution of counts if we were to repeat the series of measurements. From the values of χ^2 and v we can determine whether the measured distribution differs significantly from the expected distribution. The counting system usually is considered to be satisfactory when the chi-squared

value is within the *95 %* confidence interval [23]. Quantitatively, this means that for this confidence interval one of the following relationships shall be verified:

$$\chi_L^2 < \chi^2 < \chi_u^2 \qquad (2.19)$$

$$\sqrt{\frac{(N-1)s^2}{\chi_u^2}} < \sigma < \sqrt{\frac{(N-1)s^2}{\chi_L^2}} \qquad (2.20)$$

where χ_u^2 and χ_L^2 are the upper and lower limit values of the confidence interval, respectively. These values can be found in reference [23] for number of degrees of freedom not greater than *20*. Another possibility is to use online calculator, such as the one available on the website *www.swogstat.org/stat/public/chisq_calculator.htm*.

CHAPTER THREE

MATERIALS AND METHODS

In this chapter, the material available in the dosimetry services in Gabon and Ghana, and in the SSDL in Ghana used for the study are presented. The methodology used for all the performance assessments is also presented.

3.1 MATERIALS

3.1.1 Readers

Two dosimetry systems were used: the microStar InLight OSL system (serial number 11040681, date of installation, April 2012) and the Harshaw Model 6600 TLD system (serial number 9805167, date of installation, May 1997). The two dosimetry systems consist of a reader, a personal computer, a software (WinREMS for Harshaw and microStar for the OSL system) and dosimeters. Harshaw Model 6600 TLD system is a fully automated system with a readout capacity of *200* TLD cards, whereas the microStar system is a manual system with a capacity of one dosimeter per readout. Furthermore, the Harshaw Model 6600 contains a heating system that uses a stream of hot gas (nitrogen or air).

3.1.2 Dosimeters

The TLD dosimeters that were used here are personnel TLD cards with only two thermoluminescent elements of LiF (Ti ,Mg) per card (Figure 3.1). One element is used to estimate *Hp(10)* (readout position *2*) and another is dedicated for the measurement of the Hp(0.07) (readout position *3*).

The OSL dosimeters are also designed to monitor personnel dose. The dosimeter consists of four detector elements of Al_2O_3:C (Figure 3.2) located in read positions *1* (*E1*), *2* (*E2*), *3* (*E3*), and *4* (*E4*). An average dose is automatically computed from these four reading positions to obtain the whole body dose *Hp(10)*, the skin dose *Hp(0.07)*, and the lens dose *Hp(3)*.It is important to stress that the lower limits of the measuring range are ***0.010 mSv*** for the OSL system ***0.10 mSv*** for the TL system [14, 24]. Furthermore, a minimal reporting dose of ***0.5 mSv*** is recommended for InLight OSL systems, while the minimum detectability is said to be less than ***0.01 mSv*** for Harshaw Model 6600.

3.1.3 Annealing system

Reading a TLD card with the Harshaw model *6600* system (Figure 3.1) depletes about *100 %* of the signal. For the zero dose test purpose, the cards has to be read four times (the first at a specific time temperature profile different from the three others [25]) each to clear them further. For the microStar InLight system, the dosimeters have to be bleached only once using an InLight pocket annealer (Figure 3.2).

Figure 3.1: Harshaw 6600 system of the dosimetry service of Ghana. Here are presented the dosimeters, the gas generator, the reader and the personal computer of this dosimetry system.

Figure 3.2: microStar system of the dosimetry service of Gabon. On the picture the manual reader, the personal computer, the pocket annealer, the bar code reader and the dosimeters of this dosimetry system are presented.

3.1.5 Irradiation facility

The following is a description of relevant equipment available in the SSDL of Ghana (Figure 3.3).

Ionisation chamber

- manufacturer: PTW-FREIBURG
- type: TW 32002 (1 litre spherical ionization chamber)
- serial number: 000227
- calibrated at: PTW-FREIBURG calibration laboratory (for gamma rays, Co-60, and X-rays, N250,N200,N150,N100, N80 and N60)
- date of last calibration: 08-09-2015.

Electrometer

- manufacturer: PTW-FREIBURG
- type: T 10002 (UNIDOS)
- serial number: 020243
- calibrated at: PTW-FREIBURG calibration laboratory
- date of the last calibration: 08-09-2015.

Irradiation source (^{137}Cs)

- manufacturer: J.L SHEPHERD & Associates
- type: Type A
- serial number: USA DOT - 7A
- date of manufacture: September 1989
- dose rate at *1 m / 1.5 m*: ***1.8246 mSv/h / 0.8230 mSv/h*** (date: 11-02-2016).

Equipment for measuring temperature and pressure

- type: Compensiert (Präzisions - Barometer)
- serial number: Nr. 89729

Equipment for measuring relative humidity

- manufacturer: S. Brannan & sons
- serial number: SN 148/12

Phantom used

30 cm × 30 cm × 15 cm ISO water slab phantom.

3.2 METHODS

3.2.1 Irradiation procedure

- irradiations were performed using a ISO S-Cs quality in normal incidence;
- the distance from the Cs-137 source was *1.5 m* for irradiation of the reference group of dosimeters (reference dose = *3 mSv*) , and *1 m* for the other dosimeters;
- dosimeters were fixed on a 30 cm × 30 cm × 15 cm ISO water slab phantom using adhesive tape;
- dosimeters were irradiated in groups of 4, placed on the centre of the phantom, excepted the reference dosimeters which were irradiated in a group of 10 (Harshaw 6600), or 6 (microStar).

Figure 3.3: Irradiation facility of Radiation Protection Institute (Ghana). The figure shows the setup for irradiation of TL reference dosimeters in ^{137}Cs quality.

3.2.2 Reader performance tests

This section is limited to the reader background test, the photomultiplier tube consistency and the beam intensity test. Measurement from each of these tests must fall within acceptance limits. These limits are [14, 19]:

- DRK count: less than 30;
- PMT noise: within ± 10 % (1σ) of the observed mean;
- Reference light and CAL count: within ± 10 % (1σ) of the observed mean;
- LED count: within ± 10 % (1σ) of the observed mean;

In addition to the above procedure, counting statistics was used to check whether the counting systems are operating properly.

3.2.3 Limit of detectability and zero dose determination

It is convenient to estimate the smallest personal deep dose equivalent *Hp (10)* that can be detected reliably in order to set a detection limit for a dosimetry system. According to [14,19], the Lower Limit of Detection (*LLD*) also called the Minimum Detectable Dose (*MDD*) is simply obtained by the formula

$$LLD = k\sigma \qquad (3.1)$$

where k is a coverage factor that can be obtained from a Student t-distribution or a Gaussian distribution. σ is the standard deviation of repeated or simultaneous evaluations of unexposed dosimeters. For the Harshaw 6600 TLD system, $k = 2.26$, corresponding to a Student's t value for *10* samples at *95%* confidence. For the microStar InLight OSL system, $k = 3$ which corresponds to a confidence level of *99.73%* when a Gaussian distribution is assumed. The situation can be explained using Figure 3.4. If a Gaussian or a Student distribution is assumed for the zero dose distribution, then there is a certain confidence probability that the zero dose be located in the interval $\pm k\sigma$. This probability is *95%* for the Model *6600* Harshaw system and *99.73%* for the InLight MicroStar system. Since no negative dose can be measured, the relevant interval is $[0; +k\sigma]$. This means that there is a probability of *95%* or *99.73%* that the zero dose be located between zero and $+k\sigma$. It is then assumed that above $+k\sigma$, a certain dose is present. This is the reason why $+k\sigma$ can be taken as the *LLD*. It is then clear that there is a small probability, *5%* (TLD system) and *0.27%* (OSL system), that the zero dose be located outside the interval $[0; k\sigma]$.

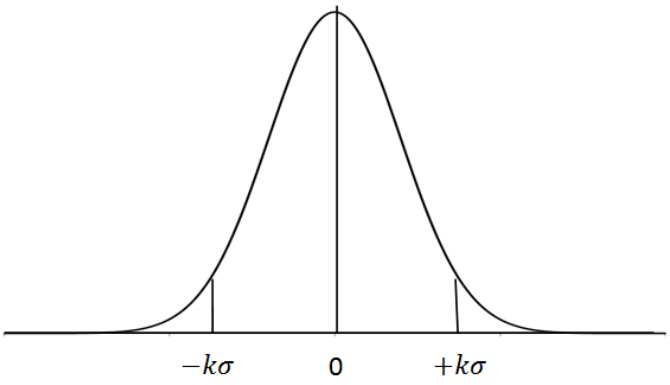

Figure 3.4: Illustration for determining the LLD by the statistical method. Ideal case where the zero dose value is *0 mSv*.

This means that there is a weak probability to conclude that a dose is present when actually there is none (false positive). In fact, Eq. 3.1 gives the *LLD* in terms of *mSv* whereas measurements are carried out in units of count (OSL system) or charge (TLD system). To obtain the *LLD* in units of personal deep dose *Hp (10)*, the standard deviation in units of count or charge is first obtained. Then the standard deviation in *mSv* is derived using Eq. 3.2.

$$\sigma = \frac{\sigma_C}{CF} \qquad (3.2)$$

where *CF* is the calibration factor obtained from the calibration curve and whose unit is either *nC/mSv* (TLD system) or *count/mSv* (OSL system). σ_C is the standard deviation in counts or *nC*.

To apply the method described above for the determination of the *LLD* and zero dose, a set of multiple measurements of the zero dose was taken. Counting statistics were also used to determine whether the multiple measurements taken show an amount of internal fluctuation that is consistent with predicted statistical fluctuation. The chain

of events that characterizes this category of counting statistics is illustrated in Figure 3.5. This diagram was followed in the present work.

The dosimeters were annealed or bleached before the reading stage. OSLDs were bleached only once, for 30 seconds, using an InLight pocket annealer. TLDs were annealed four times using the Harshaw 6600 reader and according to the time temperature profiles (TTP) listed in table 3.1 [25].

Finally, another approach was used for determining the *LLD*. That was to perform a linearity test and to consider the intercept of the linearity equation as the *LLD*. Thereafter, the trumpet curve was used to check whether the *LLDs* obtained were in accordance with IAEA requirements.

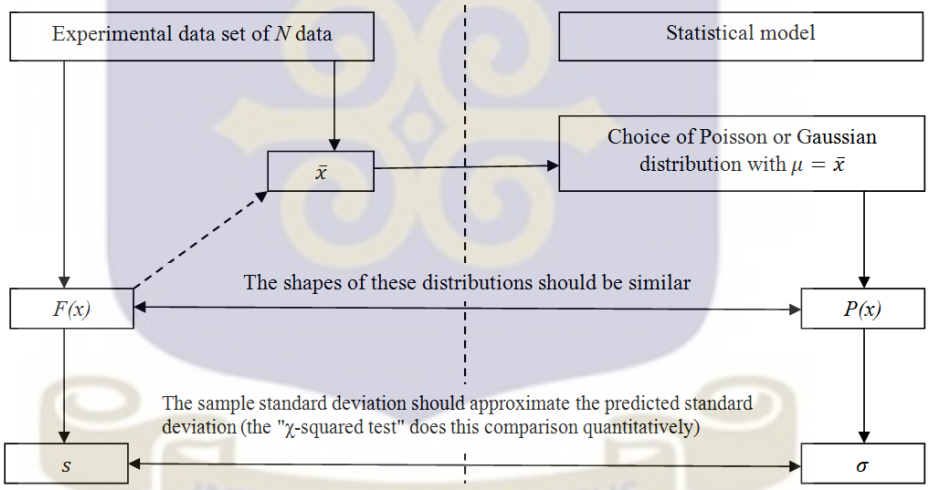

Figure 3.5: The inspection of a set of data for consistency with a statistical model [22]. The diagram is used to compare the experimental and the predicted distributions.

Table 3.1: Time temperature profiles used for zero dose and *LLD* determinations [25]. As shown in the table, the TTP used for the first readout is different from the one used for the three other readouts.

Parameter	Value First readout / Other three readouts (normal TTP)	Units
Preheat temperature	*100 / 50*	*°C*
Preheat time	*1 / 0*	*Sec*
Rate	*25 / 25*	*°C / Sec*
Maximum temperature	*300*	*°C*
Acquire time	*60 / 13*	*Sec*
Annealing temperature	*300 / 300*	*°C*
Annealing time	*0/10*	*Sec*

3.2.4 Uncertainty analysis

The procedure followed here is the one described in the IEC technical report TR62461 [7] and based on the *Guide to the Expression of Uncertainty in Measurement* (GUM). Three steps are required for the calculation of uncertainty in measurement: the construction of a model function, the collection of data and existing knowledge, and the calculation of the result of the measurement and the associated uncertainty according to the model function.

Construction of a model function

The model function that was used here is the following:

$$Hp\ (10) = N_0 K_n K_s K_{E,\varphi} K_{env}\ f(H_m) \qquad (3.3)$$

Where:

- $Hp\ (10)$ is the measuring quantity personal dose equivalent (measured value);
- N_0 is the reference calibration factor;
- K_n is the correction factor for non linearity;
- K_s is the correction factor for inhomogeneity of detector sensitivity;
- $K_{E,\varphi}$ is the correction factor for photon energy and angle of incidence;
- K_{env} is the correction factor for environmental conditions;
- H_m is the indicated value, reading of the dosimeter in units of *Hp (10)*;
- $f(H_m)$ is the linearity correction function obtained from the linearity curve.

This model function gives the relationship between the measurand (measuring quantity) $H_p(10)$, called output quantity of the evaluation, and the input quantities $N_0, K_n, K_{E,\varphi}$, ... , etc. The imperfect knowledge of the true value is taken into account in such a way that, for the evaluation, both the input quantities and the output quantity are replaced by random variables. Their possible values are denoted by small letters with asterisk, for example n_0^*, k_n^*, $k_{E,\varphi}^*$, whereas all quantities are written in capital letters as in Eq. 3.3. For each quantity, the possible values are characterized by a distribution which has an expectation value denoted by the corresponding small letter without an asterisk, for example n_0, k_n, $k_{E,\varphi}$, and a corresponding standard deviation (standard uncertainty) denoted by the letter *s* and the index given by the mean value (expectation value), for example s_{n_0}, s_{k_n}, $s_{k_{E,\varphi}}$, respectively. Since the output quantity is linked to the input quantities via the model function, then the distributions of the possible values of the input quantities lead to a distribution of the possible

values of the output quantity. This is described by the corresponding expectation value $h_p(10)$ and its standard uncertainty u. The aim of the uncertainty analysis according to the GUM is the determination of $u[h_p(10)]$(this should be read as " u associated to $h_p(10)$").

Collection of data and existing knowledge

The second step of uncertainty analysis is the collection of data and existing knowledge. This includes both mathematical methods like statistical analysis and other methods like collecting data from data sheets (like calibration certificates), or using scientific and experimental experience. This generally leads to an adequate documentation method called the uncertainty budget. The main data needed, in the present work, for the uncertainty analysis are provided by the international standard IEC 62387 (tables 8, 14 and 15) and experimental data.

Calculation of the result of a measurement and the associated uncertainty

There are three steps : the calculation of sensitivity coefficients of the inputs quantities, the calculation of the contributions of the standard uncertainties of the input quantities to the standard uncertainty associated with the output quantity, and the calculation of the total standard uncertainty u, associated with the output quantity $h_p(10)$.

The sensitivity coefficient, denoted by the symbol c with a subscript indicating the input quantities, for example c_{n_0}, c_{k_n}, $c_{k_{E,\varphi}}$, is the partial derivative of the model function of the measurement, with respect to the particular input quantity. Thus, the sensitivity coefficient of the input quantity n_0 is given by:

$$c_{n_0} = \frac{\partial h_p(10)}{\partial n_0} = \frac{\partial H_p(10)}{\partial N_0}\Big|_{N_0=n_0, K_n=k_n, K_s=k_s \; K_{E,\varphi}=k_{E,\varphi}, K_{env}=k_{env}, f(H_m)=f(h_m)}$$

$$= k_n k_s k_{E,\varphi} k_{env} f(h_m) \qquad (3.4)$$

following the same procedure, we get for the other input quantities:

$$\begin{cases} c_{k_n} = n_0 k_s k_{E,\varphi} k_{env} f(h_m) \\ c_{k_s} = n_0 k_n k_{E,\varphi} k_{env} f(h_m) \\ c_{k_{E,\varphi}} = n_0 k_n k_s k_{env} f(h_m) \\ c_{k_{env}} = n_0 k_n k_s k_{E,\varphi} f(h_m) \end{cases} \qquad (3.5)$$

The contributions of the input quantities to the standard uncertainty $u[h_p(10)]$ associated with the output quantity are obtained by the following equation:

$$u_i[h_p(10)] = |c_i| s_i \qquad (3.6)$$

where $i = n_0, k_n, k_s\ k_{E,\varphi}, k_{env}$.

The total standard uncertainty u associated with the output quantity $h_p(10)$ is then obtained by the geometrical sum of all these contributions:

$$u[h_p(10)] = \sqrt{u_i^2[h_p(10)]} \qquad (3.7)$$

where i is as above.

It is also important to stress that if a mean value of several measurements is used as an input quantity, the standard deviation of this mean value is given by the standard deviation of a single measurement divided by the square root of the number of the measurements. This standard deviation of the mean is then taken as the standard uncertainty associated to this mean value. This is the case here for the quantity h_m. The standard uncertainty associated with $f(h_m)$ is then obtained through the error propagation formula [21, 22]. For a function $f = f(x, y)$, this formula is given by:

$$\sigma_f = \sqrt{\left(\frac{\partial f(x,y)}{\partial x}\sigma_x\right)^2 + \left(\frac{\partial f(x,y)}{\partial y}\sigma_y\right)^2} \qquad (3.8)$$

where σ_x and σ_y are the standard uncertainties associated with the quantities *x* and *y*, respectively.

The standard IEC 62387 does not address any type test requirement for the reference calibration factor N_0 because this cannot be tested in a type test. But, as high precision is required for calibration facilities, limits of $\pm$ 5 % about an expectation value of *1* with a triangular distribution are usually assumed [7].

From Tables 8, 14 and 15 in standard IEC 62387, limits of $\pm$ 40 % and $\pm$ 20 % about an expectation value of *1* are derived for $K_{E,\varphi}$, and K_{env}, respectively. A Gaussian distribution and a triangular distribution are respectively assumed for $K_{E,\varphi}$, and K_{env}.

Concerning the correction factors K_n, and K_s, experimental data were used. First, relative minimum and maximum responses were calculated:

$$r_{min} = \frac{R_{min}}{R_{ref}} \quad and \quad r_{min} = \frac{R_{min}}{R_{ref}} \qquad (3.9)$$

where R_{min} and R_{max} are the minimum and maximum experimental responses, respectively. R_{ref} is the reference response which is the mean value of the responses of the reference dosimeters.

Then, the maximum and minimum correction factors are computed:

$$k_{min} = \frac{1}{r_{max}} \qquad and \qquad k_{max} = \frac{1}{r_{min}} \qquad (3.10)$$

Finally, the half - width and the expectation value of the distribution are obtained by:

$$a = \frac{k_{max} - k_{min}}{2} \qquad (3.11)$$

$$k = \frac{k_{max} + k_{min}}{2} \qquad (3.12)$$

We assumed a Gaussian distribution for K_n and K_s. The standard uncertainties associated with the distributions used are given in Table 3.2.

Table 3.2: Standard uncertainties for the distributions used in the study [7]. The standard uncertainties are given with confidence levels of *100 %* and *99.7 %* for the triangular and the Gaussian distributions, respectively.

Type of distribution	Standard uncertainty	Comment
Triangular	$a/\sqrt{6}$	*100 %* of all the possible values are within the interval $[k_{min}; k_{max}]$
Gaussian	$a/3$	*99.7 %* of all the possible values are within the interval $[k_{min}; k_{max}]$

After the uncertainty calculation according to IEC technical report TR62461, a comparison with the following international standards was performed:

- IAEA 99 (trumpet curve): $\frac{1}{5}(1 - \frac{2H_0}{H_0+H_t}) \leq \frac{H_m}{H_t} \leq 1.5(1 + \frac{H_0}{2H_0+H_t})$, 95 % level [1];
- IEC 1066: $0.33 \leq H_m/H_t \leq 1.77$, 95 % level [8];
- IEC 1283 ser.: $0.0 \leq H_m/H_t \leq 2.1$, 95 % level [8];
- PTB 99: $1 - 0.4t(H_t) \leq H_m/H_t \leq 1 + 0.4t(H_t)$, 92 % level, $H_0 \leq 0.2\ mSv$ [8].

Where H_0, H_m, H_t and H_m/H_t are as defined in the section 2.3.6 of the literature review, $t(H_t)$ is the trumpet function:

$$t(H_t) = 1 + \frac{20}{9}\frac{H_0}{H_0 + H_t} \qquad (3.13)$$

As the computed uncertainties are expressed in terms of personal dose equivalent *Hp (10)* and the standards for comparison are given in terms of response, we converted the computed uncertainties into responses. The following is the procedure to do so.

The complete result of a measurement, is given by

$$H_p(10) = h_p(10) \pm u\,, 95\ \%\ confidence\ level \qquad (3.14)$$

The minimum uncertainty of the response and the maximum uncertainty of the response are respectively given by:

$$R^{min} = \frac{h_p(10)}{h_p(10) + u} \quad and \quad R^{max} = \frac{h_p(10)}{h_p(10) - u} \qquad (3.15)$$

These were the computed limits that were compared to the standards given above.

3.2.5 Linearity test

The procedure adopted is the one described in the IEC 62387 standard [9]. The dosimeters are irradiated at known dose equivalents and the variation of the response due to the change of the dose equivalent shall not exceed the values given in the standard. This requirement is met only if the relationship below is valid:

$$0.91 - U_{t,com} \leq \left(\frac{\bar{H}_{m,i}}{\bar{H}_{m,ref}} \pm U_{com}\right).\frac{H_{t,ref}}{H_{t,i}} \leq 1.11 + U_{t,com} \qquad (3.16)$$

Where:

- $H_{t,i}$ is the conventional true value of dose equivalent delivered to dosimeters of group i ;
- $H_{t,ref}$ is the reference conventional true value of dose equivalent;
- $\bar{H}_{m,i}$ is the mean of the indicated values of dosimeters of group i;
- $\bar{H}_{m,ref}$ is the mean of indicated values of dosimeters of the reference group;
- U_{com}, is the expanded uncertainty of $\bar{H}_{m,i}/\bar{H}_{m,ref}$;
- $U_{t,com}$, is the combined relative expanded uncertainty of $H_{t,ref}/H_{t,i}$.

Eq. 3.16 can be rewritten as

$$0.91 - U_{t,com} \leq \left(\frac{\bar{R}_i}{\bar{R}_{ref}} \pm U_{com}.\frac{H_{t,ref}}{H_{t,i}}\right) \leq 1.11 + U_{t,com}$$

where $\bar{R}_i$ and $\bar{R}_{ref}$ are the mean response of dosimeters of group i and of the reference group, respectively.

$$U_{t,com} = \sqrt{U_{t,rel,ref}^2 + U_{t,rel,i}^2}$$

where $U_{t,rel,ref}$ and $U_{t,rel,i}$ are expanded uncertainties of the conventional true values $H_{t,ref}$ and $H_{t,i}$ respectively. Assuming

$$U_{t,rel,ref} = U_{t,rel,i} = 2.5\ \%$$

leads to $U_{t,com} = 0.035$ and

$$0.87 \leq \left(\frac{\bar{R}_i}{\bar{R}_{ref}} \pm U_{com}.\frac{H_{t,ref}}{H_{t,i}}\right) \leq 1.15$$

We are interested in the mean response of dosimeters of group i, therefore we have to multiply the previous equation by $\bar{R}_{ref}$. According to IEC 62387 standard, $H_{t,ref} = 3\ mSv$. $H_{m,ref}$ is obtained experimentally. Finally, we get

$$0.87 \times \bar{R}_{ref} \leq \left(\bar{R}_i \pm U_{R,com}\right) \leq 1.15 \times \bar{R}_{ref} \qquad (3.17)$$

where

$$U_{R,com} = U_{com}.\frac{H_{t,ref}}{H_{t,i}}.\bar{R}_{ref}$$

is the expanded uncertainty associated with $\bar{R}_i$. U_{com} is calculated using Eq. 3.18 as:

$$U_{com} = \frac{\bar{H}_{m,i}}{\bar{H}_{m,ref}}.\sqrt{\left(\frac{U_i^2}{\bar{H}_{m,i}^2} + \frac{U_{ref}^2}{\bar{H}_{m,ref}^2}\right)} \qquad (3.18)$$

where U_i and U_{ref} are the expanded uncertainties of $\bar{H}_{m,i}$ and $\bar{H}_{m,ref}$, respectively. They are given by

$$U = \frac{t_{n-1}}{\sqrt{n}}s$$

where t_{n-1} is the Student's *t*-value for a double sided *95 %* confidence interval, *s* is the standard deviation for the specific group of measurements, and *n* is the number of measurements.

A comparison was performed with the following standards:

- IAEA 99 (trumpet curve) [1];
- IEC 1066: $|R(H_t) - 1| \leq 0.1 - I$ (*I:=* confidence interval $\approx$ *0.03*) for *0.1mSv* $\leq H_t \leq$ *1 Sv* ($R(H_t) = H_m / H_t$) [8];
- IEC 1283 ser.: $|R(H_t) - 1| \leq 0.15$ for the "value of the coefficient of variation over the effective range of measurement [8].

3.2.6 Coefficient of variation

The procedure considered is the one described by the IEC 62387 standard [9]. The statistical fluctuations of the indicated value shall fulfil the following requirements:

$$\begin{cases} v \leq 15\ \%\ \ for\ H_t < 0.1\ mSv \\ v \leq \left(16 - \dfrac{H_t}{0.1\ mSv}\right)\%\ for\ 0.1\ mSv \leq H_t \leq 1.1\ mSv \\ v \leq 5\ \%\ for\ H_t \geq 1.1\ mSv \end{cases} \qquad (3.19)$$

where $v = s/\bar{H}_m$ is the coefficient of variation, s is the standard deviation of the group of measurement, $\bar{H}_m$ is the corresponding mean, and H_t is the conventional true value.

CHAPTER FOUR

RESULTS AND DISCUSSIONS

This chapter provides the results that have been obtained for the reader performance tests, the zero dose and minimum detectable dose assessments, the uncertainty analysis, the linearity and coefficient of variation tests.

4.1 READER PERFORMANCE TESTS

4.1.1 MicroStar InLight system

DRK count

1000 readings were taken for this test. Figure 4.1 shows the plot of DRK count against the reading number. Figure 4.2 shows the application of counting statistics to the *1000* values.

From Figure 4.1 we see that all the measurements are below *30*. This means that the requirement given in the usual manual is met. From Figure 4.2 we observe that the shapes of the experimental and the predicted distributions are similar. Table 4.1 shows the Chi - square test which compares the experimental and predicted (Gaussian) standard deviations quantitatively.

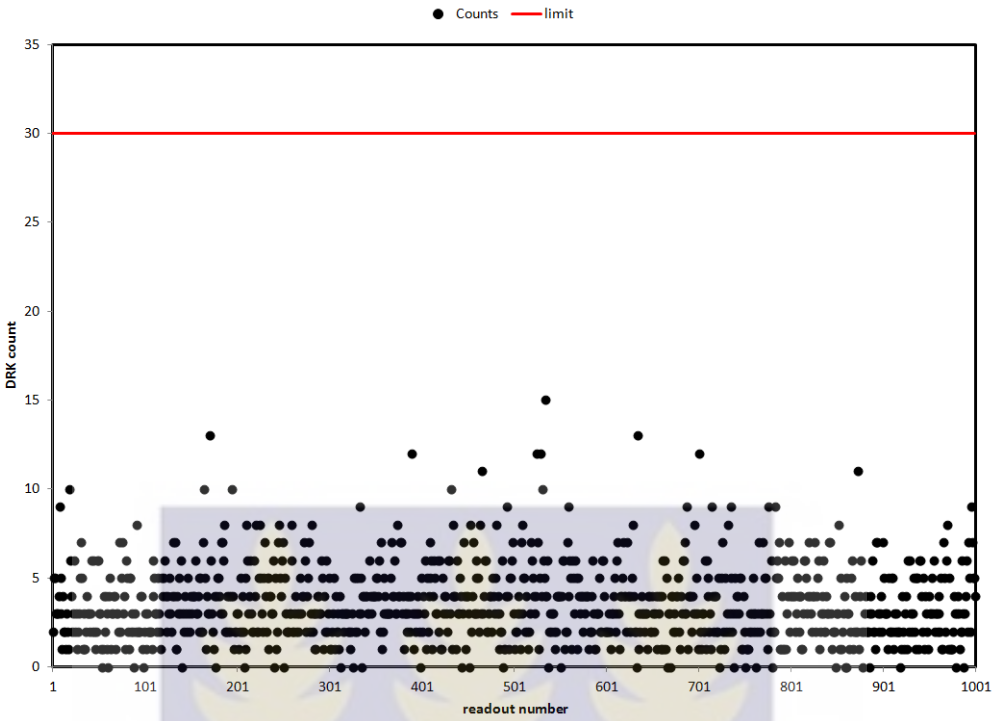

Figure 4.1: DRK count against the reading number. All the points are below the required limit.

Table 4.1: Chi - square test between the experimental and predicted distributions of DRK count measurements. The predicted standard deviation is outside the required interval.

Number of degrees of freedom *v*	*Mean (counts)*	*s (counts)*	*σ (counts)*	χ^2	Chi-square test for *σ (counts)*
999	*3.54*	*2.046*	***1.91***	1143.48	$\mathbf{1.96 < \sigma < 2.14}$

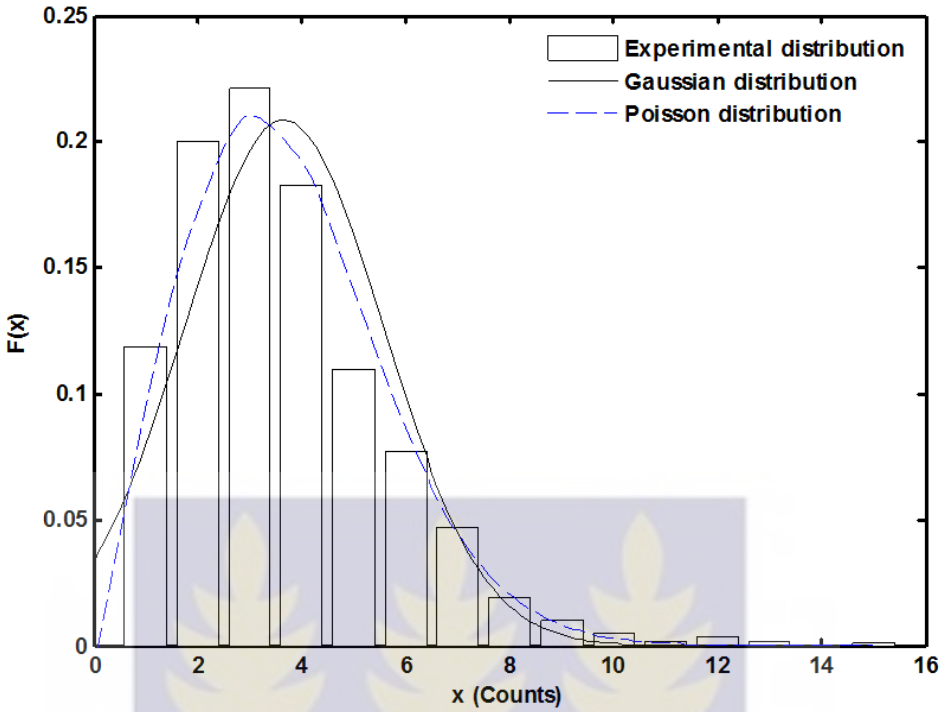

Figure 4.2: Application of counting statistics to the DRK count measurement using the Gaussian and Poisson distributions as the predicted distributions. The shapes of the predicted and experimental curves are similar. The Poisson distribution fits better the experimental distribution.

From Table 4.1 we can see that the value of σ is just outside the required interval. Therefore, the experimental and predicted standard deviations were not sufficiently close to pass the Chi - square test. If instead of the Gaussian distribution the Poisson distribution is chosen, it is observed that the predicted distribution fits better the experimental distribution (Figure 4.2), but the result of the Chi - square test remains the same.

CAL count

1000 readings were also taken for this test. Figure 4.3 shows the plot of CAL count against the reading number. Figure 4.4 illustrates the application of counting statistics to these *1000* values.

From Figure 4.3 we observe that only one measurement is outside the required limits. This means that *99.99 %* of the measurements fall within these limits. Therefore it is considered that the requirement given in the user manual is met. From Figure 4.4 we see that the experimental and predicted distributions are similar, and from Table 4.2 we can see that the value of σ is just outside the required interval so that the CAL count measurement also failed the Chi - square test.

Table 4.2: Chi - square test between the experimental and predicted distributions of CAL count measurements. The predicted standard deviation is outside the required interval.

Number of degrees of freedom v	*Mean (counts)*	*s (counts)*	σ *(counts)*	χ^2	Chi-square test for σ *(counts)*
999	*1069.77*	*34.49*	***32.71***	*1110.57*	$\mathbf{33.037 < \sigma < 36.067}$

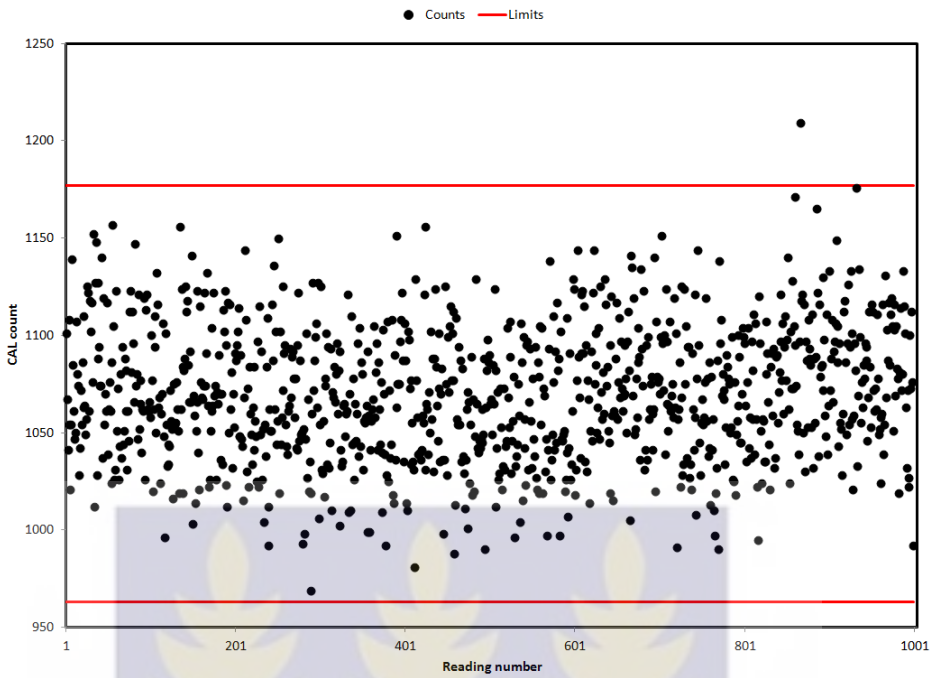

Figure 4.3: CAL count against the reading number. Only one point is outside the required limits.

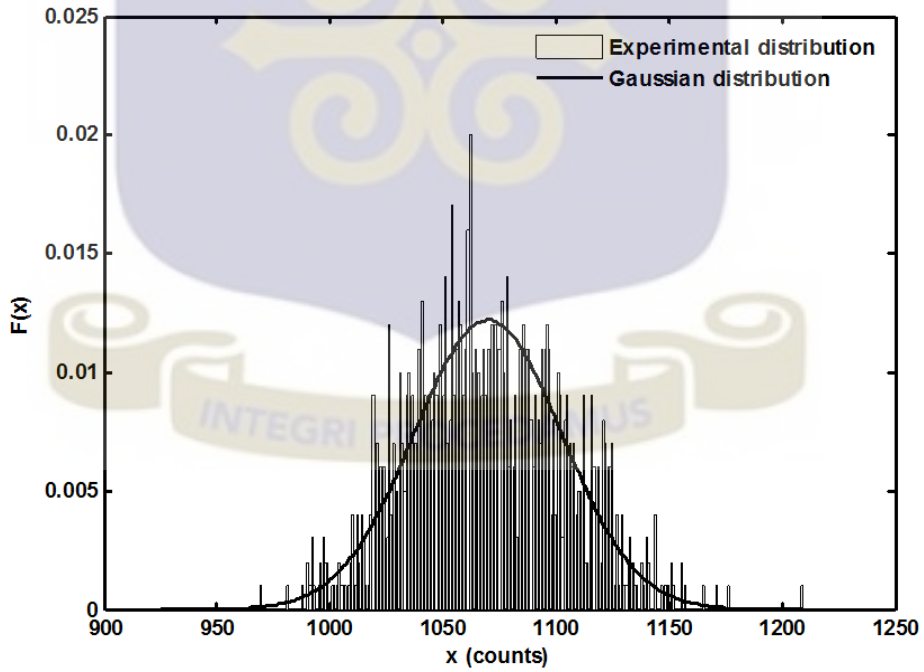

Figure 4.4: Application of counting statistics to the CAL count measurement using the Gaussian distribution as the predicted distribution. The predicted and the experimental distributions are similar.

LED count

Here also 1000 readouts were taken. Figure 4.5 shows the plot of the LED count against the reading number. Figure 4.6 illustrates the application of counting statistics to the LED count measurement. From Figure 4.5 we can see that all the measurements fall within the limits. Therefore the requirement given in the user manual is met. From Figure 4.6 we see that the experimental and predicted distributions are not similar, and from Table 4.3 we can see that the value of σ is largely outside the required interval. Therefore the LED count measurement failed the Chi - square test.

Table 4.3: Chi - square test between the experimental and predicted distributions of LED count measurements. The predicted standard deviation is outside the required interval.

Number of degrees of freedom *v*	*Mean (counts)*	*s (counts)*	σ *(counts)*	χ^2	Chi-square test for σ *(counts)*
999	*5908.21*	*111.13*	***76.86***	*2088.12*	$\mathbf{106.46 < \sigma < 116.22}$

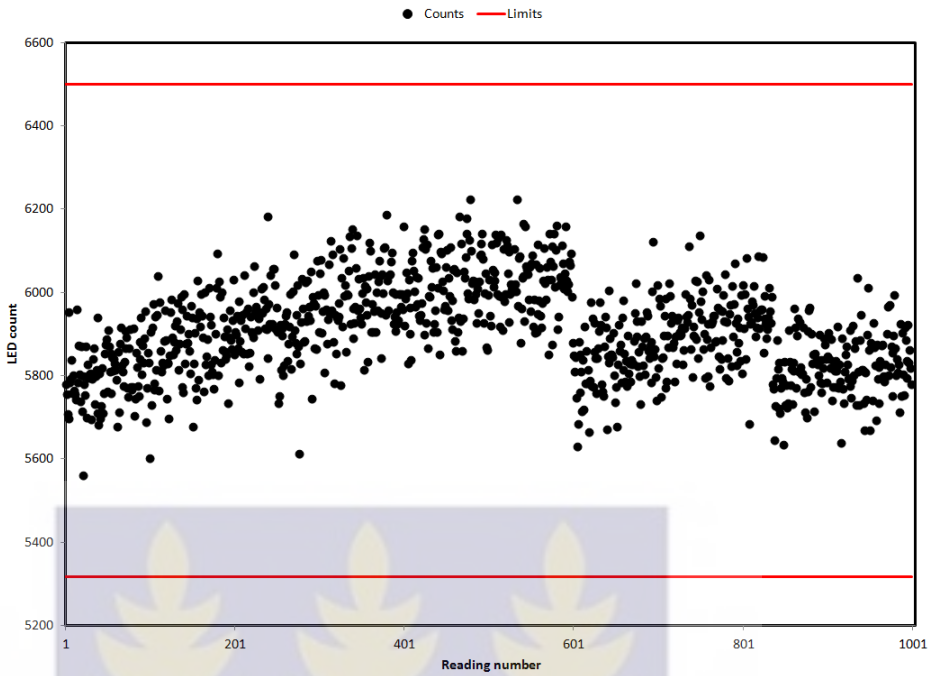

Figure 4.5: LED count against the reading number. All the points are within the required limits.

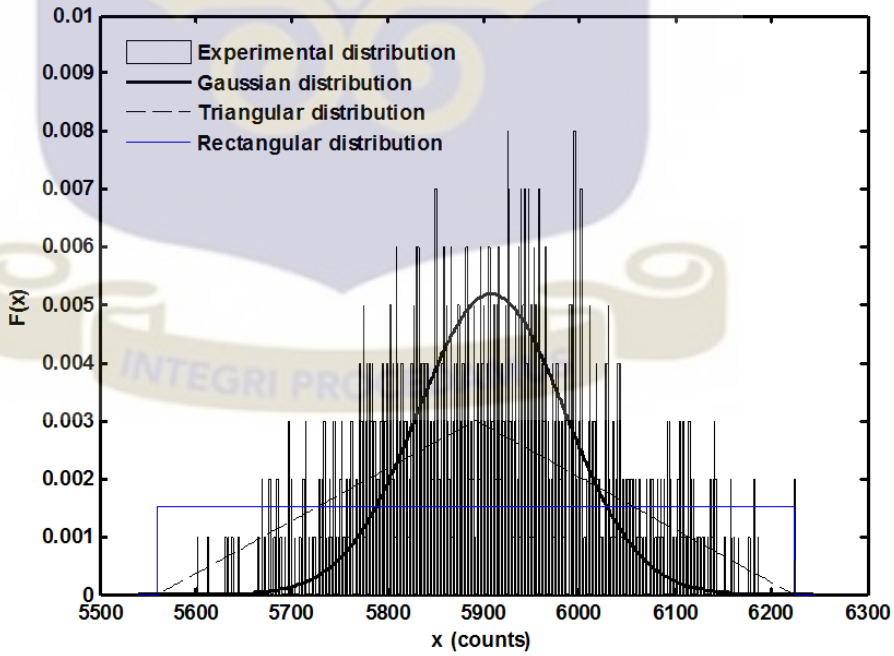

Figure 4.6: Application of counting statistics to the LED count measurement using the Gaussian distribution as the predicted distribution. The predicted distribution is not similar to the experimental distribution. The Rectangular and triangular distributions have been tested as predicted distribution but they also did not fit the experimental distribution.

Finally, concerning the microStar InLight reader, used in the Gabonese dosimetry service, on one hand, all the reader performance tests met the requirements given in the user manual. On the other hand, all these tests, in particular the CAL count measurement, failed the statistical test that is part of counting statistics. This means that there may be some abnormalities in the counting system, and that the statistical abnormalities suspected have apparently no impact on the reading results. Furthermore, since the DRK count and the CAL count did not fail the Chi - square test by very far, we can still consider a Gaussian distribution as an approximate of the experimental data distributions of these two measurements.

4.1.2 Harshaw 6600 system

PMT Noise

300 readouts were taken for this quality control measurement. Figure 4.7 shows the plot of the PMT noise measurement against the reading number. Figure 4.8 shows the application of counting statistics to these measurements.

From Figure 4.7 we can see that a significant number of readings are outside the required limits. Therefore the requirement given in the Harshaw 6600 user manual is not met. From Figure 4.8 we see that the experimental and predicted distributions are very similar. But from Table 4.4 we can see that the value of σ is outside the required interval by a small margin. Therefore the PMT noise QC measurement failed the Chi - square test.

Table 4.4: Chi - square test between the experimental and predicted (Gaussian) distributions of PMT noise measurement. The predicted standard deviation is outside the required interval by a small margin.

Number of degrees of freedom *v*	*Mean (pC)*	*s (pC)*	*σ (pC)*	χ^2	Chi-square test for *σ (pC)*
299	*12.16*	*4.00*	***3.5***	*393.45*	$\mathbf{3.70 < \sigma < 4.35}$

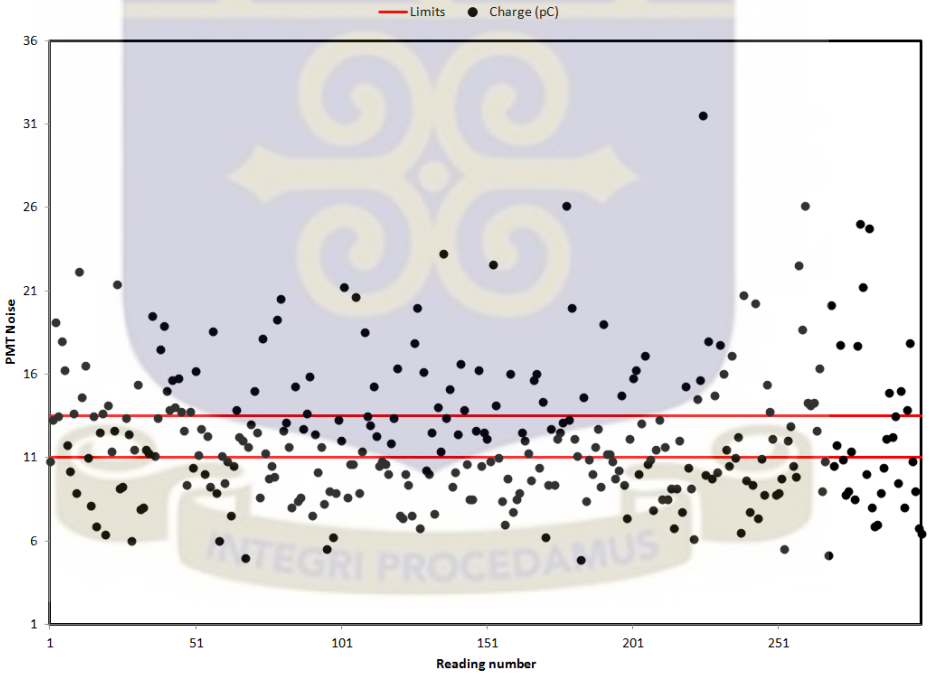

Figure 4.7: PMT noise measurement against the reading number. A significant number of readings are outside the required limits.

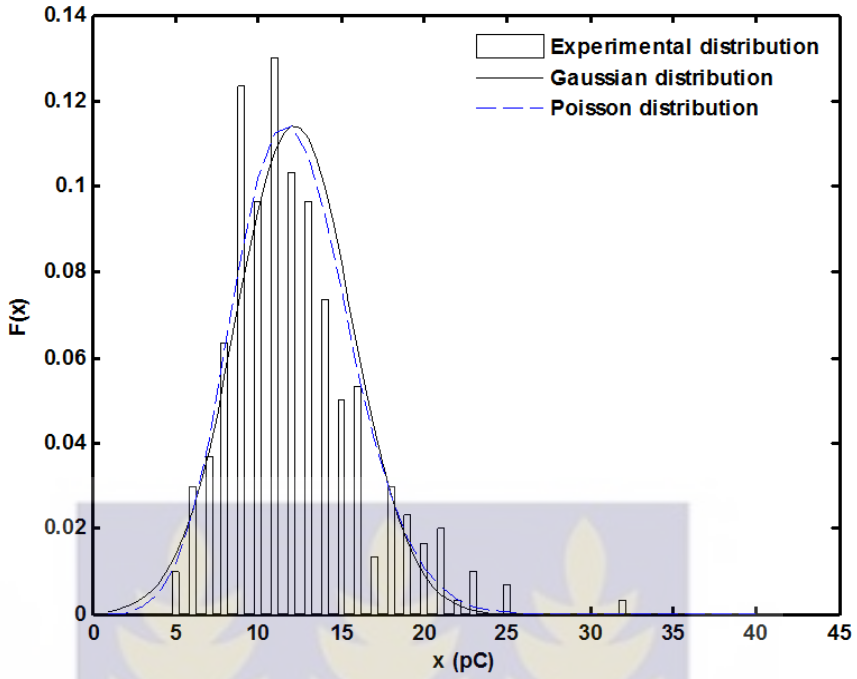

Figure 4.8 : Application of counting statistics to the PMT noise measurement using the Poisson and Gaussian distributions as predicted distributions. The shapes of the predicted and experimental distributions are very similar. The Poisson distribution fits better the experimental distribution.

Reference light

300 readouts were also taken for this QC measurement. Figure 4.9 shows the plot of the PMT noise measurement against the reading number. Figure 4.10 shows the application of counting statistics to these *300* measurements.

From Figure 4.9 we can see that the Reference light measurement meets the requirement of the user manual since all the measurements fall within the required limits. From Figure 4.10 we see that the experimental and Gaussian distributions are not similar. Table 4.5 confirm this fact since we can see that the value of σ is largely outside the required interval for the predicted standard deviation. Therefore the Reference light QC measurement failed the Chi - square test.

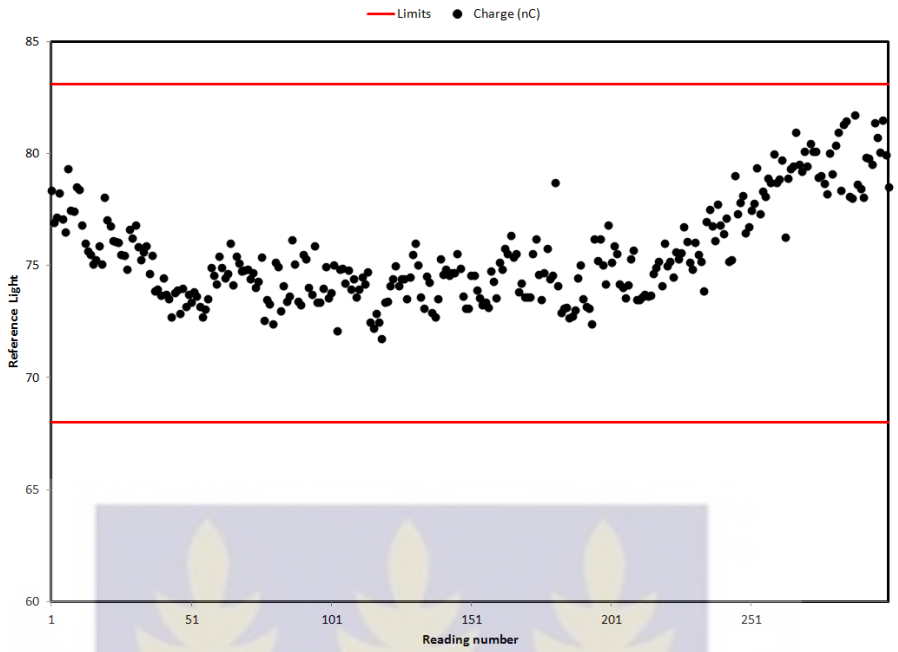

Figure 4.9: Reference light measurement against the reading number. All the points are within the required limits.

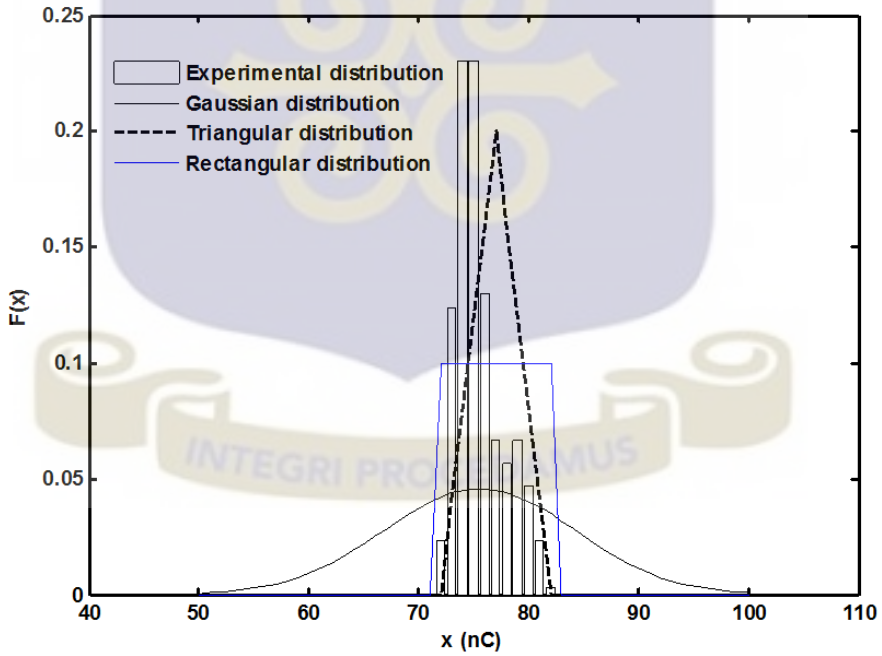

Figure 4.10 : Application of counting statistics to the Reference light measurement using the Gaussian distributions the predicted distribution. The shapes of the predicted and experimental distributions are not similar. The Rectangular and triangular distributions have been tried as predicted distributions, and only the triangular distribution seems to be close enough to the experimental distribution.

Table 4.5: Chi - square test between the experimental and predicted (Gaussian) distributions of Reference light measurement. The predicted standard deviation is largely outside the required interval.

Number of degrees of freedom *v*	*Mean (nC)*	*s (nC)*	*σ (nC)*	χ^2	Chi-square test for *σ (nC)*
299	*75.55*	*1.737*	***8.69***	*11.94*	$\mathbf{1.61 < \sigma < 1.89}$

It has been shown that only the Reference light measurement meets the requirement of the user manual. Since the Reference light and PMT noise are quality control (QC) tests that are taken before and after the measurement of a group of dosimeters so that if one of these QC measurements falls outside the required limits no measurements can be taken. Therefore, this clearly means that the limits used by the Ghanaian dosimetry service for the PMT noise are different from those given in the user manual.

Concerning the Chi - square test, it has been shown that the PMT noise measurement failed the test by a very small margin. Therefore, we can still consider a Gaussian distribution as an approximate of the experimental distribution of this measurement. The Reference light measurement failed the test by a large margin.

Finally, the intercomparison of the two dosimetry systems shows some similarities and differences regarding the application of counting statistics to the reader QC measurements. Let us recall first that the DRK count (microStar system) and PMT

noise (Harshaw 6600 system) measurements, and that the CAL count (microStar system) and Reference light (Harshaw 6600 system) measurements, are equivalent QC measurements, respectively. It has been shown for the DRK count ant PMT noise measurements that the experimental and predicted distributions were similar. Also, it has been shown that both the DRK count and PMT noise measurements failed the Chi - square test by a very small margin, so that a Gaussian distribution could still be considered as an approximate of the experimental distribution of these measurements. The results for the photomultiplier tube consistency (CAL count and Reference light measurements) were different. While the CAL count measurement failed the Chi - square test by a very small margin, so that an experimental CAL count measurement distribution could still be approached by a Gaussian distribution, the Reference light measurement failed the Chi - square test by a large margin, so that a Gaussian distribution is not convenient to approach an experimental Reference light measurement distribution. Instead, a triangular distribution seems to approach better reference light measurements. Particularly, the result obtained for the Reference light measurement is in contradiction with the results of counting statistics involving a radioactive source. Indeed, it is well known that radioactivity is well described by counting statistics [21,22,23].

4.2 ZERO DOSE AND LIMIT OF DETECTABILITY

4.2.1 Statistical method

MicroStar InLight system

Five curves are shown below corresponding to the result obtained with four different OSL dosimeters read *100* times each (Figure 4.11), and with the whole set of *10* dosimeters corresponding to *1000* readouts (Figure 4.12). Results listed in Table 4.6 were obtained from *10* readouts (one per dosimeter), *100* readouts (*10* per dosimeter) and *1000* readouts (*100* per dosimeter). From the shapes of the curves we could conclude that the experimental distribution follows the predicted distribution, but only the case for *9* degrees of freedom (Table 4.6) does not fail the chi-squared test. This means that for the two last cases the measured distributions differ significantly from the expected distributions. Rectangular and triangular distribution have also been tried as predicted distributions. From all the predicted distributions used, it appear that the triangular distribution approximate better the experimental distribution.

Table 4.6. Results per number of degrees of freedom. Only the case for 9 degrees of freedom passes the Chi - squared test.

Number of degrees of freedom *v*	*Zero dose (counts / mSv)*	*s (counts / mSv)*	*σ (counts / mSv)*	χ^2	Chi-square test for *σ (counts)*
9	*171.63 / 0.080*	*10.77 / 0.005*	***13.10** / 0.006*	*6.14*	$\mathbf{7.41 < \sigma < 19.66}$
99	*165.99 / 0.077*	*8.01 / 0.0037*	***12.88** / 0.006*	*38.27*	$\mathbf{7.03 < \sigma < 9.31}$
999	*167.78 / 0.078*	*8.04 / 0.0037*	***12.95** / 0.006*	385.27	$\mathbf{7.70 < \sigma < 8.41}$

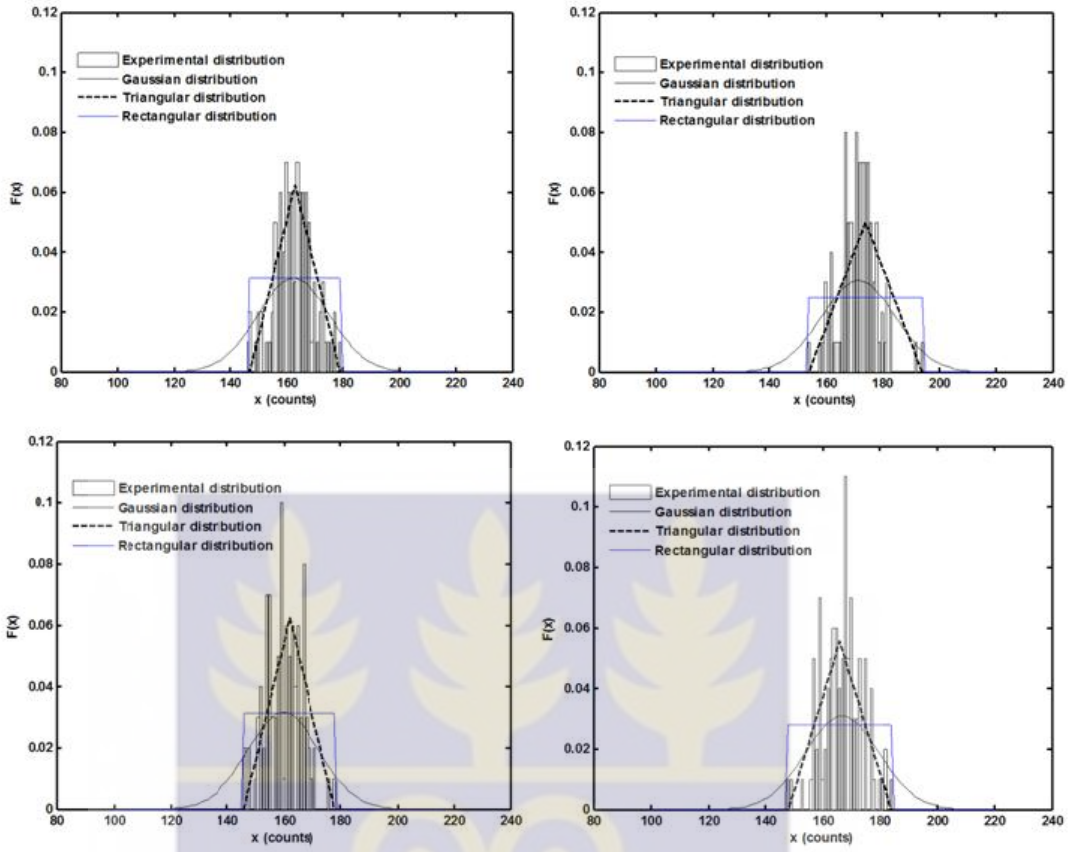

Figure 4.11: Experimental and predicted distributions for four OSL InLight dosimeters read 100 times each. The Gaussian distribution and particularly the triangular distribution are similar to the experimental distributions.

Taking only into account the Gaussian distribution as the predicted distribution, we came to the conclusion that for accuracy purposes the zero dose of the dosimetry system is ***≈ 168 counts / 0.08 mSv***, and for statistical reasons the *LLD* is $3\sigma = \mathbf{39.3}$ ***counts / 0.018 mSv ≈ 0.020 mSv.*** Table 4.7 compares the values of the *LLD* computed, the *LLD* reported on the reader certificate, and other relevant quantities. It can be seen that the *LLD* calculated according to the statistical method presented here is above the lower limit of the measuring range of the dosimeters, but is lower than the *LLD* specified in the reader certificate.

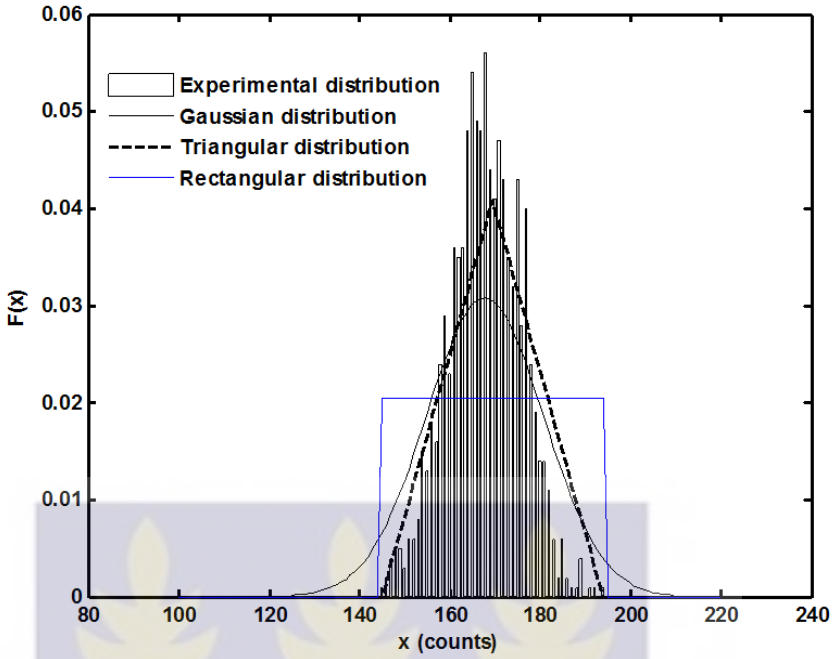

Figure 4.12: Experimental and Gaussian distributions corresponding to 1000 readouts of OSL InLight dosimeters resulting from the combination of the readouts of the 10 dosimeters of the set considered (100 readouts per dosimeter). The predicted and experimental distributions are similar. Rectangular and triangular distributions have also been tried as predicted distributions. It can be seen that the triangular distribution fits better the experimental distribution.

Table 4.7: Comparison between the *LLD* computed, the *LLD* specified in the reader certificate, and other relevant quantities.

LLD calculated	*LLD* (reader certificate)	Minimal reporting dose (manufacturer)	Recording level (one month, IAEA)	Zero dose (calculated)	Lower limit of the measuring range
0.020 mSv	*0.042 mSv*	*0.05 mSv*	*0.083 mSv*	***0.080 mSv***	*0.01 mSv*

Harshaw 6600 system

Here *100* repeated measurements were taken and the application of counting statistics to the data obtained did not lead to results that can be exploited. Therefore, only the results from these repeated measurements, following the annealing process given by Table 3.1, are presented. The zero dose value of the Harshaw *6600* system used by the Ghanaian dosimetry service is then given by the mean value of the *100* repeated measurements. We found ***0.026 mSv***. The *LLD* were determined according to the procedure given in [25]. The first *10* measurements were used. we found ***LLD = 0.00975 mSv = 0.975 mrem***, value in accordance with the user manual requirement which states that the *LLD* should be lower than ***1 mrem***. Table 4.8 compares the values of the *LLD* computed and other relevant quantities. In particular, it is observed that the value of the *LLD* calculated according to the statistical method is lower than the lower limit of the measuring range of the dosimeters and the zero dose calculated.

Table 4.8: Comparison between the *LLD* computed and other relevant quantities.

LLD calculated	Recording level (one month, IAEA)	Zero dose (calculated)	Lower limit of the measuring range
0.00975 mSv	*0.083 mSv*	***0.026 mSv***	*0.1 mSv*

4.2.2 Experimental method

Table 4.9 compares the operational quantity *Hp(10)* measured by the two systems.

Table 4.9: Comparison of the quantity *Hp(10)* measured by the two systems. A global and very significant underestimation is observed for the TL system, while an overestimation is generally observed for the OSL system.

Delivered dose *(mSv)*	Measured dose *(mSv)* (Harshaw 6600)	Measured dose *(mSv)* (microStar)
0.01	0.083705	0.03624988
0.02	0.092724	---
0.03	0.08003475	---
0.04	0.11326475	0.04874992
0.05	0.1993975	0.04375005
0.06	0.139195	0.05375004
0.07	0.15539	0.11124992
0.08	0.1081965	0.08875012
0.09	0.13094	0.09208353
0.1	0.1989625	0.13625002
0.2	0.1976	0.22874975
0.4	0.3321425	0.4537499
0.8	0.6193275	0.83874917
1	0.8541	1.00124955
2	1.571175	1.95124841
3	2.32423	3.12541477
5	3.9329	5.15873742
10	7.538875	10.6612399

Table 4.9 shows that, for the TLD system, apart from the doses lower than *0.2 mSv* and the abnormal measurement observed at the delivered dose *0.1 mSv*, the measured dose are systematically underestimated. For the OSL system, an overestimation of the quantity *Hp (10)* is generally observed for delivered doses above *0.06 mSv*.

For the OSL system, the measured doses corresponding to the true doses *0.02 mSv* and *0.03 mSv* were negative since their values were lower than the mean background and transport dose measured by the control dosimeters. This is why they are not presented in Table 4.9.

At this stage, the first conclusion is that the microStar gives better results than the Harshaw 6600 in the measurement of the operational quantity *Hp (10)*. The second conclusion is that both systems require corrections in order to obtain better results.

LLD for the TL system

A curve of the measured dose against the conventional true dose was plotted. The intercept of the equation obtained was considered as the experimental *LLD*. Then after, the trumpet curve was used to check whether the *LLD* obtained is in accordance with IAEA requirements.

From Figures 4.13 and 4.14 we can verify the linearity of the TL system. The user manual requirement states that the linearity of the system is established from *0.1 mSv* to *1 Sv*. The results obtained are better since the experimental linearity has been established from *0.01 mSv*.

From Figure 4.13, which is a plot of the mean raw doses measured against the true dose, we obtain a *LLD* of ***0.081 mSv***. From Figure 4.14, which is the curve of the mean dose values corrected for the zero dose against the true dose, a *LLD* of ***0.055 mSv*** is obtained.

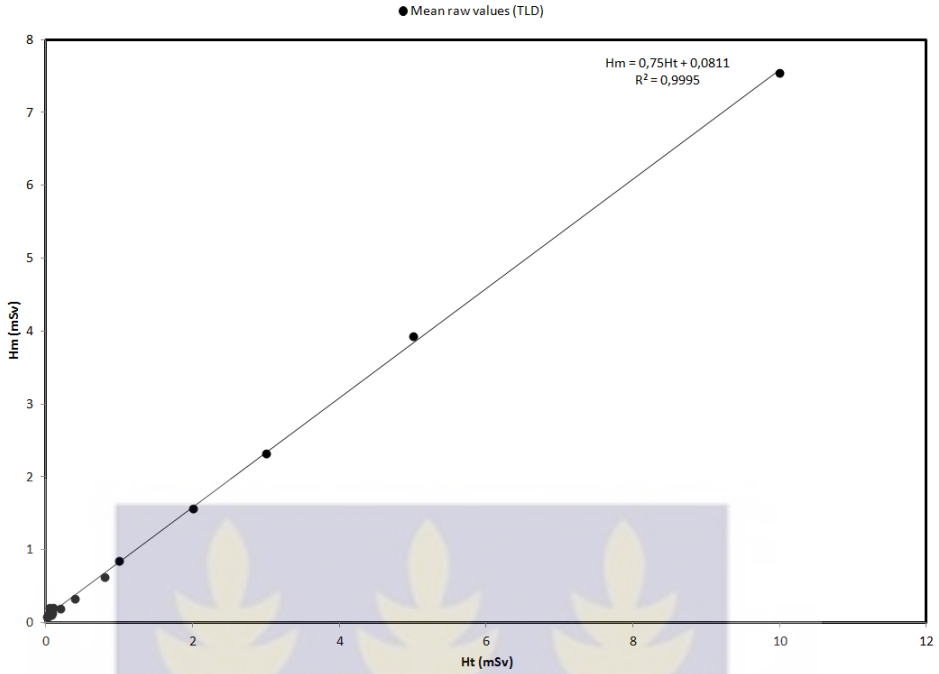

Figure 4.13: Curve of the measured dose against the delivered dose using the mean raw values measured. The linearity is established from the true dose *0.01 mSv*.

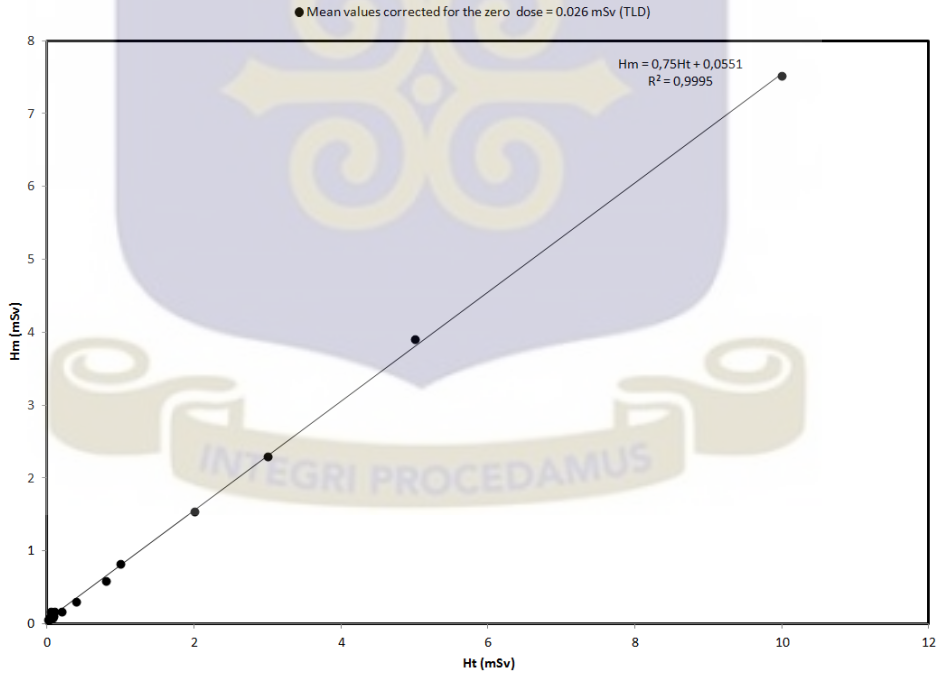

Figure 4.14: Curve of the mean measured doses corrected for the zero dose against the delivered dose. The linearity is established from the true dose *0.01 mSv*.

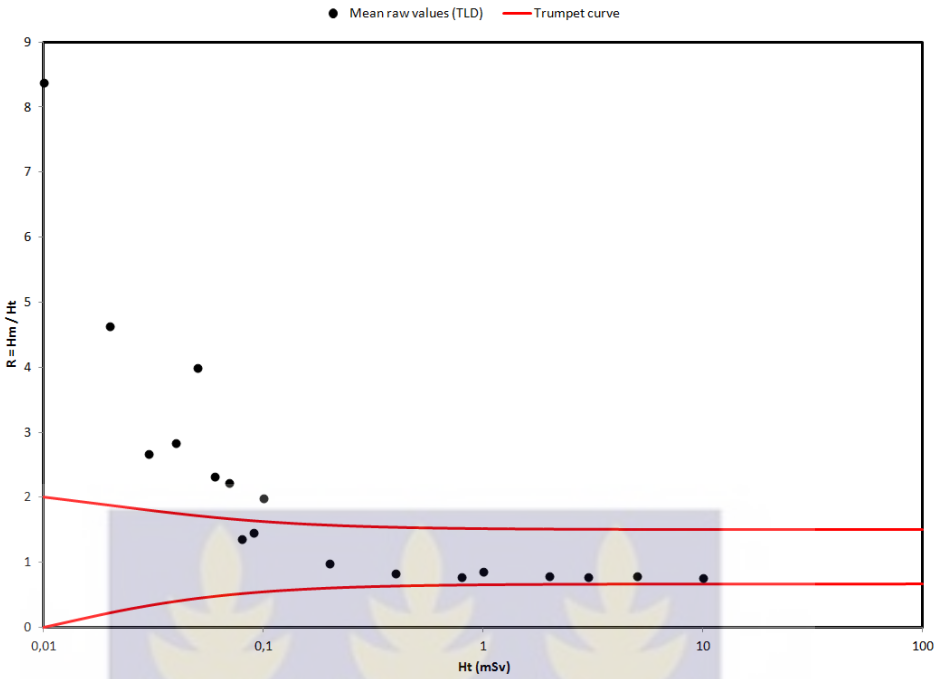

Figure 4.15: Verification of the choice of the LLD by the use of the trumpet curve. Here is represented the mean raw measured dose against the true dose.

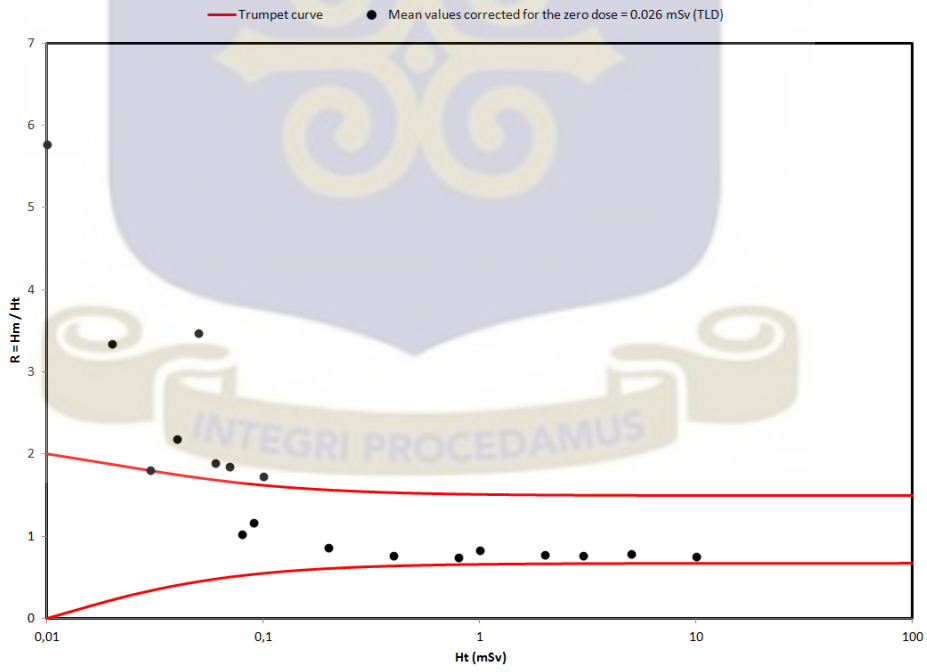

Figure 4.16: Verification of the choice of the LLD by the use of the trumpet curve. Here is represented the mean measured dose corrected for the zero dose against the true dose.

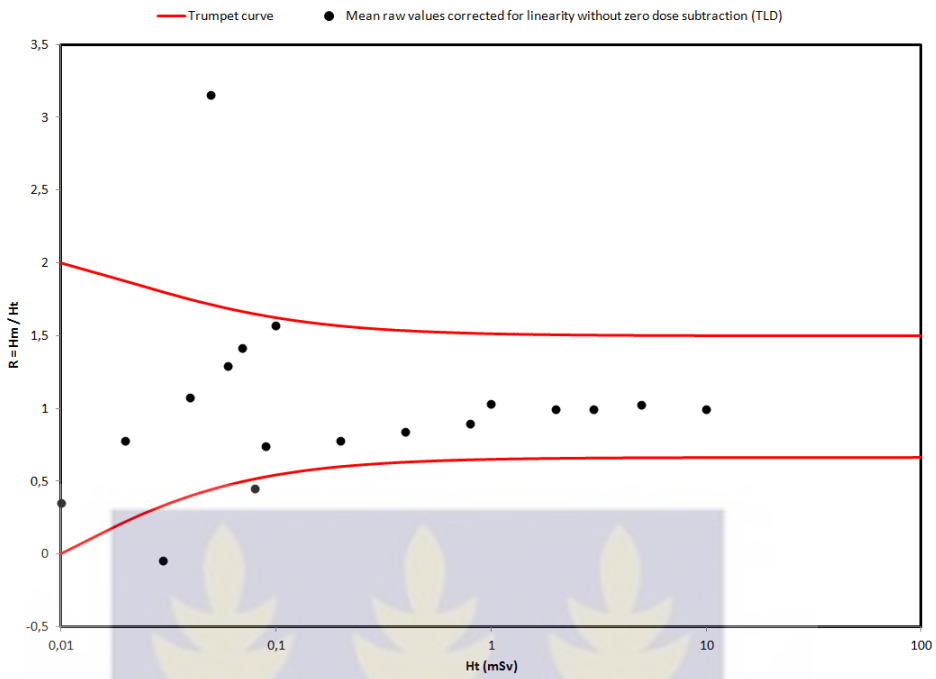

Figure 4.17: Verification of the choice of the LLD by the use of the trumpet curve. Here is represented the mean raw measured dose corrected for linearity without zero dose subtraction against the true dose.

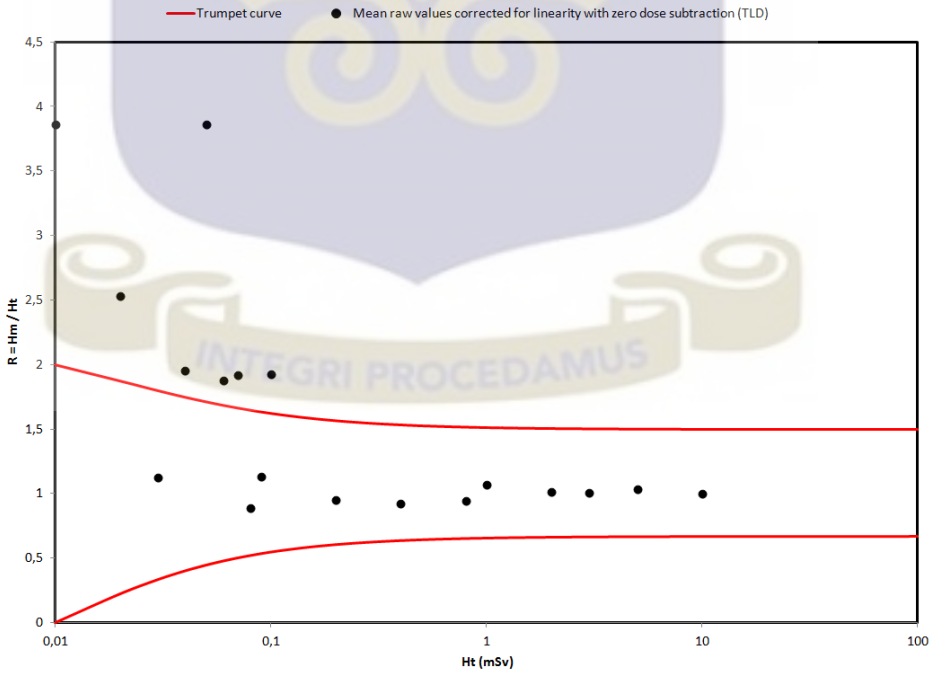

Figure 4.18: Verification of the choice of the LLD by the use of the trumpet curve. Here is represented the mean raw measured dose corrected for linearity with zero dose subtraction against the true dose.

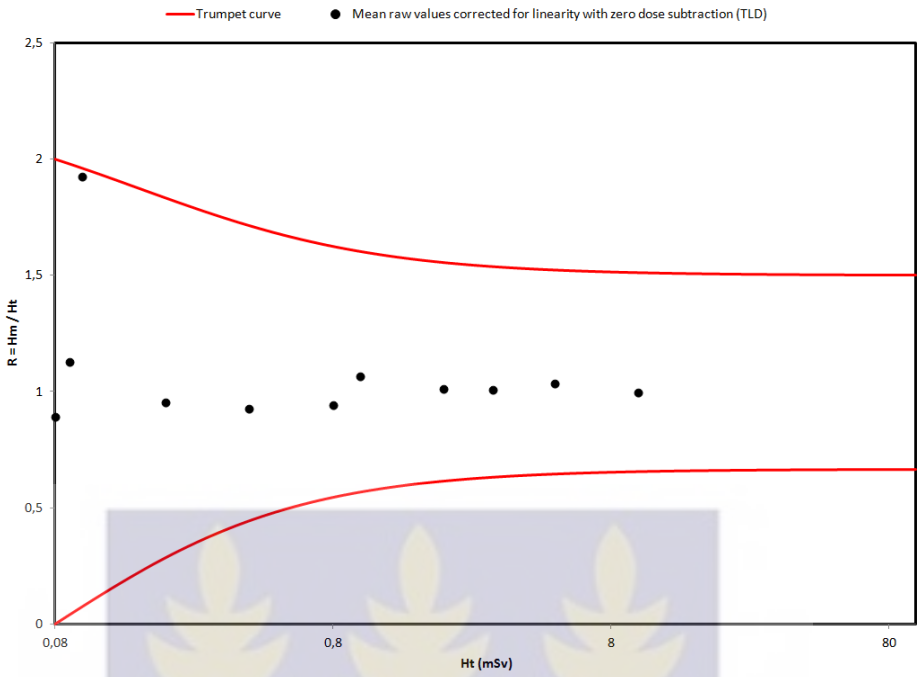

Figure 4.19: Verification of the choice of the *LLD* by the use of the trumpet curve. Here is represented the mean raw measured dose corrected for linearity with zero dose subtraction against the true dose for a *LLD* of *0.08 mSv*.

Figure 4.16 is a slight improvement of Figure 4.15. Both Figure 4.15 and Figure 4.16 suggest a *LLD* of *0.08 mSv*. But an improvement of the results is still needed. Figure 4.17 is obtained by correcting the raw measured dose values using the linearity equation $H_t = 1.333\ H_m - 0.108\ (in\ mSv)$ derived from equation given in Figure 4.13. A significant improvement is observed. When applying the linearity equation $H_t = 1.333\ H_m - 0.073\ (in\ mSv)$, derived from equation given in Figure 4.14, we obtain Figure 4.18. We can see a better distribution of the points about the line $R = 1$. A recording level (minimal reporting dose) of ***0.08 mSv*** is suggested. Figure 4.19 is the same as Figure 4.18 but with a recording level of *0.08 mSv*. This means that all the dose values below *0.08 mSv* are considered to be zero and are not reported. Table 4.10 does a comparison between the *LLDs* determined statistically and experimentally, and

other relevant quantities. It is observed, in particular, that the value of the experimental *LLD* is about equal to the IAEA monthly recording level.

Table 4.10: Comparison between the computed and measured *LLDs* and other relevant quantities.

LLD calculated (statistically)	*LLD* (experimental)	Recording level (one month, IAEA)	Zero dose (calculated)	Lower limit of the measuring range
0.00975 mSv	*0.08 mSv*	*0.083 mSv*	*0.026 mSv*	*0.1 mSv*

LLD for the OSL system

As done for the TL system, the linearity and the trumpet curves were used for the determination of the experimental *LLD* of the OSL system. Here correction for the zero dose is not required because of the use of control dosimeters for the subtraction of background and transport dose. Let us suppose that a field dosimeter has recorded a dose of *(x + y) mSv*, *x* being the real dose measured and *y* the zero dose value, and that the control dosimeter has recorded a dose of *(z + y) mSv*, where *y* is as previously and *z* is the real natural background dose measured. Therefore, the net dose recorded by the dosimeter will be

$$(x + y)mSv - (z + y)mSv = (x - z)\ mSv$$

We can see that the zero dose values cancel.

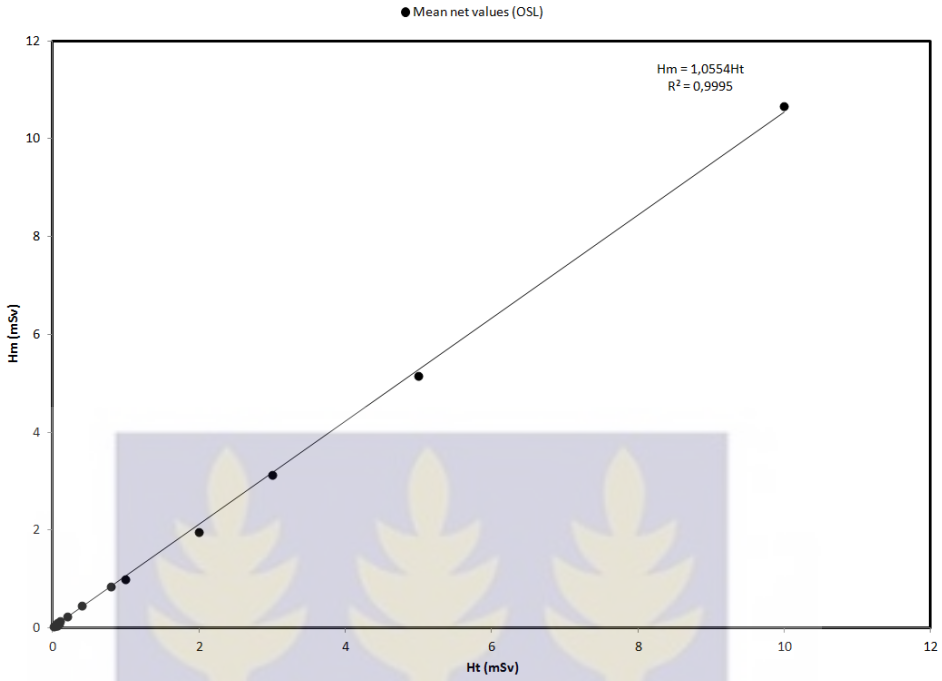

Figure 4.20: Curve of the measured net dose against the delivered dose. The linearity is established from the true dose *0.01 mSv*.

From Figure 4.20, the linearity equation $H_m = 1.0554H_t$ suggests a *LLD* of *0 mSv*. Figure 4.21 shows acceptable results but a general overestimation of the results is observed. Correction of the results using the equation $H_t = 0.95H_m$, derived from the previous linearity equation, led to Figure 4.22 which shows better results. Figure 4.23 is identical to Figure 4.22 but with a recording level of *0.05 mSv*. From Figures 4.21 and 4.22 we can see that only the response corresponding to the true dose $H_t = 0.01\ mSv$ is outside the limits. Since the measurements corresponding to true doses *0.02 mSv* and *0.03 mSv* were not good, we can take the value of *0.04 mSv* as the *LLD*. This value is in accordance with the value given in the manufacturer's reader certificate. We can also adopt the manufacturer's minimal reporting dose of *0.05 mSv* [23]. Table 4.11 compares the *LLDs* determined statistically and experimentally, and other relevant quantities. It is observed, in particular, that the value of the

experimental *LLD* is very close to the *LLD* given in the reader certificate and lower than the IAEA monthly recording level.

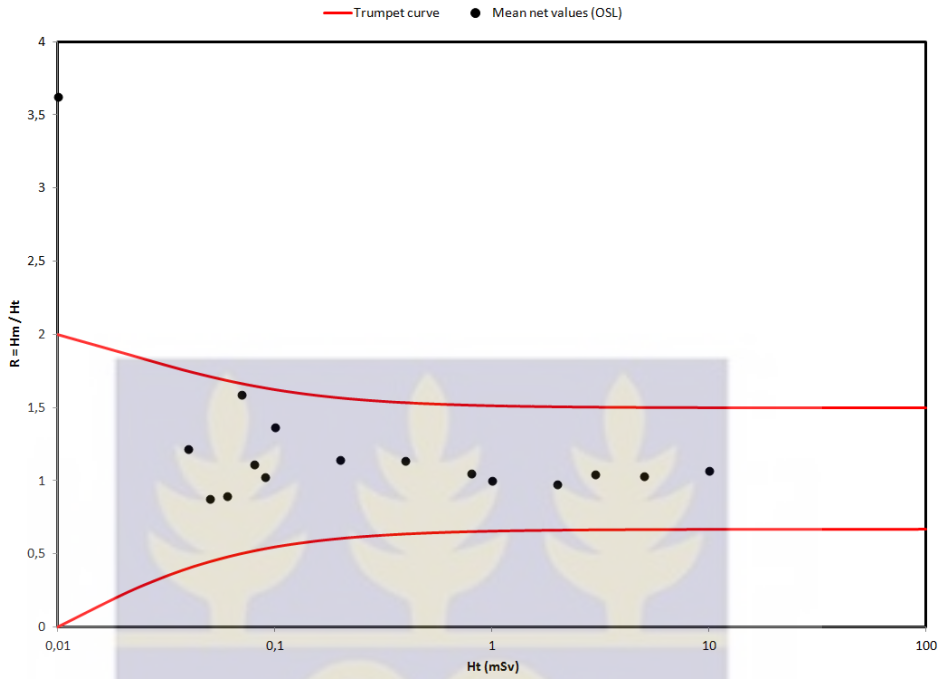

Figure 4.21: Verification of the choice of the *LLD* by the use of the trumpet curve. Here is represented the mean measured net dose as a function of the conventional true dose.

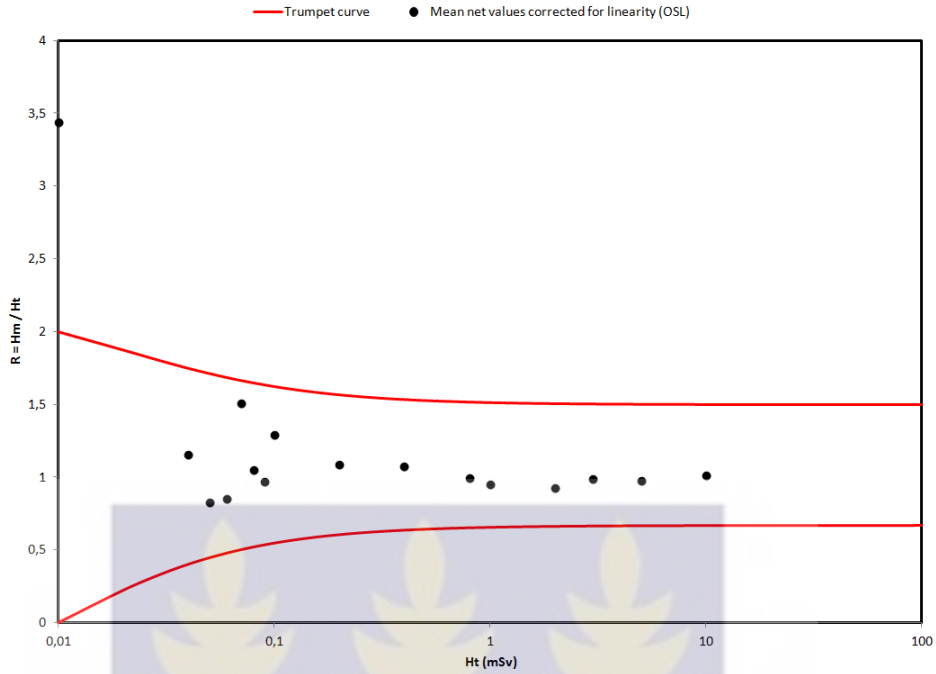

Figure 4.22: Verification of the choice of the *LLD* by the use of the trumpet curve. Here is represented the mean measured net dose corrected for linearity as a function of the conventional true dose.

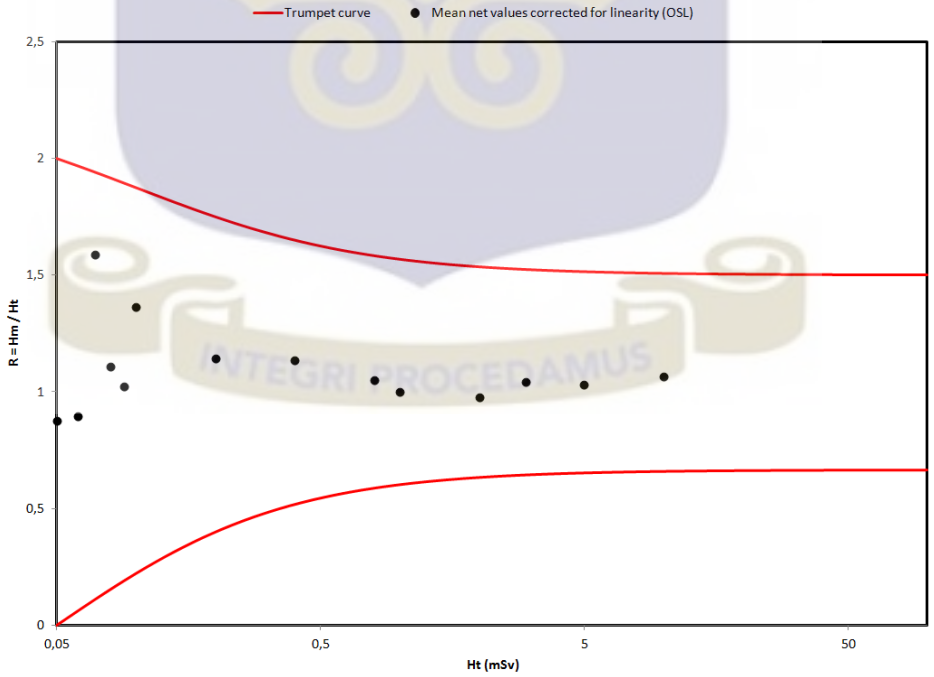

Figure 4.23: Verification of the choice of the *LLD* by the use of trumpet curve.

Here is represented the mean measured net dose corrected for linearity as a function of the conventional true dose for a *LLD* of *0.05 mSv*.

Table 4.11: Comparison between the *LLDs* determined experimentally and statistically and other relevant quantities.

LLD calculated (statistically)	*LLD* (experimental)	*LLD* (reader certificate)	Minimal reporting dose (manufacturer)	Recording level (one month, IAEA)	Lower limit of the measuring range
0.020 mSv	*0.04 mSv*	*0.042 mSv*	*0.05 mSv*	*0.083 mSv*	*0.01 mSv*

Quarterly LLD

Two monitoring periods are generally chosen in routine : monthly and quarterly monitoring periods. The *LLDs* that have been determined in the present work can be considered as monthly *LLDs*. For the Harshaw 6600 system whose *LLD* has been determined to be *0.08 mSv*, just like the IAEA monthly recording level, the IAEA quarterly recording level can be adopted. For the microStar system, Eq. 2.2 can be used to calculate the quarterly *LLDs*. In order to have the same maximum annual missed dose, *L* in Eq. 2.2 is calculated to be *0.6 mSv* (instead of *1 mSv* as in [1, 6]). We found the quarterly *LLDs* to be *0.15 mSv*. Table 4.12 shows monthly and quarterly *LLDs* as determined in the present work and the corresponding maximum annual missed doses.

Table 4.12: *LLDs* and corresponding maximum annual missed doses.

Monthly *LLD* (TL)	Monthly *LLD* (OSL)	IAEA monthly recording level	Quarterly *LLD* (TL)	Quarterly *LLD* (OSL)	IAEA quarterly recording level
0.08 mSv	*0.05 mSv*	*0.083 mSv*	*0.25 mSv*	*0.15 mSv*	*0.25*
			Corresponding maximum missed doses		
0.96 mSv	*0.6 mSv*	*0.996 mSv*	*1 mSv*	*0.6 mSv*	*1 mSv*

We end this section by presenting the mean measured dose values corrected in order to appreciate the improvement that has been realized to allow both the dosimetry systems to better measure the operational quantity *Hp (10)*. Table 4.13 compares the measured doses of the two systems corrected for linearity.

Table 4.13: Comparison of the doses measured by the two systems after correction for linearity.

Delivered dose *(mSv)*	Measured dose *(mSv)* (Harshaw 6600)	Measured dose *(mSv)* (microStar)
0.05	---	0.04145352
0.06	---	0.05092859
0.07	---	0.1054102
0.08	0.07125839	0.08409146
0.09	0.1015823	0.08724989
0.1	0.1922767	0.12909799
0.2	0.19046008	0.21674223
0.4	0.3698456	0.42993168
0.8	0.75274936	0.79472159
1	1.06577153	0.94869201
2	2.02184763	1.84882357
3	3.02589586	2.96135565
5	5.17073557	4.88794523
10	9.97858204	10.1016106

Table 4.13 shows a clear improvement for both of the systems. Finally, we can conclude that after correction for linearity of the measured doses, the two dosimetry systems gave better and comparable results starting from the recording levels (*0.08 mSv* and *0.05 mSv* for the Harshaw 6600 and microStar systems, respectively), and they show a very good capability of measuring the operational quantity *Hp (10)*.

4.3 LINEARITY AND COEFFICIENT OF VARIATION

As already said linearity and coefficient of variation performance tests were performed according to the performance standard IEC 62387. For linearity , comparisons were done with other performance standards (from Figure 4.25 to Figure 4.27).

4.3.1 Harshaw 6600 system

The IEC 62387 linearity limits, dependent on the reference response $\bar{R}_{ref} = 1.0086$, were calculated to be ***0.088*** (lower limit) and ***1.16*** (upper limit).

Figure 4.24 shows that the results are globally in accordance with the IEC 62387 linearity requirement**.**

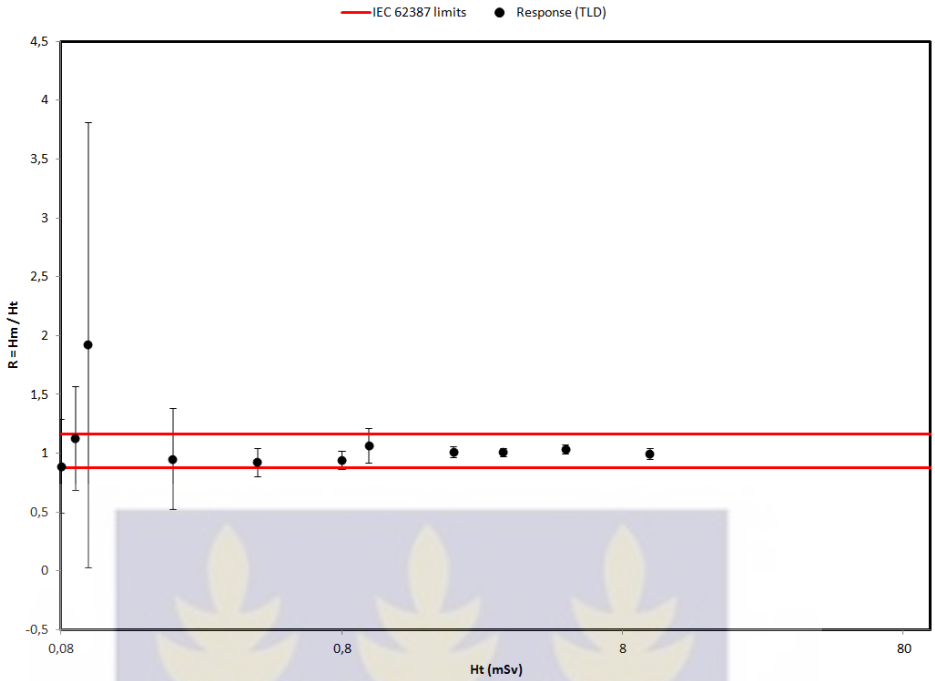

Figure 4.24: Linearity results obtained for the TL system using IEC 62387 performance standard.

We can see that the linearity results are globally in accordance with the performance standards tested. However the results, in particular the statistical uncertainties of the points close to the recording level, can be significantly improved by increasing the number of dosimeters to be irradiated simultaneously to deliver a certain dose.

Concerning the coefficient of variation test, results were not good enough (Figure 4.28). Again, a solution to the problem could be to increase the number of dosimeters for each dose delivered.

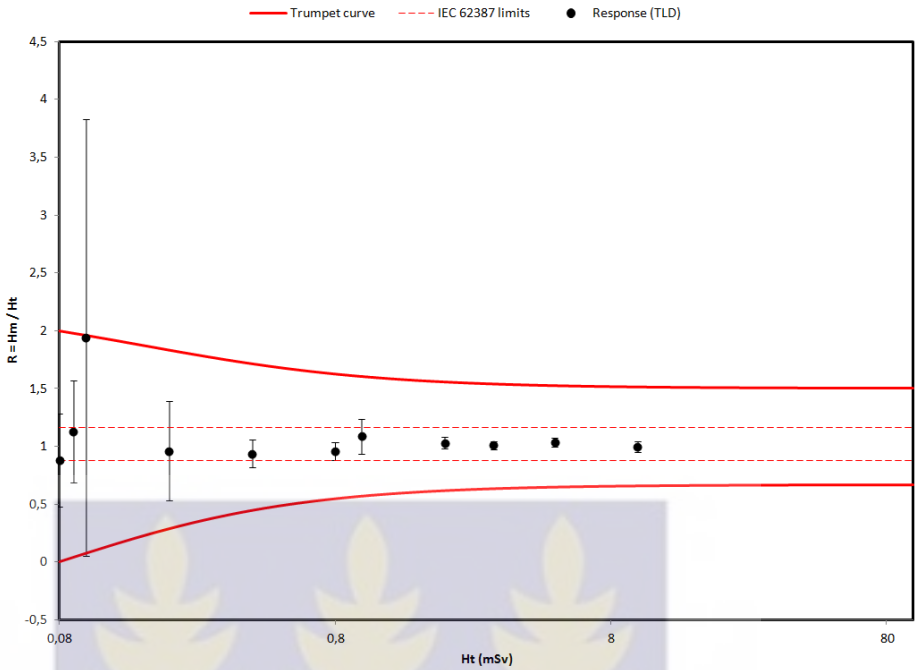

Figure 4.25: Linearity results obtained for the TL system. Comparison between the performance standards IEC 62387 and IAEA 99.

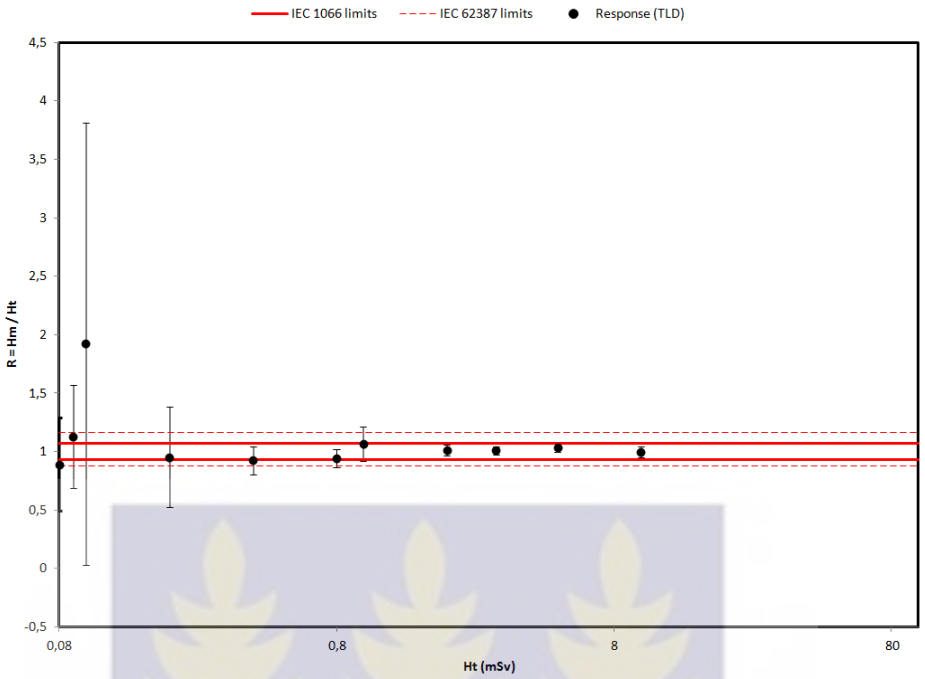

Figure 4.26: Linearity results obtained for the TL system. Comparison between the performance standards IEC 62387 and IEC 1066.

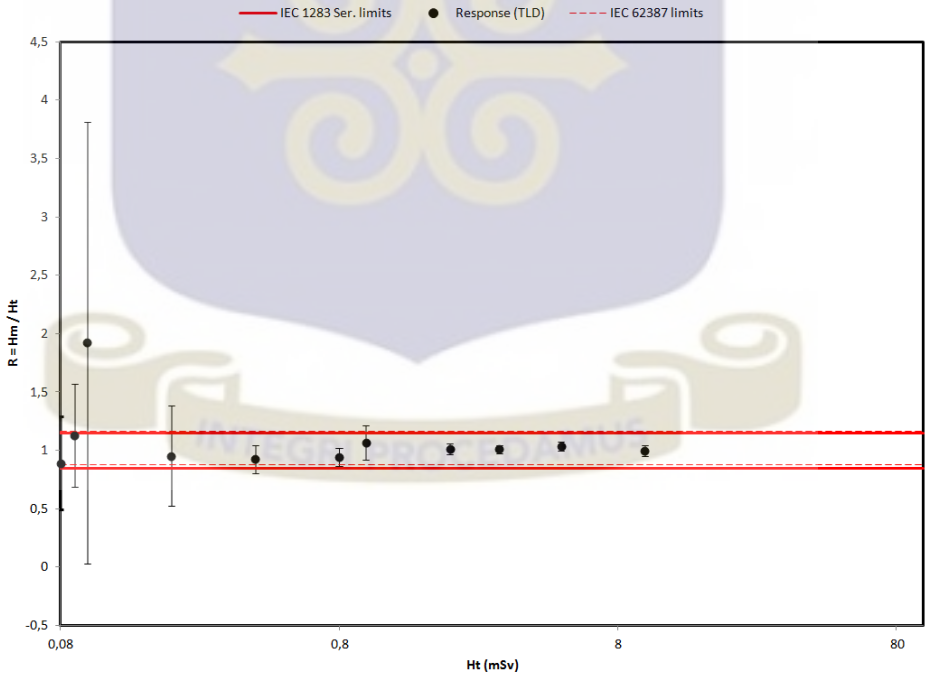

Figure 4.27: Linearity results obtained for the TL system. Comparison between the performance standards IEC 62387 and IEC 1283 Ser.

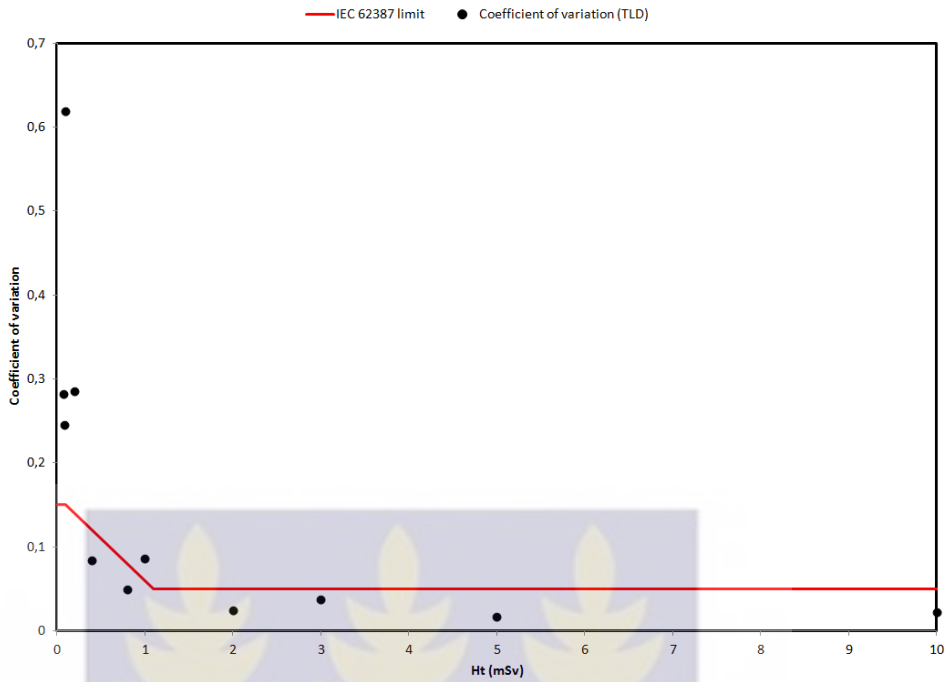

Figure 4.28: Coefficient of variation results obtained for the TL system.

4.3.2 MicroStar system

The linearity and coefficient of variation results obtained for the microStar system according to the performance standard IEC 62387 are presented below. Concerning linearity, comparisons with other performance standards are also presented (from Figure 4.30 to Figure 4.32). The IEC 62387 linearity limits, dependent on the reference response $\bar{R}_{ref} = 0.9871$, were calculated to be ***0.086*** (lower limit) and ***1.14*** (upper limit).

We can observe that, concerning the microStar, the linearity results are also globally in good accordance with the performance standards used. But the results, especially the statistical uncertainties of the points about the recording level, can be significantly improved by increasing the number of dosimeters per dose delivered.

Regarding the coefficient of variation test, results were not good at all for the OSL system (Figure 4.33). Here also, a solution to the problem could be to increase the number of dosimeters for each dose delivered

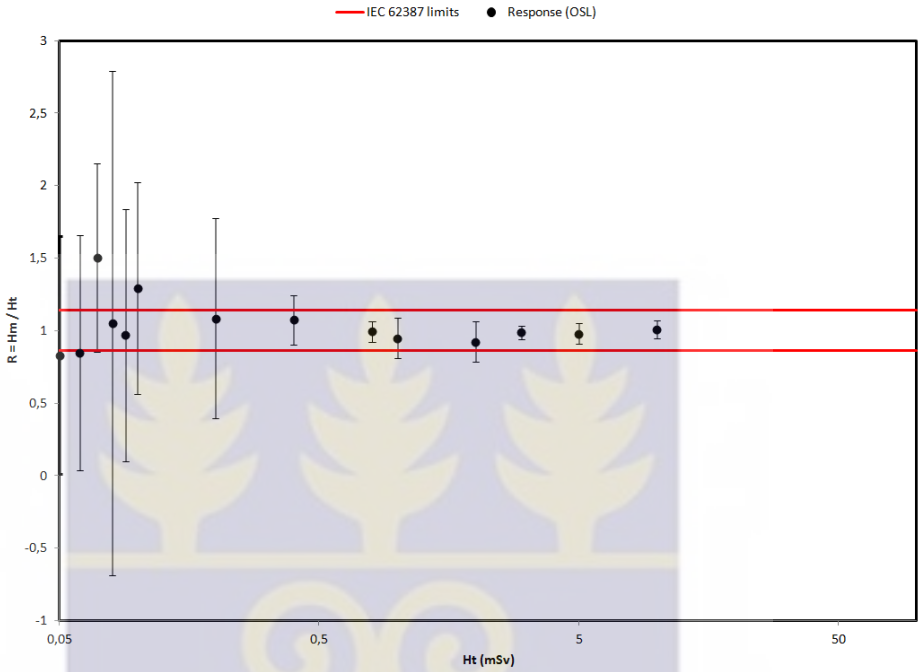

Figure 4.29: Linearity results obtained for the OSL system using IEC 62387 performance standard.

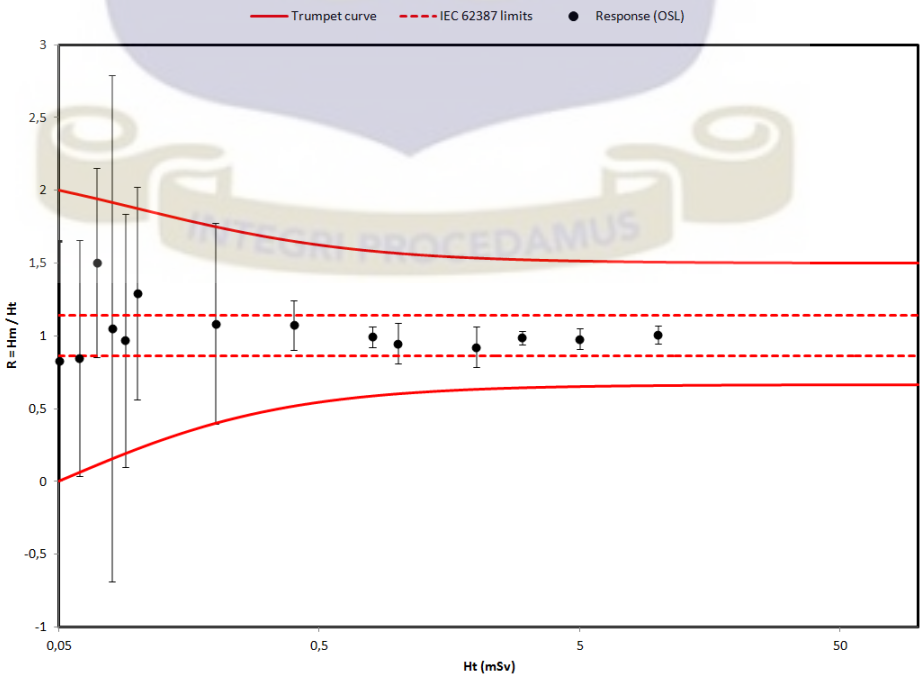

Figure 4.30: Linearity results obtained for the OSL system. Comparison between the performance standards IEC 62387 and IAEA 99.

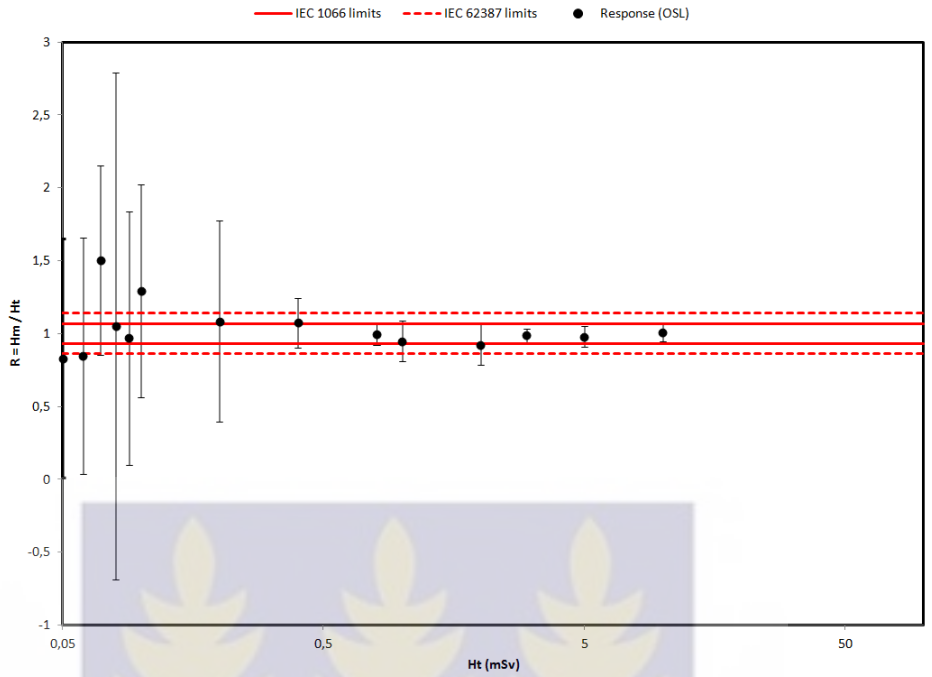

Figure 4.31: Linearity results obtained for the OSL system. Comparison between the performance standards IEC 62387 and IEC 1066.

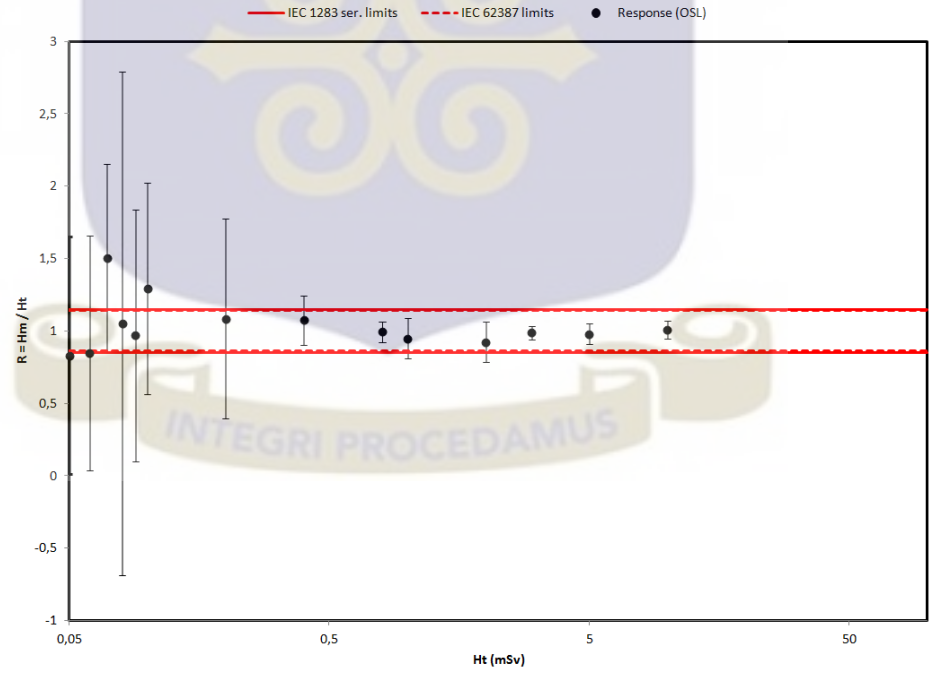

Figure 4.32: Linearity results obtained for the OSL system. Comparison between the performance standards IEC 62387 and IEC 1283 Ser.

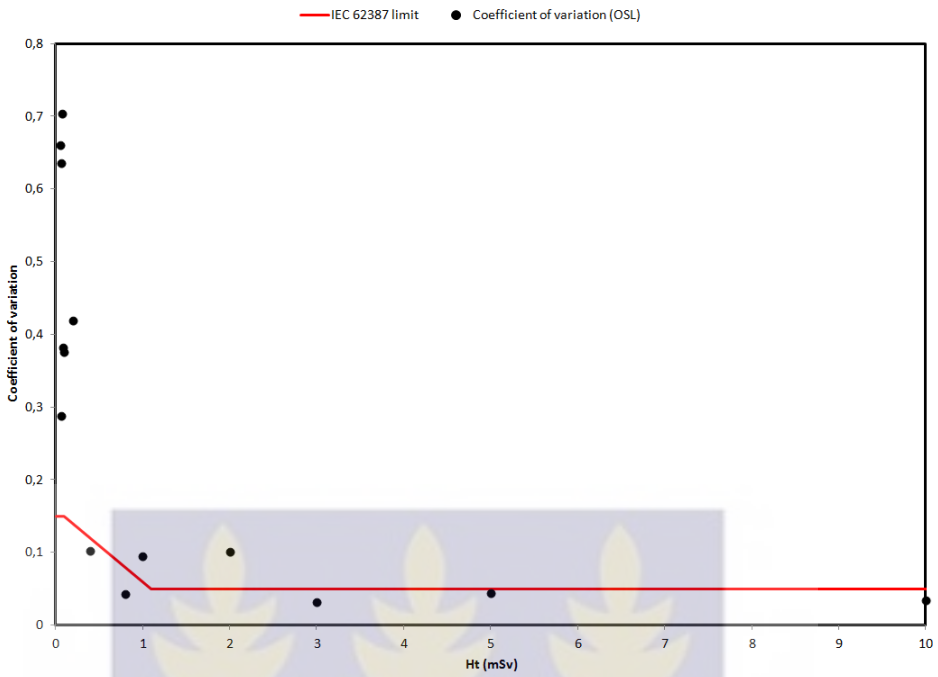

Figure 4.33: Coefficient of variation results obtained for the OSL system.

4.4 UNCERTAINTY ANALYSIS

The procedure given in the IEC technical report TR 62461 has been followed. Presented here are the uncertainty budget obtained for the reference measured doses (Table 4.14). The results for the other measured doses are presented in the annexes. The model function used is that given by Eq. 3.3. The relevance of the work was to express the uncertainties in terms of response and then to compare the result with relevant international performance standards, which are also expressed in terms of response (from Figure 4.34 to Figure 4.37).

4.4.1 Harshaw 6600 system

The results obtained for the TL system used by the dosimetry service of Ghana are presented below.

Table 4.14: Uncertainty budget of the TL reference measured dose.

Quantity	Best estimate	Absolute standard uncertainty	Uncertainty type	Number of observations	Confidence level	Distribution	Sensitivity coefficient	Uncertainty contribution to output quantity
N_0	*1.00*	$0.05/\sqrt{6} = 0.0204$	B	---	*100 %*	Triangular	1.025 x 1.02 x 3.026 *mSv*	0.0204 x 1.025 x 1.02 x 3.026 *mSv*
K_n	*1.025*	$0.125/3 = 0.0417$	B	78	*99.7 %*	Gaussian	1.02 x 3.026 *mSv*	0.0417 x 1.02 x 3.026 *mSv*
K_s	*1.02*	$0.24/3 = 0.08$	B	107	*99.7 %*	Gaussian	1.025 x 3.026 *mSv*	0.08 x 1.025 x 3.026 *mSv*
$K_{E,\varphi}$	*1.00*	$0.40/3 = 0.133$	B	---	*99.7 %*	Gaussian	1.025 x 1.02 x 3.026 *mSv*	0.133 x 1.025 x 1.02 x 3.026 *mSv*
K_{env}	*1.00*	$0.20/\sqrt{6} = 0.0816$	B	---	*100 %*	Triangular	1.025 x 1.02 x 3.026 *mSv*	0.0816 x 1.025 x 1.02 x 3.026 *mSv*
H_m	2.324 *mSv*	0,0361 *mSv*	A	10	*68.27 %*	Gaussian	*1*	1 x 0,0361 *mSv*
$H_p(10)$	3,16 *mSv*	0,57 *mSv (18,11 %)*	Combined	---	*68.27 %*	Gaussian	---	---
Complete result of the measurement						$3.16\ mSv \pm 1.12\ mSv$	$(k_{cov} = 1.96)$	

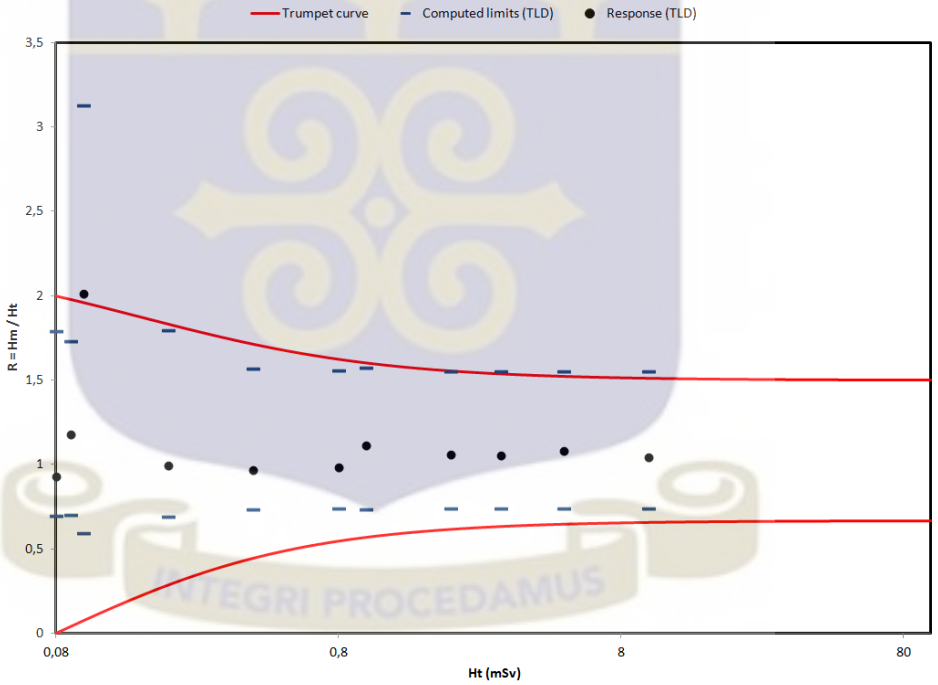

Figure 4.34: Harshaw 6600 system results for uncertainty analysis. Comparison with the performance standard IAEA 99.

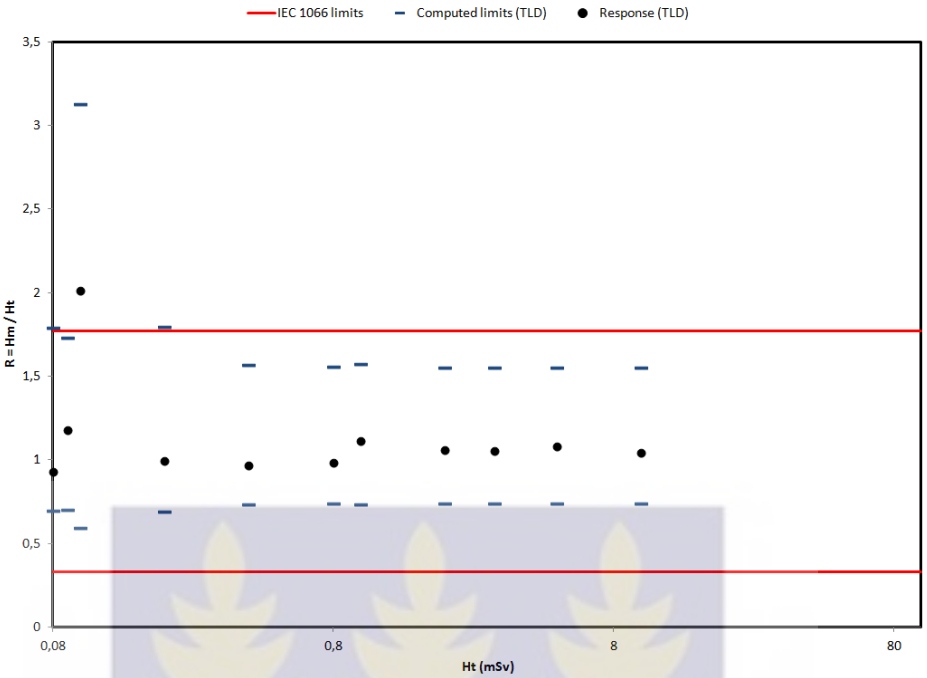

Figure 4.35: Harshaw 6600 system results for uncertainty analysis. Comparison with the performance standard IEC 1066.

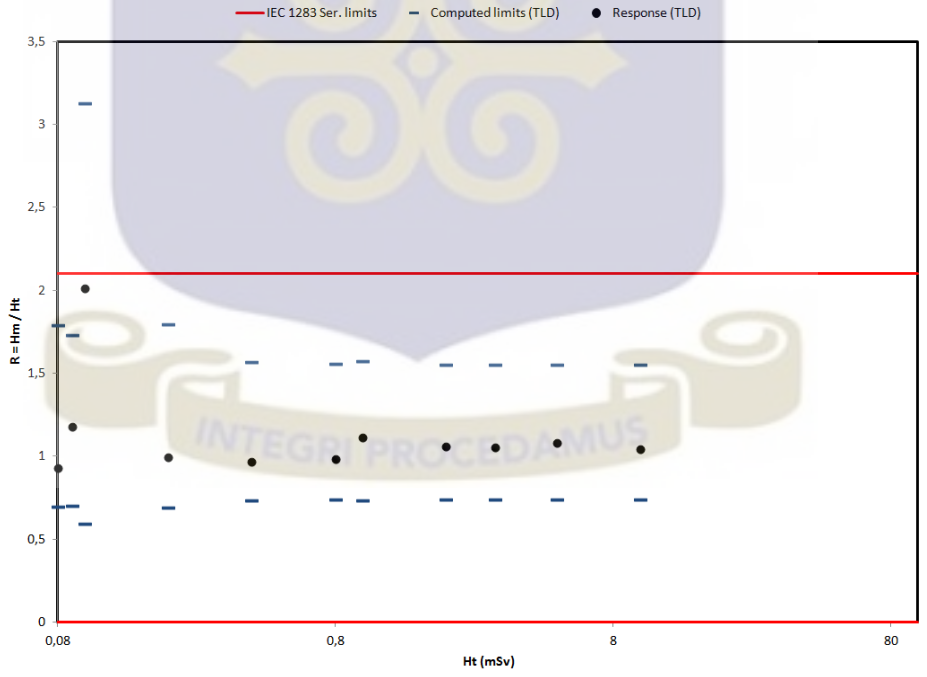

Figure 4.36: Harshaw 6600 system results for uncertainty analysis. Comparison with the performance standard IEC 1283 Ser.

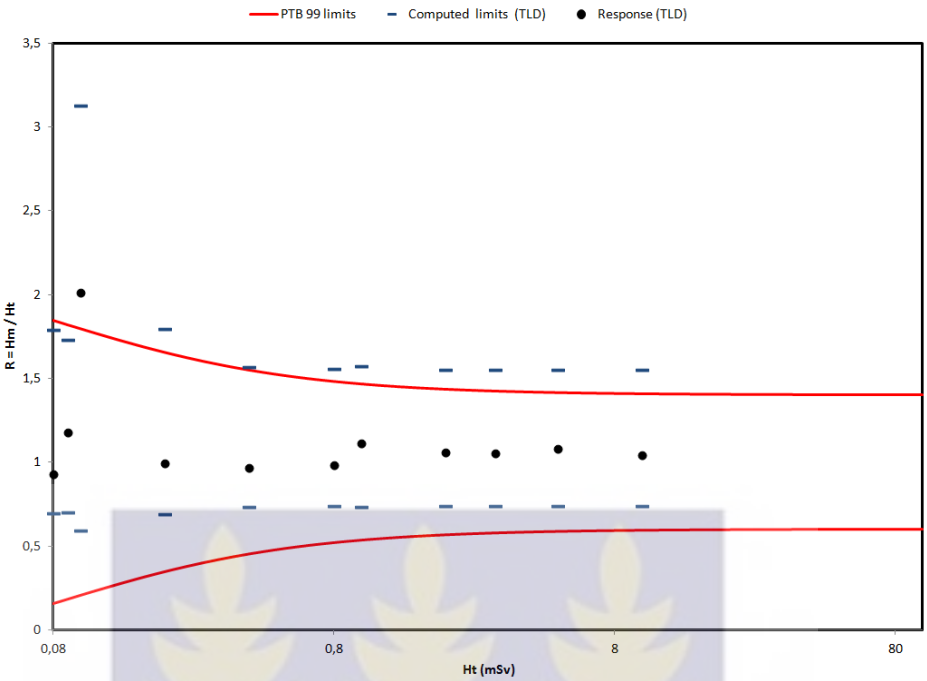

Figure 4.37: Harshaw 6600 system results for uncertainty analysis. Comparison with the performance standard PTB 99.

We can see that the results for uncertainty assessment according to the IEC technical report TR 62461 are globally in good accordance with the requirements of the performance standards that have been used for comparison. It is believed that the results can be improved by increasing the number of dosimeters to be irradiated for each dose level delivered.

4.4.2 MicroStar system

The results obtained for the OSL system of the dosimetry service of Gabon are presented below (Table 4.15 and from Figure 4.38 to Figure 4.41). The use of Eq. 3.3 is not suitable for true doses lower *0.07 mSv* and underestimates significantly the results of measured doses. To overcome the latter difficulty the multiplicative factor of *1.08* has been used in Eq. 3.3. This factor was obtained with the help of the

software Matlab, taking into account the fact that the results should be multiplied by a coefficient whose value is greater that one to avoid the underestimation.

Table 4.15: Uncertainty budget of the OSL reference measured dose.

Quantity	Best estimate	Absolute standard uncertainty	Uncertainty type	Number of observations	Confidence level	Distribution	Sensitivity coefficient	Uncertainty contribution to output quantity
N_0	*1.00*	$0.05/\sqrt{6} = 0.0204$	B	---	*100 %*	Triangular	1.08 x 0.93 x 2.96 *mSv*	0.0204 x 1.08 x 0.93 x 2.96 *mSv*
K_n	*0.93*	$0.27/3 = 0.09$	B	78	*99.7 %*	Gaussian	1.08 x 2.96 *mSv*	0.09 x 1.08 x 2.96 *mSv*
K_s	*1*	0	B	---	*99.7 %*	Gaussian	1.08 x 0.93 x 2.96 *mSv*	0 x 1.08 x 0.93 x 2.96 *mSv*
$K_{E,\varphi}$	*1.00*	$0.40/3 = 0.133$	B	---	*99.7 %*	Gaussian	1.08 x 0.93 x 2.96 *mSv*	0.133 x 1.08 x 0.93 x 2.96 *mSv*
K_{env}	*1.00*	$0.20/\sqrt{6} = 0.0816$	B	---	*100 %*	Triangular	1.08 x 0.93 x 2.96 *mSv*	0.0816 x 1.08 x 0.93 x 2.96 *mSv*
H_m	*3,13 mSv*	*0,03819 mSv*	A	4	*68.27 %*	Gaussian	*1*	1 x 0,03819 *mSv*
$H_p(10)$	*2,97 mSv*	*0,55 mSv (18,55 %)*	Combined	---	*68.27 %*	Gaussian	---	---
Complete result of the measurement						$2.97\ mSv \pm 1.081\ mSv$	$(k_{cov} = 1.96)$	

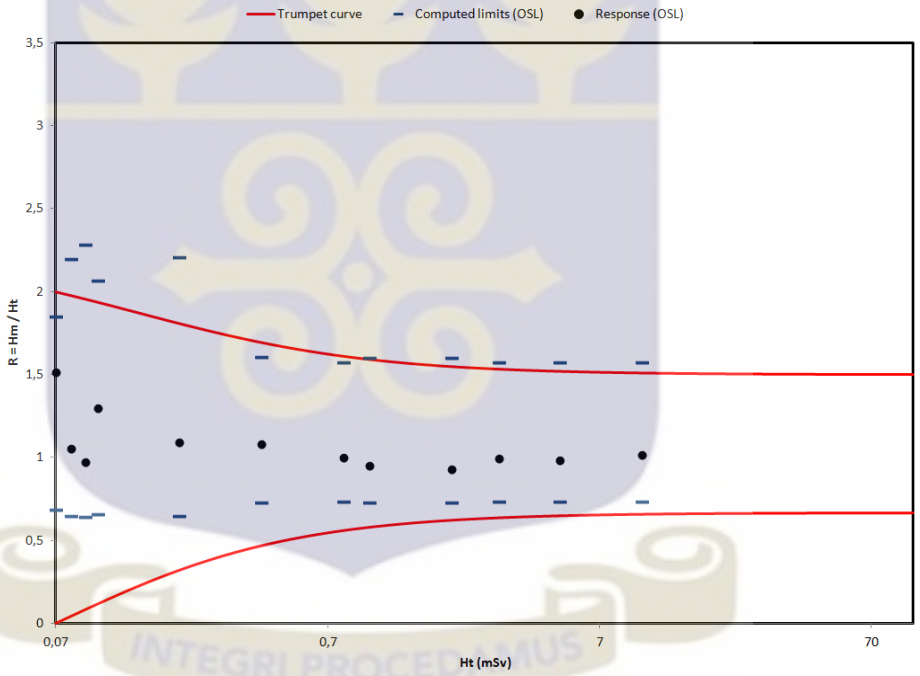

Figure 4.38: MicroStar system results for uncertainty analysis. Comparison with the performance standard IAEA 99.

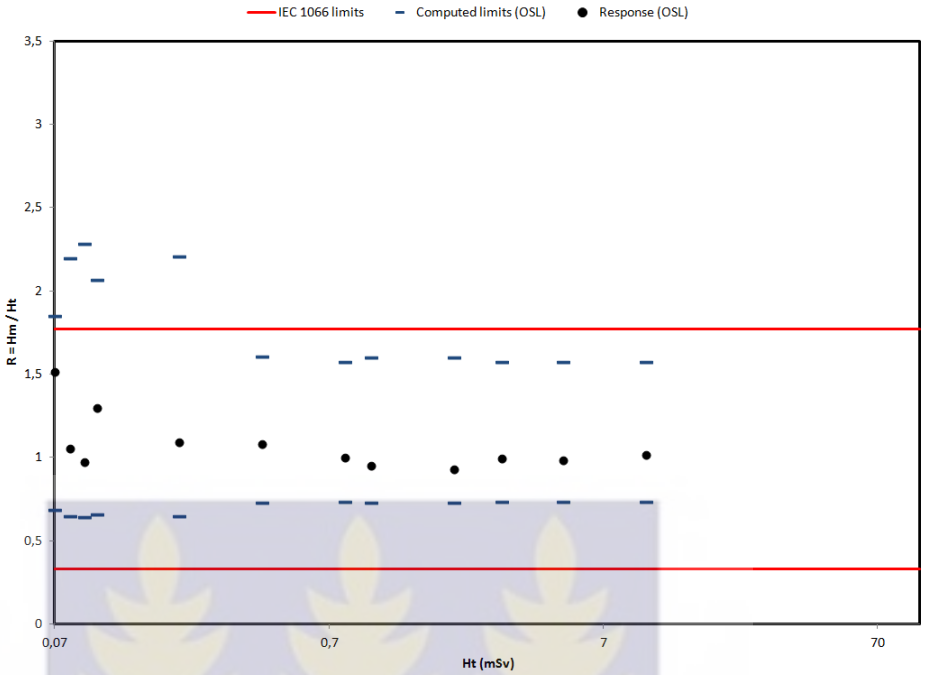

Figure 4.39: MicroStar system results for uncertainty analysis. Comparison with the performance standard IEC 1066.

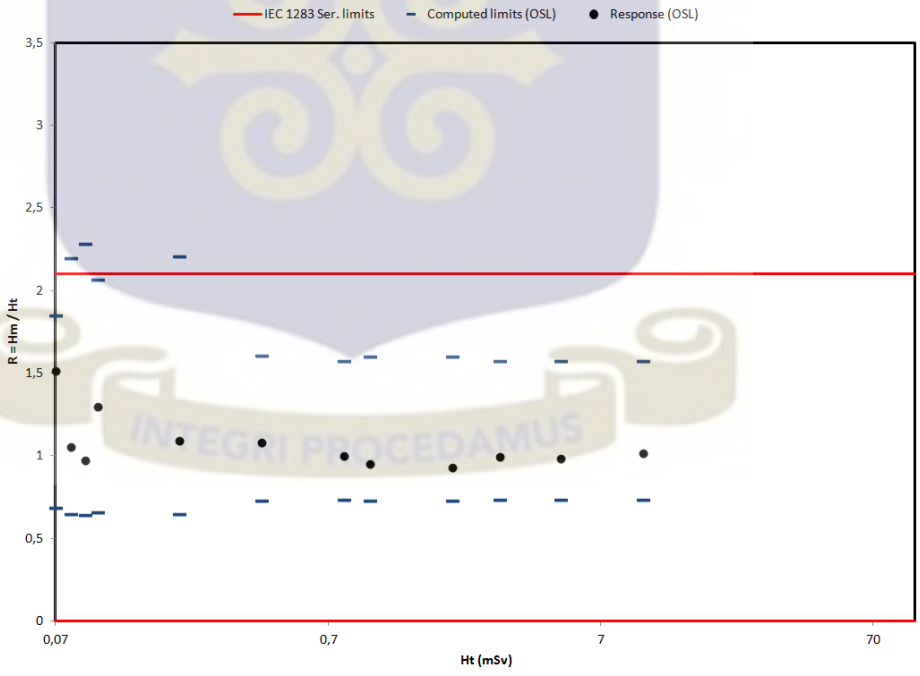

Figure 4.40: MicroStar system results for uncertainty analysis. Comparison with the performance standard IEC 1283 Ser.

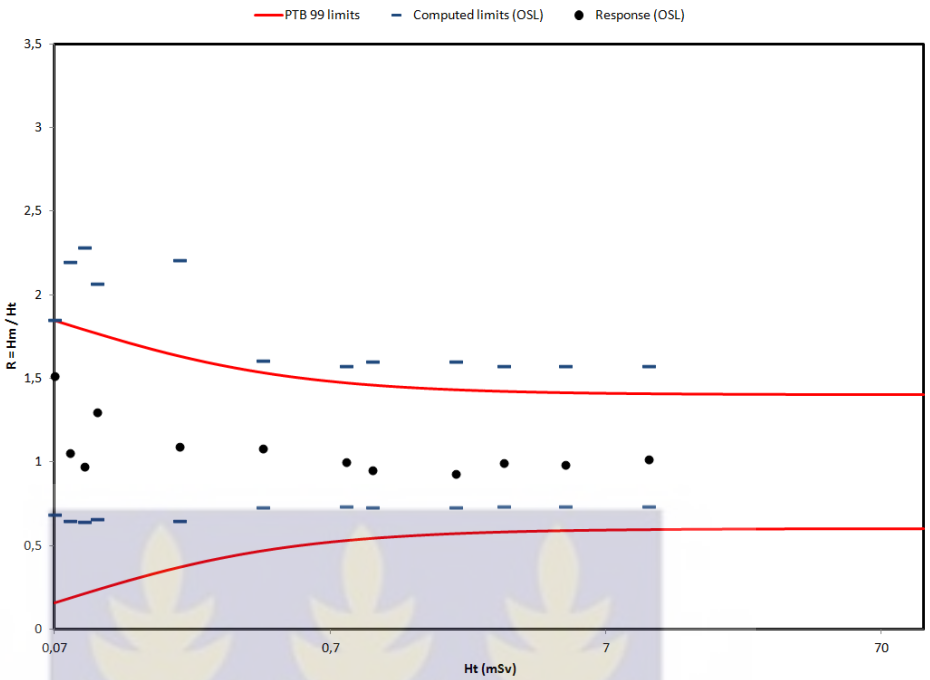

Figure 4.41: MicroStar system results for uncertainty analysis. Comparison with the performance standard PTB 99.

Although some abnormal points are observed for the computed upper limit in the region of the recording level, and even though the computed upper limit is slightly greater than the upper limit of the standard PTB 99, it can be seen that the results for uncertainty analysis according to the IEC technical report TR 62461 are globally in good accordance with the requirements of the other performance standards that have been used for comparison. As for the TL system, it is believed that the results can be improved by increasing the number of dosimeters for each dose delivered.

CHAPTER FIVE

CONCLUSIONS AND RECOMMENDATIONS

This chapter ends the work that has been undertaken. It provides the main conclusions that have been derived for all the performance tests carried out for both the dosimetry systems in Ghana and Gabon. Recommendations that should be followed by the two dosimetry services are also given.

5.1 CONCLUSION

Reader performance test

For the Harshaw 6600 TLD system of the dosimetry service of Ghana, only the Reference light QC test met the requirement given in the user manual. The PMT noise test did not meet the standard possibly due to the difference in the methodology in use in practice and that given in the user manual. It has been shown that both Reference light and the PMT noise measurements failed the Chi - square test. But since the PMT noise measurement failed this test by a very small margin, a Gaussian distribution can still be considered as an approximation of the experimental distribution of this measurement.

For the microStar OSL system of the dosimetry service of Gabon, the three QC tests, DRK count, CAL count and LED count, meet the user manual requirements. However all these tests failed the statistical test that is part of counting statistics. This led to the conclusion that there may be some abnormalities in the counting system, and that the statistical abnormalities suspected have apparently no impact on the

reading results. It was also concluded that since the DRK count and the CAL count failed the Chi - square test by very small margin , a Gaussian distribution could still be considered as an approximation of the experimental data distributions of these two QC measurements.

Zero dose and limit of detectability

The zero dose for the Harshaw TLD 6600 and the microStar systems were found to be ***0.026 mSv*** and ***0.08 mSv***. respectively . The TLD Reader retains lower doses at about three times lower than the microStar system after readout.

A statistical method and an experimental method were used for the lower limit of detection tests . For TLD system, the application of the statistical method led to a *LLD* value of ***0.00975 mSv*** in accordance with the user manual requirement. A value of ***0.020 mSv*** was estimated for the microStar system. By applying the experimental method the values ***0.055 mSv*** and ***0 mSv*** were estimated for the TLD and OSL systems respectively. Applying the accepted IAEA acceptance limits, the trumpet curve, the estimated recording levels are ***0.08 mSv*** and ***0.05 mSv*** for the TLD and OSL systems respectively. In particular, The value ***0.05 mSv*** is in accordance with the minimal reporting dose stated by the microStar system's manufacturer.

Quarterly recording levels, ***0.25 mSv*** and ***0.15 mSv,*** are proposed for the Harshaw 6600 system and the microStar system, respectively. These quarterly minimum reporting doses have been calculated so that the maximum annual missed dose remains the same whether or not a monthly or quarterly monitoring period is chosen.

Linearity and coefficient of variation

A linearity test has been performed, for both the OSL and TL systems, according to the international performance standards of IEC 62387 , IAEA99 ,IEC1066 and IEC 1283. The results obtained for the two systems showed that they are globally in accordance with the performance standards tested.

The coefficient of variation test was also performed according to the performance standard IEC 62387. The coefficient of variation results of the two systems did not meet the IEC 62387 requirement.

Uncertainty analysis

The uncertainty assessment was performed according to IEC technical report TR 62461. Comparisons have been performed with some relevant standards. Although some abnormal points were observed in the computed upper limit in the region of the recording level, and even though, in particular, the computed upper limit is slightly greater than the upper limit of PTB 99 standard, the results for uncertainty analysis are roughly in accordance with the requirements of all the performance standards tested.

Regarding the results for linearity test, uncertainty analysis, and for the reader QC tests, it is considered that the overall objective of the work is met. Concerning the coefficient of variation test it is believed that increasing significantly the number of dosimeters per delivered dose equivalent will reduced the standard deviation so that the results for the coefficient of variation could also meet the overall objective of the study.

5.2 RECOMMENDATIONS

5.2.1 Dosimetry service of Ghana

Since it has been shown that the Harshaw 6600 system of the RPI dosimetry service underestimates significantly and systematically the operational quantity *Hp (10)*, corrections shall be used to overcome this difficulty. In particular, the model function used for the uncertainty determination in this work should be used. Another and simple solution is to correct the measured doses for linearity using the linearity equation with zero dose subtraction as used in this study.

The model function and the linearity equation should be improved on a regular basis. particularly, the number of dosimeters for each delivered dose should be significantly increased. Doing so will generally improve the results of all the performance tests that were performed in this work.

The dosimetry service of Ghana should keep participating, when possible, in regional and interregional intercomparisons to make sure that the reliability of its measurements is maintained.

5.2.2 Dosimetry service of Gabon

Even though it was shown that the microStar system of Gabon is capable of measuring the quantity *Hp (10)* without corrections, an overestimation of this quantity was globally observed. Therefore corrections should be applied to measured doses in order to obtain more accurate estimation of *Hp(10).* A simpler way of doing this is to apply the linearity correction equation to the measured doses as applied in this work. The use of the model function for the uncertainty assessment in this work is another

option to explore. However, this is only possible for true doses equal to or greater than ***0.07 mSv***.

The model function and the linearity equation should be improved regularly. In particular, the improvement of the model function should be done so that this function could be used accurately for true doses equal to or greater than ***0.05 mSv***, the monthly recording level. Furthermore, increasing the number of dosimeters for each delivered dose will improve the model function and the linearity equation, and will generally improve the results of all the performance tests that have been performed in this work.

The dosimetry service of Gabon should continue to take part when possible, in regional and interregional intercomparisons to validate the reliability of its measurements.

REFERENCES

[1] International Atomic Energy Agency, *Assessment of Occupational Exposure Due to External Sources of Radiation*, IAEA Safety Standards Series, Safety Guide No. RS-G-1.3, Vienna, Austria, 1999.

[2] International Atomic Energy Agency, *Assessment of Occupational Exposure Due to Intakes of Radionuclides*, IAEA safety Standards Series, Safety Guide No. RS-G-1.2, Vienna, Austria, 1999.

[3] International Atomic Energy Agency, *Occupational Radiation Protection*, IAEA safety Standards Series, Safety Guide No. RS-G-1.1, Vienna, Austria, 1999.

[4] International Atomic Energy Agency, *Radiation Protection and Safety of Radiation Sources: International Basic Safety Standards*, IAEA Safety Standards, General Safety Requirements Part 3, No. GSR Part 3, Vienna, Austria, 2014.

[5] M. Arib, A. Herrati, F. Dari, J. Ma, Z. Lounis-Mokrani, *Intercomparison 2013 on Measurements of the Personal Dose Equivalent Hp (10) in Photon Fields in the African Region*, Radiation Protection Dosimetry, pp. 1-8, 2014.

[6] International Commission on Radiological Protection, *General Principles for the Radiation Protection of Workers*, Publication No.75, Pergamon Press, Oxford and New York, 1997.

[7] International Electrotechnical Commission, *Radiation Protection Instrumentation - Determination of Uncertainty in Measurement*, Technical Report TR 62461, First Edition, Geneva, Switzerland, 2006.

[8] P. Ambrosi, D.T. Bartlett, *Dosimeter Characteristics and service performance requirements*, Intercomparison for Individual Monitoring of External Exposure from Photon Radiation, Result of a Co-ordinated Research Project 1996 - 1998, IAEA - TECDOC -1126, pp 119 - 140, Vienna, Austria, December 1999.

[9] International Electrotechnical Commission, *Radiation Protection Instrumentation - Passive Integrating Dosimetry Systems for Personal and Environmental Monitoring of Photon and Beta Radiation*, International Standard IEC 62387, First Edition, Geneva, Switzerland, 2012.

[10] International Atomic Energy Agency, *Intercomparison of Measurements of Personal Dose Equivalent Hp (10) in Photon Fields in the West Asia Region*, IAEA - TECDOC - CD - 1567, Vienna, Austria, August 2007.

[11] International Atomic Energy Agency, *Intercomparison for Individual Monitoring of External Exposure from Photon Radiation*, Result of a Co-ordinated Research Project 1996 - 1998, IAEA - TECDOC -1126, Vienna, Austria, December 1999.

[12] M. Gustafsson, R.V. Griffith, *IAEA Activities in the Field of Occupational Radiation Protection*, Intercomparison for Individual Monitoring of External Exposure from Photon Radiation, Result of a Co-ordinated Research Project 1996 - 1998, IAEA - TECDOC -1126, pp 3 - 7, Vienna, Austria, December 1999.

[13] Ramat HISSEINE ISSA, *A Comparative Study Between the Performance Characteristics of Optically Stimulated Luminescent Dosimeters and Thermoluminescent Dosimeters*, MPhil thesis, pp 50 - 70, School of Nuclear and Allied Sciences, University of Ghana, July 2015.

[14] Saint-Gobain Crystals & detectors, *Model 6600 Automated TLD Reader with WinREMS*, Operator's manual, Publication No. 6600-W-O-0602-005, 2002.

[15] V.E. Aleinikov, P. Ambrosi, L. Bürmann, D.T. Bartlett, D.R. McClure, I. Csete, V.I. Fominykh, A.V. Oborin, H. Stadtmann, *Dosimeter Irradiations for the 1996 - 1998 Co-ordinated Research Project on Intercomparison for Individual Monitoring of External Exposure from Photon Radiation*, Intercomparison for Individual Monitoring of External Exposure from Photon Radiation, Result of a Co-ordinated Research Project 1996 - 1998, IAEA - TECDOC -1126, pp 13 - 26, Vienna, Austria, December 1999.

[16] International Organisation for Standardisation, *X and Gamma Reference Radiation for Calibrating Dosemeters and Doserate Meters and for Determining their Response as a Function of Photon Energy - Part 3: Calibration of Area and Personal Dosemeters and the Measurement of their Response as a Function of Energy and Angle of Incidence*, International Standard ISO 4037-3, First Edition, Geneva, Switzerland, 1999.

[17] International Atomic Energy Agency, *Calibration of Radiation Protection Monitoring Instruments*, Safety Reports Series No. 16, Vienna, Austria, 2000.

[18] European Commission, *Technical Recommendations for monitoring individuals occupationally exposed to external radiation*, Radiation Protection 73, Directorate-General for environment, Nuclear Safety, and Civil Protection,1994.

[19] Landauer Inc, microStar InLight system user manual, 2010.

[20] International Organisation for Standardisation, *X and Gamma Reference Radiation for Calibrating Dosemeters and Doserate Meters and for Determining their*

Response as a Function of Photon Energy - Part 1: Radiation Characteristics and Production Methods, International Standard ISO 4037-1, First Edition, Geneva, Switzerland, 1996.

[21] James E. Turner, *Atoms, Radiation and Radiation Protection*, third edition. Wiley (2007).

[22] Glenn F. Knoll, *Radiation Detection and Measurement*, third edition. Wiley (2000).

[23] Herman Cember, Thomas E. Johnson, *Introduction to Health Physics*, fourth edition. McGraw-Hill Medical (2009).

[24] www.landauer.com/Dosimeters.aspx (accessed on March 2016).

[25] Bicron RMP, *Model 6600 Automated TLD Reader 6600*, QC Acceptance Procedures. Publication No. 6600-0-Q-1197-001 (1997).

APPENDIX A

LINEARITY CURVES OF TL AND OSL SYSTEMS FOR RAW AND NET VALUES, RESPECTIVELY

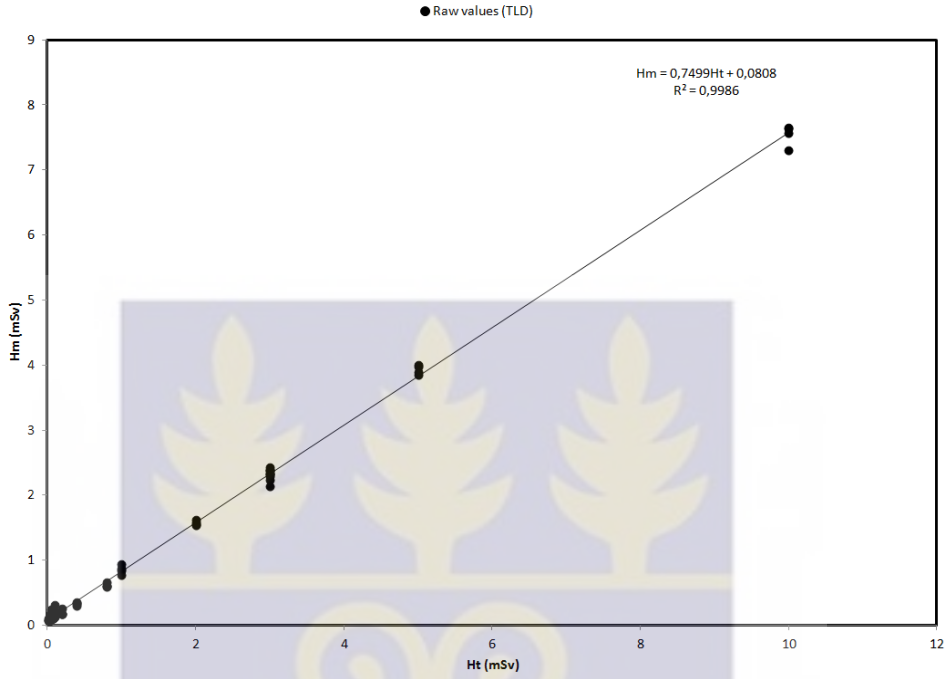

Figure A.1: Curve of the raw measured dose against the delivered dose (TLD).

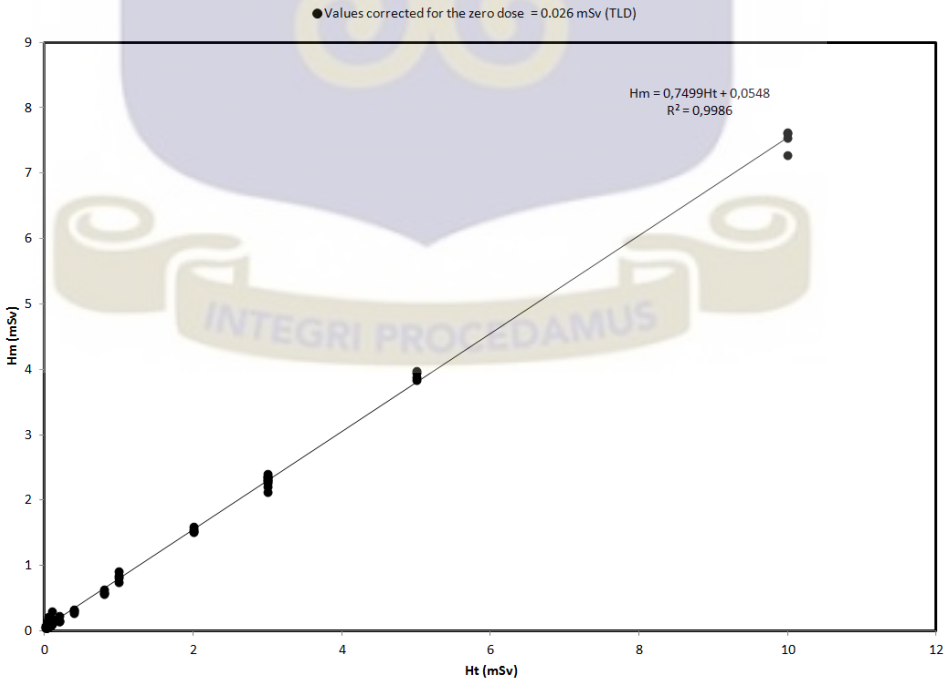

Figure A.2: Curve of the raw measured dose corrected for the zero dose against the delivered dose (TLD).

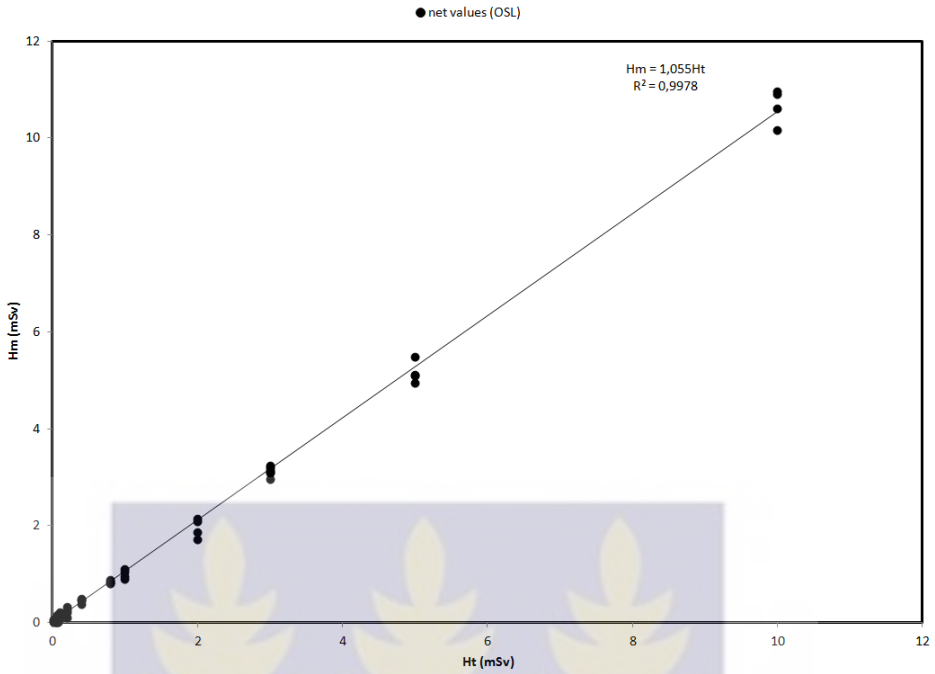

Figure A.3: Curve of net measured dose against the delivered dose (OSL).

APPENDIX B

VERIFICATION OF THE CHOICE OF LLDs

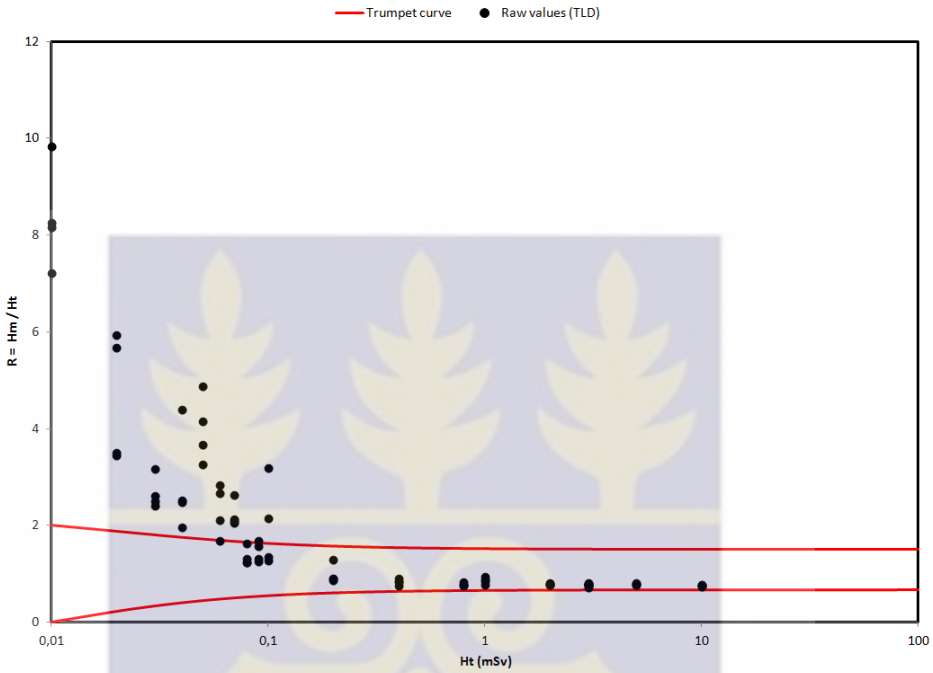

Figure B.1: Verification of the choice of the LLD by the use of the trumpet curve. Here is represented the raw measured dose as a function of the conventional true dose.

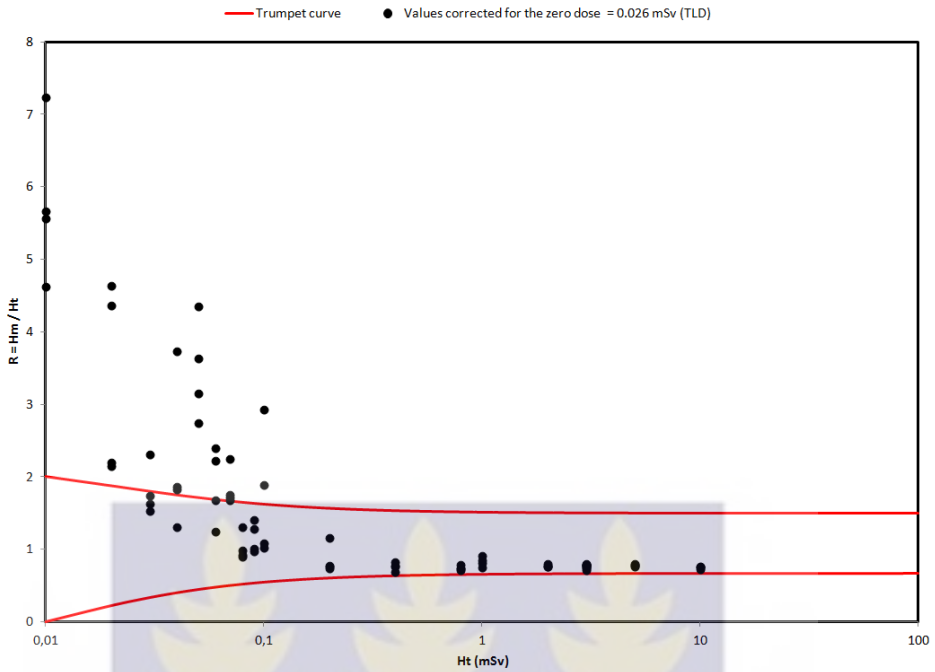

Figure B.2: Verification of the choice of the LLD by the use of the trumpet curve. Here is represented the raw measured dose corrected for the zero dose as a function of the conventional true dose.

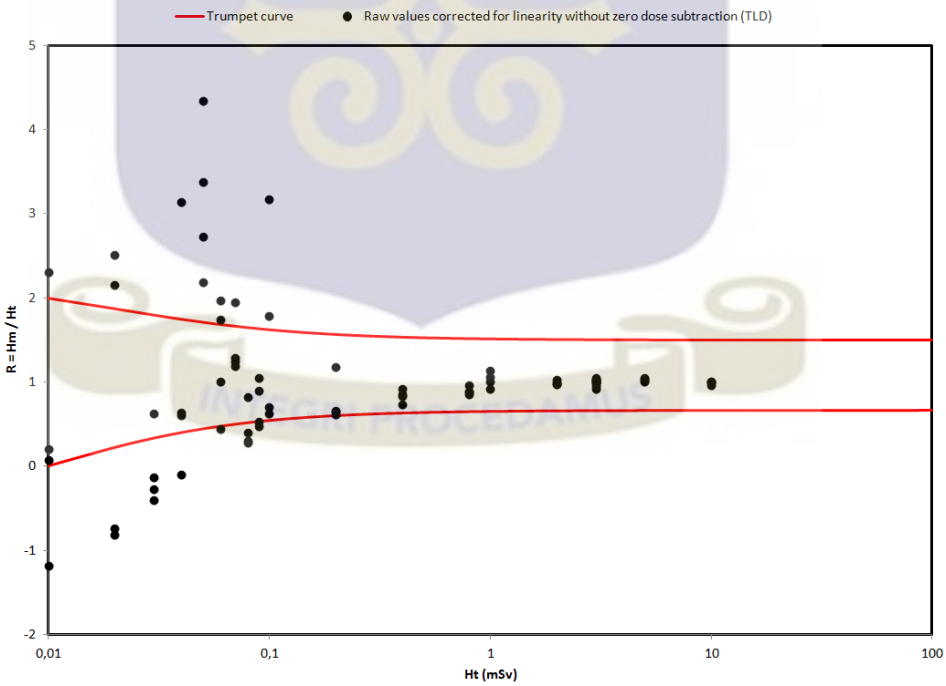

Figure B.3: Verification of the choice of the LLD by the use of the trumpet curve. Here is represented the raw measured dose corrected for linearity without zero dose subtraction as a function of the conventional true dose.

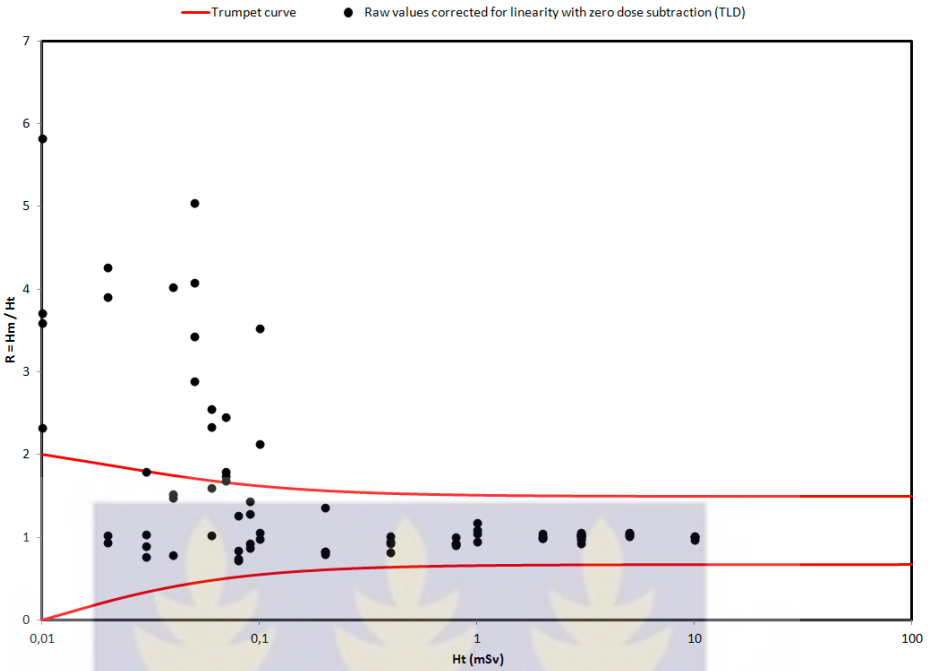

Figure B.4: Verification of the choice of the LLD by the use of the trumpet curve. Here is represented the raw measured dose corrected for linearity with zero dose subtraction as a function of the conventional true dose.

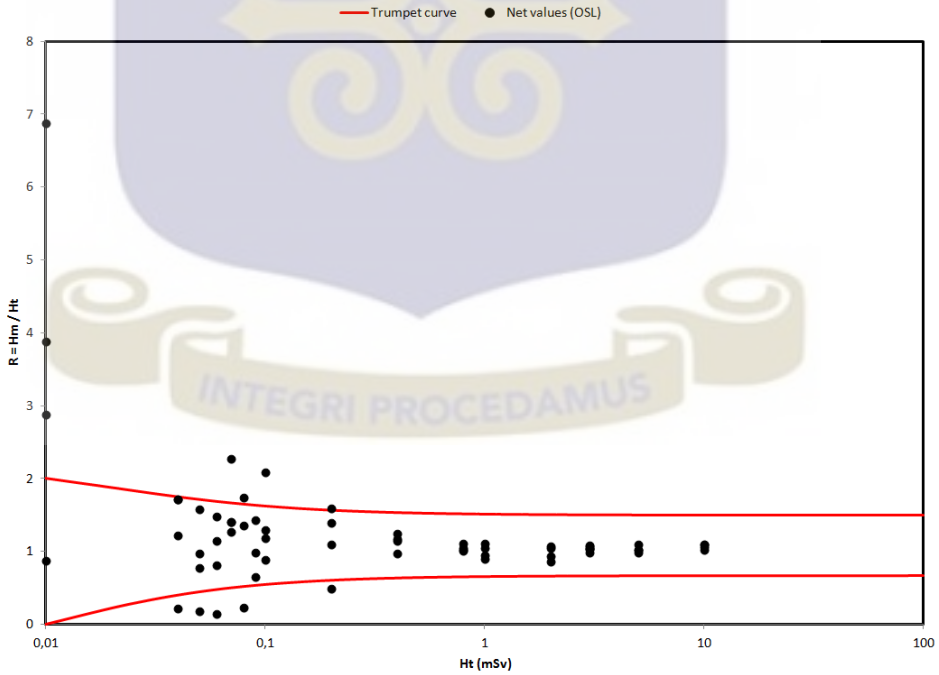

Figure B.5: Verification of the choice of the LLD by the use of the trumpet curve. Here is represented the measured net dose as a function of the conventional true dose.

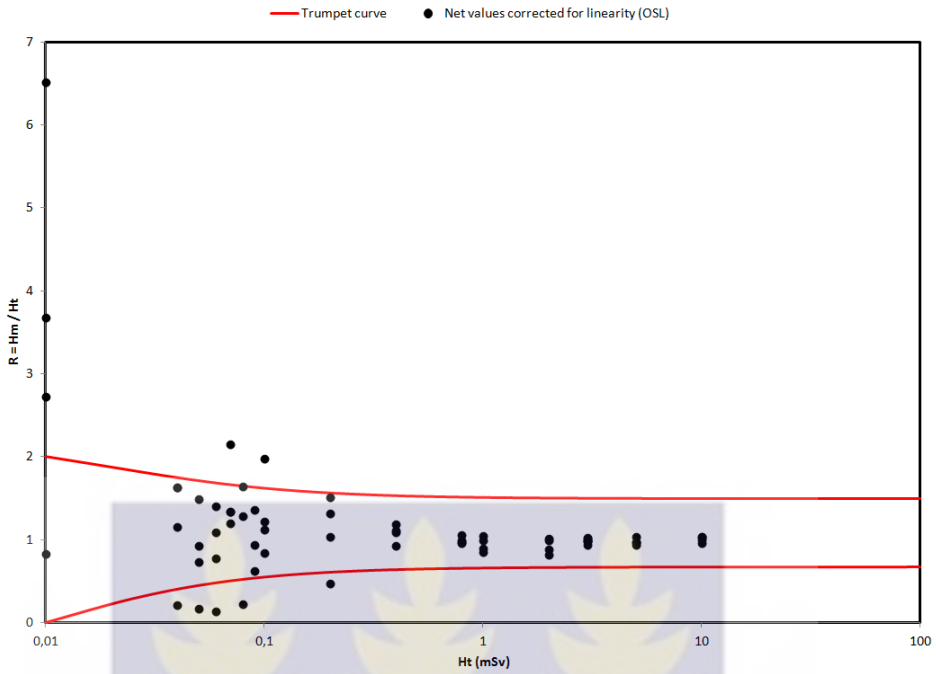

Figure B.6: Verification of the choice of the LLD by the use of the trumpet curve. Here is represented the measured net dose corrected for linearity as a function of true dose

APPENDIX C

UNCERTAINTY BUDGETS

Harshaw 6600 TL system

Table C.1: Uncertainty budget of the raw measured dose *0.108 mSv* corresponding to the true dose *0.08 mSv* (TLD).

Quantity	Best estimate	Absolute standard uncertainty	Uncertainty type	Number of observations	Confidence level	Distribution	Sensitivity coefficient	Uncertainty contribution to output quantity
$\boldsymbol{N_0}$	*1.00*	$0.05/\sqrt{6} = 0.0204$	B	---	*100 %*	Triangular	$1.025 \times 1.02 \times 0.071\ mSv$	$0.0204 \times 1.025 \times 1.02 \times 0.071\ mSv$
$\boldsymbol{K_n}$	*1.025*	$0.125/3 = 0.0417$	B	*78*	*99.7 %*	Gaussian	$1.02 \times 0.071\ mSv$	$0.0417 \times 1.02 \times 0.071\ mSv$
$\boldsymbol{K_s}$	*1.02*	$0.24/3 = 0.08$	B	*107*	*99.7 %*	Gaussian	$1.025 \times 0.071\ mSv$	$0.08 \times 1.025 \times 0.071\ mSv$
$\boldsymbol{K_{E,\varphi}}$	*1.00*	$0.40/3 = 0.133$	B	---	*99.7 %*	Gaussian	$1.025 \times 1.02 \times 0.071\ mSv$	$0.133 \times 1.025 \times 1.02 \times 0.071\ mSv$
$\boldsymbol{K_{env}}$	*1.00*	$0.20/\sqrt{6} = 0.0816$	B	---	*100 %*	Triangular	$1.025 \times 1.02 \times 0.071\ mSv$	$0.0816 \times 1.025 \times 1.02 \times 0.071\ mSv$
$\boldsymbol{H_m}$	*0.108 mSv*	*0.010 mSv*	A	4	*68.27 %*	Gaussian	*1*	$1 \times 0.010\ mSv$
$\boldsymbol{H_p(10)}$	*0.075 mSv*	*0.017 mSv* (22,55 %)	Combined	---	*68.27 %*	Gaussian	---	---
Complete result of the measurement							$0.075\ mSv \pm 0.033\ mSv \quad (k_{cov} = 1.96)$	

Table C.2: Uncertainty budget of the raw measured dose *0.13 mSv* corresponding to the true dose *0.09 mSv* (TLD).

Quantity	Best estimate	Absolute standard uncertainty	Uncertainty type	Number of observations	Confidence level	Distribution	Sensitivity coefficient	Uncertainty contribution to output quantity
$\boldsymbol{N_0}$	*1.00*	$0.05/\sqrt{6} = 0.0204$	B	---	*100 %*	Triangular	$1.025 \times 1.02 \times 0.102\ mSv$	$0.0204 \times 1.025 \times 1.02 \times 0.102\ mSv$
$\boldsymbol{K_n}$	*1.025*	$0.125/3 = 0.0417$	B	*78*	*99.7 %*	Gaussian	$1.02 \times 0.102\ mSv$	$0.0417 \times 1.02 \times 0.102\ mSv$
$\boldsymbol{K_s}$	*1.02*	$0.24/3 = 0.08$	B	*107*	*99.7 %*	Gaussian	$1.025 \times 0.102\ mSv$	$0.08 \times 1.025 \times 0.102\ mSv$
$\boldsymbol{K_{E,\varphi}}$	*1.00*	$0.40/3 = 0.133$	B	---	*99.7 %*	Gaussian	$1.025 \times 1.02 \times 0.102\ mSv$	$0.133 \times 1.025 \times 1.02 \times 0.102\ mSv$
$\boldsymbol{K_{env}}$	*1.00*	$0.20/\sqrt{6} = 0.0816$	B	---	*100 %*	Triangular	$1.025 \times 1.02 \times 0.102\ mSv$	$0.0816 \times 1.025 \times 1.02 \times 0.102\ mSv$
$\boldsymbol{H_m}$	*0.13 mSv*	*0.012 mSv*	A	4	*68.27 %*	Gaussian	*1*	$1 \times 0.012\ mSv$
$\boldsymbol{H_p(10)}$	*0.106 mSv*	*0.023 mSv (21.56 %)*	Combined	---	*68.27 %*	Gaussian	---	---
Complete result of the measurement							$0.106\ mSv \pm 0.045\ mSv \quad (k_{cov} = 1.96)$	

Table C.3: Uncertainty budget of the raw measured dose *0.198 mSv* corresponding to the true dose *0.20 mSv* (TLD).

Quantity	Best estimate	Absolute standard uncertainty	Uncertainty type	Number of observations	Confidence level	Distribution	Sensitivity coefficient	Uncertainty contribution to output quantity
N_0	*1.00*	$0.05/\sqrt{6} = 0.0204$	B	---	*100 %*	Triangular	$1.025 \times 1.02 \times 0.19\ mSv$	$0.0204 \times 1.025 \times 1.02 \times 0.19\ mSv$
K_n	*1.025*	$0.125/3 = 0.0417$	B	*78*	*99.7 %*	Gaussian	$1.02 \times 0.19\ mSv$	$0.0417 \times 1.02 \times 0.19\ mSv$
K_s	*1.02*	$0.24/3 = 0.08$	B	*107*	*99.7 %*	Gaussian	$1.025 \times 0.19\ mSv$	$0.08 \times 1.025 \times 0.19\ mSv$
$K_{E,\varphi}$	*1.00*	$0.40/3 = 0.133$	B	---	*99.7 %*	Gaussian	$1.025 \times 1.02 \times 0.19\ mSv$	$0.133 \times 1.025 \times 1.02 \times 0.19\ mSv$
K_{env}	*1.00*	$0.20/\sqrt{6} = 0.0816$	B	---	*100 %*	Triangular	$1.025 \times 1.02 \times 0.19\ mSv$	$0.0816 \times 1.025 \times 1.02 \times 0.19\ mSv$
H_m	*0.198 mSv*	*0.027 mSv*	A	4	*68.27 %*	Gaussian	*1*	$1 \times 0.027\ mSv$
$H_p(10)$	*0.199 mSv*	*0.045 mSv (22.63 %)*	Combined	---	*68.27 %*	Gaussian	---	---
Complete result of the measurement							$0.199\ mSv \pm 0.088\ mSv \quad (k_{cov} = 1.96)$	

Table C.4: Uncertainty budget of the raw measured dose *0.33 mSv* corresponding to the true dose *0.40 mSv* (TLD).

Quantity	Best estimate	Absolute standard uncertainty	Uncertainty type	Number of observations	Confidence level	Distribution	Sensitivity coefficient	Uncertainty contribution to output quantity
$\boldsymbol{N_0}$	*1.00*	$0.05/\sqrt{6} = 0.0204$	B	---	*100 %*	Triangular	$1.025 \times 1.02 \times 0.37\ mSv$	$0.0204 \times 1.025 \times 1.02 \times 0.37\ mSv$
$\boldsymbol{K_n}$	*1.025*	$0.125/3 = 0.0417$	B	*78*	*99.7 %*	Gaussian	$1.02 \times 0.37\ mSv$	$0.0417 \times 1.02 \times 0.37\ mSv$
$\boldsymbol{K_s}$	*1.02*	$0.24/3 = 0.08$	B	*107*	*99.7 %*	Gaussian	$1.025 \times 0.37\ mSv$	$0.08 \times 1.025 \times 0.37\ mSv$
$\boldsymbol{K_{E,\varphi}}$	*1.00*	$0.40/3 = 0.133$	B	---	*99.7 %*	Gaussian	$1.025 \times 1.02 \times 0.37\ mSv$	$0.133 \times 1.025 \times 1.02 \times 0.37\ mSv$
$\boldsymbol{K_{env}}$	*1.00*	$0.20/\sqrt{6} = 0.0816$	B	---	*100 %*	Triangular	$1.025 \times 1.02 \times 0.37\ mSv$	$0.0816 \times 1.025 \times 1.02 \times 0.37\ mSv$
$\boldsymbol{H_m}$	*0.33 mSv*	*0.015 mSv*	A	4	*68.27 %*	Gaussian	*1*	$1 \times 0.015\ mSv$
$\boldsymbol{H_p(10)}$	*0.39 mSv*	*0.072 mSv (18.51 %)*	Combined	---	*68.27 %*	Gaussian	---	---
Complete result of the measurement						$0.39\ mSv \pm 0.14\ mSv \quad (k_{cov} = 1.96)$		

Table C.5: Uncertainty budget of the raw measured dose *0.62 mSv* corresponding to the true dose *0.8 mSv* (TLD).

Quantity	Best estimate	Absolute standard uncertainty	Uncertainty type	Number of observations	Confidence level	Distribution	Sensitivity coefficient	Uncertainty contribution to output quantity
$\boldsymbol{N_0}$	*1.00*	$0.05/\sqrt{6} = 0.0204$	B	---	*100 %*	Triangular	$1.025 \times 1.02 \times 0.75\ mSv$	$0.0204 \times 1.025 \times 1.02 \times 0.75\ mSv$
$\boldsymbol{K_n}$	*1.025*	$0.125/3 = 0.0417$	B	*78*	*99.7 %*	Gaussian	$1.02 \times 0.75\ mSv$	$0.0417 \times 1.02 \times 0.75\ mSv$
$\boldsymbol{K_s}$	*1.02*	$0.24/3 = 0.08$	B	*107*	*99.7 %*	Gaussian	$1.025 \times 0.75\ mSv$	$0.08 \times 1.025 \times 0.75\ mSv$
$\boldsymbol{K_{E,\varphi}}$	*1.00*	$0.40/3 = 0.133$	B	---	*99.7 %*	Gaussian	$1.025 \times 1.02 \times 0.75\ mSv$	$0.133 \times 1.025 \times 1.02 \times 0.75\ mSv$
$\boldsymbol{K_{env}}$	*1.00*	$0.20/\sqrt{6} = 0.0816$	B	---	*100 %*	Triangular	$1.025 \times 1.02 \times 0.75\ mSv$	$0.0816 \times 1.025 \times 1.02 \times 0.75\ mSv$
$\boldsymbol{H_m}$	*0.62 mSv*	*0.018 mSv*	A	4	*68.27 %*	Gaussian	*1*	$1 \times 0.018\ mSv$
$\boldsymbol{H_p(10)}$	*0.79 mSv*	*0.14 mSv (18.22 %)*	Combined	---	*68.27 %*	Gaussian	---	---
Complete result of the measurement							$0.79\ mSv \pm 0.28\ mSv \quad (k_{cov} = 1.96)$	

Table C.6: Uncertainty budget of the raw measured dose *0.85 mSv* corresponding to the true dose *1 mSv* (TLD).

Quantity	Best estimate	Absolute standard uncertainty	Uncertainty type	Number of observations	Confidence level	Distribution	Sensitivity coefficient	Uncertainty contribution to output quantity
$\boldsymbol{N_0}$	*1.00*	$0.05/\sqrt{6} = 0.0204$	B	---	*100 %*	Triangular	$1.025 \times 1.02 \times 1.07\ mSv$	$0.0204 \times 1.025 \times 1.02 \times 1.07\ mSv$
$\boldsymbol{K_n}$	*1.025*	$0.125/3 = 0.0417$	B	*78*	*99.7 %*	Gaussian	$1.02 \times 1.07\ mSv$	$0.0417 \times 1.02 \times 1.07\ mSv$
$\boldsymbol{K_s}$	*1.02*	$0.24/3 = 0.08$	B	*107*	*99.7 %*	Gaussian	$1.025 \times 1.07\ mSv$	$0.08 \times 1.025 \times 1.07\ mSv$
$\boldsymbol{K_{E,\varphi}}$	*1.00*	$0.40/3 = 0.133$	B	---	*99.7 %*	Gaussian	$1.025 \times 1.02 \times 1.07\ mSv$	$0.133 \times 1.025 \times 1.02 \times 1.07\ mSv$
$\boldsymbol{K_{env}}$	*1.00*	$0.20/\sqrt{6} = 0.0816$	B	---	*100 %*	Triangular	$1.025 \times 1.02 \times 1.07\ mSv$	$0.0816 \times 1.025 \times 1.02 \times 1.07\ mSv$
$\boldsymbol{H_m}$	*0.85 mSv*	*0.046 mSv*	A	4	*68.27 %*	Gaussian	*1*	$1 \times 0.046\ mSv$
$\boldsymbol{H_p(10)}$	*1.11 mSv*	*0.21 mSv (18.53 %)*	Combined	---	*68.27 %*	Gaussian	---	---
Complete result of the measurement							$1.11\ mSv \pm 0.40\ mSv \quad (k_{cov} = 1.96)$	

Table C.7: Uncertainty budget of the raw measured dose *1.57 mSv* corresponding to the true dose *2 mSv* (TLD).

Quantity	Best estimate	Absolute standard uncertainty	Uncertainty type	Number of observations	Confidence level	Distribution	Sensitivity coefficient	Uncertainty contribution to output quantity
$\boldsymbol{N_0}$	*1.00*	$0.05/\sqrt{6} = 0.0204$	B	---	*100 %*	Triangular	$1.025 \times 1.02 \times 2.02\ mSv$	$0.0204 \times 1.025 \times 1.02 \times 2.02\ mSv$
$\boldsymbol{K_n}$	*1.025*	$0.125/3 = 0.0417$	B	*78*	*99.7 %*	Gaussian	$1.02 \times 2.02\ mSv$	$0.0417 \times 1.02 \times 2.02\ mSv$
$\boldsymbol{K_s}$	*1.02*	$0.24/3 = 0.08$	B	*107*	*99.7 %*	Gaussian	$1.025 \times 2.02\ mSv$	$0.08 \times 1.025 \times 2.02\ mSv$
$\boldsymbol{K_{E,\varphi}}$	*1.00*	$0.40/3 = 0.133$	B	---	*99.7 %*	Gaussian	$1.025 \times 1.02 \times 2.02\ mSv$	$0.133 \times 1.025 \times 1.02 \times 2.02\ mSv$
$\boldsymbol{K_{env}}$	*1.00*	$0.20/\sqrt{6} = 0.0816$	B	---	*100 %*	Triangular	$1.025 \times 1.02 \times 2.02\ mSv$	$0.0816 \times 1.025 \times 1.02 \times 2.02\ mSv$
$\boldsymbol{H_m}$	*1.57 mSv*	*0.025 mSv*	A	4	*68.27 %*	Gaussian	*1*	$1 \times 0.025\ mSv$
$\boldsymbol{H_p(10)}$	*2.11 mSv*	*0.38 mSv (18.11 %)*	Combined	---	*68.27 %*	Gaussian	---	---
Complete result of the measurement							$2.11\ mSv \pm 0.75\ mSv \quad (k_{cov} = 1.96)$	

Table C.8: Uncertainty budget of the raw measured dose *3.93 mSv* corresponding to the true dose *5 mSv* (TLD).

Quantity	Best estimate	Absolute standard uncertainty	Uncertainty type	Number of observations	Confidence level	Distribution	Sensitivity coefficient	Uncertainty contribution to output quantity
$\boldsymbol{N_0}$	*1.00*	$0.05/\sqrt{6} = 0.0204$	B	---	*100 %*	Triangular	$1.025 \times 1.02 \times 5.17\ mSv$	$0.0204 \times 1.025 \times 1.02 \times 5.17\ mSv$
$\boldsymbol{K_n}$	*1.025*	$0.125/3 = 0.0417$	B	*78*	*99.7 %*	Gaussian	$1.02 \times 5.17\ mSv$	$0.0417 \times 1.02 \times 5.17\ mSv$
$\boldsymbol{K_s}$	*1.02*	$0.24/3 = 0.08$	B	*107*	*99.7 %*	Gaussian	$1.025 \times 5.17\ mSv$	$0.08 \times 1.025 \times 5.17\ mSv$
$\boldsymbol{K_{E,\varphi}}$	*1.00*	$0.40/3 = 0.133$	B	---	*99.7 %*	Gaussian	$1.025 \times 1.02 \times 5.17\ mSv$	$0.133 \times 1.025 \times 1.02 \times 5.17\ mSv$
$\boldsymbol{K_{env}}$	*1.00*	$0.20/\sqrt{6} = 0.0816$	B	---	*100 %*	Triangular	$1.025 \times 1.02 \times 5.17\ mSv$	$0.0816 \times 1.025 \times 1.02 \times 5.17\ mSv$
$\boldsymbol{H_m}$	*3.93 mSv*	*0.045 mSv*	A	4	*68.27 %*	Gaussian	*1*	$1 \times 0.045\ mSv$
$\boldsymbol{H_p(10)}$	*5.41 mSv*	*0.98 mSv (18.09 %)*	Combined	---	*68.27 %*	Gaussian	---	---
Complete result of the measurement							$5.41\ mSv \pm 1.92\ mSv \quad (k_{cov} = 1.96)$	

Table C.9: Uncertainty budget of the raw measured dose *7.54 mSv* corresponding to the true dose *10 mSv* (TLD).

Quantity	Best estimate	Absolute standard uncertainty	Uncertainty type	Number of observations	Confidence level	Distribution	Sensitivity coefficient	Uncertainty contribution to output quantity
$\boldsymbol{N_0}$	*1.00*	$0.05/\sqrt{6} = 0.0204$	B	---	*100 %*	Triangular	$1.025 \times 1.02 \times 9.98\ mSv$	$0.0204 \times 1.025 \times 1.02 \times 9.98\ mSv$
$\boldsymbol{K_n}$	*1.025*	$0.125/3 = 0.0417$	B	*78*	*99.7 %*	Gaussian	$1.02 \times 9.98\ mSv$	$0.0417 \times 1.02 \times 9.98\ mSv$
$\boldsymbol{K_s}$	*1.02*	$0.24/3 = 0.08$	B	*107*	*99.7 %*	Gaussian	$1.025 \times 9.98\ mSv$	$0.08 \times 1.025 \times 9.98\ mSv$
$\boldsymbol{K_{E,\varphi}}$	*1.00*	$0.40/3 = 0.133$	B	---	*99.7 %*	Gaussian	$1.025 \times 1.02 \times 9.98\ mSv$	$0.133 \times 1.025 \times 1.02 \times 9.98\ mSv$
$\boldsymbol{K_{env}}$	*1.00*	$0.20/\sqrt{6} = 0.0816$	B	---	*100 %*	Triangular	$1.025 \times 1.02 \times 9.98\ mSv$	$0.0816 \times 1.025 \times 1.02 \times 9.98\ mSv$
$\boldsymbol{H_m}$	*7.54 mSv*	*0.11 mSv*	A	4	*68.27 %*	Gaussian	*1*	$1 \times 0.11\ mSv$
$\boldsymbol{H_p(10)}$	*10.43 mSv*	*1.89 mSv (18.10 %)*	Combined	---	*68.27 %*	Gaussian	---	---
Complete result of the measurement							$10.43\ mSv \pm 3.70\ mSv \quad (k_{cov} = 1.96)$	

MicroStar OSL system

Table C.10: Uncertainty budget of the net measured dose *0.11 mSv* corresponding to the true dose *0.07 mSv* (OSL).

Quantity	Best estimate	Absolute standard uncertainty	Uncertainty type	Number of observations	Confidence level	Distribution	Sensitivity coefficient	Uncertainty contribution to output quantity
$\boldsymbol{N_0}$	*1.00*	$0.05/\sqrt{6} = 0.0204$	B	---	*100 %*	Triangular	$1.08 \times 0.93 \times 0.105\ mSv$	$0.0204 \times 1.08 \times 0.93 \times 0.105\ mSv$
$\boldsymbol{K_n}$	*0.93*	$0.27/3 = 0.09$	B	*64*	*99.7 %*	Gaussian	$1.08 \times 0.105\ mSv$	$0.09 \times 1.08 \times 0.105\ mSv$
$\boldsymbol{K_s}$	*1*	0	B	---	*99.7 %*	Gaussian	$1.08 \times 0.93 \times 0.105\ mSv$	$0 \times 1.08 \times 0.93 \times 0.105\ mSv$
$\boldsymbol{K_{E,\varphi}}$	*1.00*	$0.40/3 = 0.133$	B	---	*99.7 %*	Gaussian	$1.08 \times 0.93 \times 0.105\ mSv$	$0.133 \times 1.08 \times 0.93 \times 0.105\ mSv$
$\boldsymbol{K_{env}}$	*1.00*	$0.20/\sqrt{6} = 0.0816$	B	---	*100 %*	Triangular	$1.08 \times 0.93 \times 0.105\ mSv$	$0.0816 \times 1.08 \times 0.93 \times 0.105\ mSv$
$\boldsymbol{H_m}$	*0.11 mSv*	*0.015 mSv*	A	*4*	*68.27 %*	Gaussian	*1*	$1 \times 0.015\ mSv$
$\boldsymbol{H_p(10)}$	*0.106 mSv*	*0.025 mSv (23.40 %)*	Combined	---	*68.27 %*	Gaussian	---	---
Complete result of the measurement							$0.106\ mSv \pm 0.049\ mSv \quad (k_{cov} = 1.96)$	

Table C.11: Uncertainty budget of the net measured dose *0.089 mSv* corresponding to the true dose *0.08 mSv* (OSL).

Quantity	Best estimate	Absolute standard uncertainty	Uncertainty type	Number of observations	Confidence level	Distribution	Sensitivity coefficient	Uncertainty contribution to output quantity
$\boldsymbol{N_0}$	*1.00*	$0.05/\sqrt{6} = 0.0204$	B	---	*100 %*	Triangular	$1.08 \times 0.93 \times 0.084\ mSv$	$0.0204 \times 1.08 \times 0.93 \times 0.084\ mSv$
$\boldsymbol{K_n}$	*0.93*	$0.27/3 = 0.09$	B	*64*	*99.7 %*	Gaussian	$1.08 \times 0.084\ mSv$	$0.09 \times 1.08 \times 0.084\ mSv$
$\boldsymbol{K_s}$	*1*	0	B	---	*99.7 %*	Gaussian	$1.08 \times 0.93 \times 0.084\ mSv$	$0 \times 1.08 \times 0.93 \times 0.084\ mSv$
$\boldsymbol{K_{E,\varphi}}$	*1.00*	$0.40/3 = 0.133$	B	---	*99.7 %*	Gaussian	$1.08 \times 0.93 \times 0.084\ mSv$	$0.133 \times 1.08 \times 0.93 \times 0.084\ mSv$
$\boldsymbol{K_{env}}$	*1.00*	$0.20/\sqrt{6} = 0.0816$	B	---	*100 %*	Triangular	$1.08 \times 0.93 \times 0.084\ mSv$	$0.0816 \times 1.08 \times 0.93 \times 0.084\ mSv$
$\boldsymbol{H_m}$	*0.089 mSv*	*0.018 mSv*	A	*3*	*68.27 %*	Gaussian	*1*	$1 \times 0.018\ mSv$
$\boldsymbol{H_p(10)}$	*0.0845 mSv*	*0.0235 mSv (27.79 %)*	Combined	---	*68.27 %*	Gaussian	---	---
Complete result of the measurement							$0.0845\ mSv \pm 0.046\ mSv \quad (k_{cov} = 1.96)$	

Table C.12: Uncertainty of the net measured dose *0.092 mSv* corresponding to the true dose *0.09 mSv* (OSL).

Quantity	Best estimate	Absolute standard uncertainty	Uncertainty type	Number of observations	Confidence level	Distribution	Sensitivity coefficient	Uncertainty contribution to output quantity
$\boldsymbol{N_0}$	*1.00*	$0.05/\sqrt{6} = 0.0204$	B	---	*100 %*	Triangular	$1.08 \times 0.93 \times 0.087\ mSv$	$0.0204 \times 1.08 \times 0.93 \times 0.087\ mSv$
$\boldsymbol{K_n}$	*0.93*	$0.27/3 = 0.09$	B	*64*	*99.7 %*	Gaussian	$1.08 \times 0.087\ mSv$	$0.09 \times 1.08 \times 0.087\ mSv$
$\boldsymbol{K_s}$	*1*	0	B	---	*99.7 %*	Gaussian	$1.08 \times 0.93 \times 0.087\ mSv$	$0 \times 1.08 \times 0.93 \times 0.087\ mSv$
$\boldsymbol{K_{E,\varphi}}$	*1.00*	$0.40/3 = 0.133$	B	---	*99.7 %*	Gaussian	$1.08 \times 0.93 \times 0.087\ mSv$	$0.133 \times 1.08 \times 0.93 \times 0.087\ mSv$
$\boldsymbol{K_{env}}$	*1.00*	$0.20/\sqrt{6} = 0.0816$	B	---	*100 %*	Triangular	$1.08 \times 0.93 \times 0.087\ mSv$	$0.0816 \times 1.08 \times 0.93 \times 0.087\ mSv$
$\boldsymbol{H_m}$	*0.092 mSv*	*0.019 mSv*	A	*3*	*68.27 %*	Gaussian	*1*	$1 \times 0.019\ mSv$
$\boldsymbol{H_p(10)}$	*0.088 mSv*	*0.025 mSv (28.69 %)*	Combined	---	*68.27 %*	Gaussian	---	---
Complete result of the measurement							$0.088\ mSv \pm 0.049\ mSv \quad (k_{cov} = 1.96)$	

Table C.13: Uncertainty budget of the net measured dose *0.136 mSv* corresponding to the true dose *0.1 mSv* (OSL).

Quantity	Best estimate	Absolute standard uncertainty	Uncertainty type	Number of observations	Confidence level	Distribution	Sensitivity coefficient	Uncertainty contribution to output quantity
$\boldsymbol{N_0}$	*1.00*	$0.05/\sqrt{6} = 0.0204$	B	---	*100 %*	Triangular	$1.08 \times 0.93 \times 0.13\ mSv$	$0.0204 \times 1.08 \times 0.93 \times 0.13\ mSv$
$\boldsymbol{K_n}$	*0.93*	$0.27/3 = 0.09$	B	*64*	*99.7 %*	Gaussian	$1.08 \times 0.13\ mSv$	$0.09 \times 1.08 \times 0.13\ mSv$
$\boldsymbol{K_s}$	*1*	0	B	---	*99.7 %*	Gaussian	$1.08 \times 0.93 \times 0.13\ mSv$	$0 \times 1.08 \times 0.93 \times 0.13\ mSv$
$\boldsymbol{K_{E,\varphi}}$	*1.00*	$0.40/3 = 0.133$	B	---	*99.7 %*	Gaussian	$1.08 \times 0.93 \times 0.13\ mSv$	$0.133 \times 1.08 \times 0.93 \times 0.13\ mSv$
$\boldsymbol{K_{env}}$	*1.00*	$0.20/\sqrt{6} = 0.0816$	B	---	*100 %*	Triangular	$1.08 \times 0.93 \times 0.13\ mSv$	$0.0816 \times 1.08 \times 0.93 \times 0.13\ mSv$
$\boldsymbol{H_m}$	*0.136 mSv*	*0.024 mSv*	A	*4*	*68.27 %*	Gaussian	*1*	$1 \times 0.024\ mSv$
$\boldsymbol{H_p(10)}$	*0.13 mSv*	*0.034 mSv (26.32 %)*	Combined	---	*68.27 %*	Gaussian	---	---
Complete result of the measurement							$0.13\ mSv \pm 0.067\ mSv \quad (k_{cov} = 1.96)$	

Table C.14: Uncertainty budget of the net measured dose *0.23 mSv* corresponding to the true dose *0.2 mSv* (OSL).

Quantity	Best estimate	Absolute standard uncertainty	Uncertainty type	Number of observations	Confidence level	Distribution	Sensitivity coefficient	Uncertainty contribution to output quantity
$\boldsymbol{N_0}$	*1.00*	$0.05/\sqrt{6} = 0.0204$	B	---	*100 %*	Triangular	$1.08 \times 0.93 \times 0.217\ mSv$	$0.0204 \times 1.08 \times 0.93 \times 0.217\ mSv$
$\boldsymbol{K_n}$	*0.93*	$0.27/3 = 0.09$	B	*64*	*99.7 %*	Gaussian	$1.08 \times 0.217\ mSv$	$0.09 \times 1.08 \times 0.217\ mSv$
$\boldsymbol{K_s}$	*1*	0	B	---	*99.7 %*	Gaussian	$1.08 \times 0.93 \times 0.217\ mSv$	$0 \times 1.08 \times 0.93 \times 0.217\ mSv$
$\boldsymbol{K_{E,\varphi}}$	*1.00*	$0.40/3 = 0.133$	B	---	*99.7 %*	Gaussian	$1.08 \times 0.93 \times 0.217\ mSv$	$0.133 \times 1.08 \times 0.93 \times 0.217\ mSv$
$\boldsymbol{K_{env}}$	*1.00*	$0.20/\sqrt{6} = 0.0816$	B	---	*100 %*	Triangular	$1.08 \times 0.93 \times 0.217\ mSv$	$0.0816 \times 1.08 \times 0.93 \times 0.217\ mSv$
$\boldsymbol{H_m}$	*0.23 mSv*	*0,045 mSv*	A	*4*	*68.27 %*	Gaussian	*1*	$1 \times 0.045\ mSv$
$\boldsymbol{H_p(10)}$	*0.22 mSv*	*0.061 mSv (27.89 %)*	Combined	---	*68.27 %*	Gaussian	---	---
Complete result of the measurement							$0.22\ mSv \pm 0.12\ mSv \quad (k_{cov} = 1.96)$	

Table C.15: Uncertainty budget for the net measured dose *0.45 mSv* corresponding to the true dose *0.40 mSv* (OSL).

Quantity	Best estimate	Absolute standard uncertainty	Uncertainty type	Number of observations	Confidence level	Distribution	Sensitivity coefficient	Uncertainty contribution to output quantity
$\boldsymbol{N_0}$	*1.00*	$0.05/\sqrt{6} = 0.0204$	B	---	*100 %*	Triangular	$1.08 \times 0.93 \times 0.43\ mSv$	$0.0204 \times 1.08 \times 0.93 \times 0.43\ mSv$
$\boldsymbol{K_n}$	*0.93*	$0.27/3 = 0.09$	B	*64*	*99.7 %*	Gaussian	$1.08 \times 0.43\ mSv$	$0.09 \times 1.08 \times 0.43\ mSv$
$\boldsymbol{K_s}$	*1*	0	B	---	*99.7 %*	Gaussian	$1.08 \times 0.93 \times 0.43\ mSv$	$0 \times 1.08 \times 0.93 \times 0.43\ mSv$
$\boldsymbol{K_{E,\varphi}}$	*1.00*	$0.40/3 = 0.133$	B	---	*99.7 %*	Gaussian	$1.08 \times 0.93 \times 0.43\ mSv$	$0.133 \times 1.08 \times 0.93 \times 0.43\ mSv$
$\boldsymbol{K_{env}}$	*1.00*	$0.20/\sqrt{6} = 0.0816$	B	---	*100 %*	Triangular	$1.08 \times 0.93 \times 0.43\ mSv$	$0.0816 \times 1.08 \times 0.93 \times 0.43\ mSv$
$\boldsymbol{H_m}$	*0.45 mSv*	*0.022 mSv*	A	*4*	*68.27 %*	Gaussian	*1*	$1 \times 0.022\ mSv$
$\boldsymbol{H_p(10)}$	*0.43 mSv*	*0.083 mSv (19.19 %)*	Combined	---	*68.27 %*	Gaussian	---	---
Complete result of the measurement							$0.43\ mSv \pm 0.16\ mSv \quad (k_{cov} = 1.96)$	

Table C.16: Uncertainty budget of the net measured dose *0.84 mSv* corresponding to the true dose *0.8 mSv* (OSL).

Quantity	Best estimate	Absolute standard uncertainty	Uncertainty type	Number of observations	Confidence level	Distribution	Sensitivity coefficient	Uncertainty contribution to output quantity
$\boldsymbol{N_0}$	*1.00*	$0.05/\sqrt{6} = 0.0204$	B	---	*100 %*	Triangular	$1.08 \times 0.93 \times 0.79\ mSv$	$0.0204 \times 1.08 \times 0.93 \times 0.79\ mSv$
$\boldsymbol{K_n}$	*0.93*	$0.27/3 = 0.09$	B	*64*	*99.7 %*	Gaussian	$1.08 \times 0.79\ mSv$	$0.09 \times 1.08 \times 0.79\ mSv$
$\boldsymbol{K_s}$	*1*	0	B	---	*99.7 %*	Gaussian	$1.08 \times 0.93 \times 0.79\ mSv$	$0 \times 1.08 \times 0.93 \times 0.79\ mSv$
$\boldsymbol{K_{E,\varphi}}$	*1.00*	$0.40/3 = 0.133$	B	---	*99.7 %*	Gaussian	$1.08 \times 0.93 \times 0.79\ mSv$	$0.133 \times 1.08 \times 0.93 \times 0.79\ mSv$
$\boldsymbol{K_{env}}$	*1.00*	$0.20/\sqrt{6} = 0.0816$	B	---	*100 %*	Triangular	$1.08 \times 0.93 \times 0.79\ mSv$	$0.0816 \times 1.08 \times 0.93 \times 0.79\ mSv$
$\boldsymbol{H_m}$	*0.84 mSv*	*0.017 mSv*	A	*4*	*68.27 %*	Gaussian	*1*	$1 \times 0.017\ mSv$
$\boldsymbol{H_p(10)}$	*0.80 mSv*	*0.15 mSv (18.62 %)*	Combined	---	*68.27 %*	Gaussian	---	---
Complete result of the measurement							$0.80\ mSv \pm 0.29\ mSv \quad (k_{cov} = 1.96)$	

Table C.17: Uncertainty budget of the net measured dose *1.00 mSv* corresponding to the true dose *1 mSv* (OSL).

Quantity	Best estimate	Absolute standard uncertainty	Uncertainty type	Number of observations	Confidence level	Distribution	Sensitivity coefficient	Uncertainty contribution to output quantity
$\boldsymbol{N_0}$	*1.00*	$0.05/\sqrt{6} = 0.0204$	B	---	*100 %*	Triangular	$1.08 \times 0.93 \times 0.949\ mSv$	$0.0204 \times 1.08 \times 0.93 \times 0.949\ mSv$
$\boldsymbol{K_n}$	*0.93*	$0.27/3 = 0.09$	B	*64*	*99.7 %*	Gaussian	$1.08 \times 0.949\ mSv$	$0.09 \times 1.08 \times 0.949\ mSv$
$\boldsymbol{K_s}$	*1*	0	B	---	*99.7 %*	Gaussian	$1.08 \times 0.93 \times 0.949\ mSv$	$0 \times 1.08 \times 0.93 \times 0.949\ mSv$
$\boldsymbol{K_{E,\varphi}}$	*1.00*	$0.40/3 = 0.133$	B	---	*99.7 %*	Gaussian	$1.08 \times 0.93 \times 0.949\ mSv$	$0.133 \times 1.08 \times 0.93 \times 0.949\ mSv$
$\boldsymbol{K_{env}}$	*1.00*	$0.20/\sqrt{6} = 0.0816$	B	---	*100 %*	Triangular	$1.08 \times 0.93 \times 0.949\ mSv$	$0.0816 \times 1.08 \times 0.93 \times 0.949\ mSv$
$\boldsymbol{H_m}$	*1.00 mSv*	*0.045 mSv*	A	*4*	*68.27 %*	Gaussian	*1*	$1 \times 0.045\ mSv$
$\boldsymbol{H_p(10)}$	*0.95 mSv*	*0.18 mSv (19.1 %)*	Combined	---	*68.27 %*	Gaussian	---	---
Complete result of the measurement							$0.95\ mSv \pm 0.36\ mSv \quad (k_{cov} = 1.96)$	

Table C.18: Uncertainty budget of the net measured dose *1.95 mSv* corresponding to the true dose *2 mSv* (OSL).

Quantity	Best estimate	Absolute standard uncertainty	Uncertainty type	Number of observations	Confidence level	Distribution	Sensitivity coefficient	Uncertainty contribution to output quantity
$\boldsymbol{N_0}$	*1.00*	$0.05/\sqrt{6} = 0.0204$	B	---	*100 %*	Triangular	$1.08 \times 0.93 \times 1.85\ mSv$	$0.0204 \times 1.08 \times 0.93 \times 1.85\ mSv$
$\boldsymbol{K_n}$	*0.93*	$0.27/3 = 0.09$	B	*64*	*99.7 %*	Gaussian	$1.08 \times 1.85\ mSv$	$0.09 \times 1.08 \times 1.85\ mSv$
$\boldsymbol{K_s}$	*1*	0	B	---	*99.7 %*	Gaussian	$1.08 \times 0.93 \times 1.85\ mSv$	$0 \times 1.08 \times 0.93 \times 1.85\ mSv$
$\boldsymbol{K_{E,\varphi}}$	*1.00*	$0.40/3 = 0.133$	B	---	*99.7 %*	Gaussian	$1.08 \times 0.93 \times 1.85\ mSv$	$0.133 \times 1.08 \times 0.93 \times 1.85\ mSv$
$\boldsymbol{K_{env}}$	*1.00*	$0.20/\sqrt{6} = 0.0816$	B	---	*100 %*	Triangular	$1.08 \times 0.93 \times 1.85\ mSv$	$0.0816 \times 1.08 \times 0.93 \times 1.85\ mSv$
$\boldsymbol{H_m}$	*1.95 mSv*	*0.093 mSv*	A	*4*	*68.27 %*	Gaussian	*1*	$1 \times 0.093\ mSv$
$\boldsymbol{H_p(10)}$	*1.86 mSv*	*0.36 mSv (19.17 %)*	Combined	---	*68.27 %*	Gaussian	---	---
Complete result of the measurement							$1.86\ mSv \pm 0.70\ mSv \quad (k_{cov} = 1.96)$	

Table C.19: Uncertainty budget of the net measured dose *5.16 mSv* corresponding to the true dose *5 mSv* (OSL).

Quantity	Best estimate	Absolute standard uncertainty	Uncertainty type	Number of observations	Confidence level	Distribution	Sensitivity coefficient	Uncertainty contribution to output quantity
$\boldsymbol{N_0}$	*1.00*	$0.05/\sqrt{6} = 0.0204$	B	---	*100 %*	Triangular	$1.08 \times 0.93 \times 4.89\ mSv$	$0.0204 \times 1.08 \times 0.93 \times 4.89\ mSv$
$\boldsymbol{K_n}$	*0.93*	$0.27/3 = 0.09$	B	*64*	*99.7 %*	Gaussian	$1.08 \times 4.89\ mSv$	$0.09 \times 1.08 \times 4.89\ mSv$
$\boldsymbol{K_s}$	*1*	0	B	---	*99.7 %*	Gaussian	$1.08 \times 0.93 \times 4.89\ mSv$	$0 \times 1.08 \times 0.93 \times 4.89\ mSv$
$\boldsymbol{K_{E,\varphi}}$	*1.00*	$0.40/3 = 0.133$	B	---	*99.7 %*	Gaussian	$1.08 \times 0.93 \times 4.89\ mSv$	$0.133 \times 1.08 \times 0.93 \times 4.89\ mSv$
$\boldsymbol{K_{env}}$	*1.00*	$0.20/\sqrt{6} = 0.0816$	B	---	*100 %*	Triangular	$1.08 \times 0.93 \times 4.89\ mSv$	$0.0816 \times 1.08 \times 0.93 \times 4.89\ mSv$
$\boldsymbol{H_m}$	*5.16 mSv*	*0.11 mSv*	A	*4*	*68.27 %*	Gaussian	*1*	$1 \times 0.11\ mSv$
$\boldsymbol{H_p(10)}$	*4.91 mSv*	*0.91 mSv (18.63 %)*	Combined	---	*68.27 %*	Gaussian	---	---
Complete result of the measurement							$4.91\ mSv \pm 1.79\ mSv \quad (k_{cov} = 1.96)$	

Table C.20: Uncertainty budget of the net measured dose *10.66 mSv* corresponding to the true dose *10 mSv* (OSL).

Quantity	Best estimate	Absolute standard uncertainty	Uncertainty type	Number of observations	Confidence level	Distribution	Sensitivity coefficient	Uncertainty contribution to output quantity
$\boldsymbol{N_0}$	*1.00*	$0.05/\sqrt{6} = 0.0204$	B	---	*100 %*	Triangular	$1.08 \times 0.93 \times 10.10\ mSv$	$0.0204 \times 1.08 \times 0.93 \times 10.10\ mSv$
$\boldsymbol{K_n}$	*0.93*	$0.27/3 = 0.09$	B	*64*	*99.7 %*	Gaussian	$1.08 \times 10.10\ mSv$	$0.09 \times 1.08 \times 10.10\ mSv$
$\boldsymbol{K_s}$	*1*	0	B	---	*99.7 %*	Gaussian	$1.08 \times 0.93 \times 10.10\ mSv$	$0 \times 1.08 \times 0.93 \times 10.10\ mSv$
$\boldsymbol{K_{E,\varphi}}$	*1.00*	$0.40/3 = 0.133$	B	---	*99.7 %*	Gaussian	$1.08 \times 0.93 \times 10.10\ mSv$	$0.133 \times 1.08 \times 0.93 \times 10.10\ mSv$
$\boldsymbol{K_{env}}$	*1.00*	$0.20/\sqrt{6} = 0.0816$	B	---	*100 %*	Triangular	$1.08 \times 0.93 \times 10.10\ mSv$	$0.0816 \times 1.08 \times 0.93 \times 10.10\ mSv$
$\boldsymbol{H_m}$	*10.66 mSv*	*0.17 mSv*	A	*4*	*68.27 %*	Gaussian	*1*	$1 \times 0.17\ mSv$
$\boldsymbol{H_p(10)}$	*10.15 mSv*	*1.88 mSv (18.58 %)*	Combined	---	*68.27 %*	Gaussian	---	---
Complete result of the measurement							$10.15\ mSv \pm 3.69\ mSv \quad (k_{cov} = 1.96)$	

APPENDIX D

MATLAB CODE USED FOR UNCERTAINTY ASSESSMENT

Harshaw 6600 TL system

```
clear all; close all;format compact;format short g;
%Hmref=3.025895859;Htref=3; Rref=1.008631953;
hm=2.32423;% values of hm=[0.1081965 0.13094 0.1989625 0.1976 0.3321425
0.6193275 0.8541 1.571175 2.32423 3.9329 7.538875];
%Correction of hm
hmcor=1.3333*hm-0.073;
%Calculation of Hp
n0=1;kn=1.025;ks=1.02;kefi=1;kenv=1;
hp=n0*kn*ks*kefi*kenv*hmcor;
%calculation of sensitivity coefficients;
Cn0=1.025*1.02*hmcor;
Ckn=1.02*hmcor;
Cks=1.025*hmcor;
Ckefi=1.025*1.02*hmcor;
Ckenv=1.025*1.02*hmcor;
Sn0=0.05/sqrt(6);
Skn=0.125/3;
Sks=0.24/3;
Skefi=0.4/3;
Skenv=0.2/sqrt(6);
%contributions of input quantities to the output quantity
Ucontr=[Cn0*Sn0 Ckn*Skn Cks*Sks Ckefi*Skefi Ckenv*Skenv];
%type A uncertainty
s=0.085505036;% values of s =[0.01506095 0.01871481 0.08931786 0.04069192
0.02323192 0.02762292 0.06853126 0.03700012 0.085505036 0.067144719
0.165734715];
Uhm=(1.3333*s)/sqrt(10);% The denominator is sqrt(10) for Ht = 3 mSv.
%output uncertainty
U=sqrt((Ucontr(1))^2+(Ucontr(2))^2+(Ucontr(3))^2+(Ucontr(4))^2+(Ucontr(5))^2+U
hm^2);
Urel=(U/hp)*100;
Uexpand=U*1.96;
RangeLow=hp-Uexpand;
RangeUp=hp+Uexpand;RespRangeLow=hp/RangeUp;RespRangeUp=hp/RangeLow;
% Values displayed in command window
U
Urel
hp
Uexpand
RangeLow
RangeUp
RespRangeLow
```

RespRangeUp
Uhm

MicroStar OSL system

```
clear all; close all;format compact;format short g;
%Hmref=2.961355653;Htref=3;Rref=0.987118551;
hm=10.66123986;% values of hm=[0.111249924 0.088750124 0.092083534
0.136250019 0.228749752 0.453749895 0.83874917 1.001249552 1.951248407
3.125414769 5.158737421 10.66123986];
%Correction of hm
hmcor=0.94750805*hm;
%Calculation of Hp
n0=1;kn=0.93;ks=1;kefi=1;kenv=1;
hp=1.08*n0*kn*ks*kefi*kenv*hmcor;
%calculation of sensitivity coefficients;
Cn0=1.08*0.93*hmcor;
Ckn=1.08*hmcor;
Cks=1.08*0.93*hmcor;
Ckefi=1.08*0.93*hmcor;
Ckenv=1.08*0.93*hmcor;
Sn0=0.05/sqrt(6);
Skn=0.27/3;
Sks=0;
Skefi=0.4/3;
Skenv=0.2/sqrt(6);
%contributions of input quantities to the output quantity
Ucontr=[Cn0*Sn0 Ckn*Skn Cks*Sks Ckefi*Skefi Ckenv*Skenv];
%type A uncertainty
s=0.362893462;% values of s =[0.032014939 0.032014939 0.035118699
0.051234732 0.095916009 0.04654703 0.035589646 0.094999414 0.197208083
0.098724917 0.22583139 0.362893462];
Uhm=(0.94750805*s)/sqrt(4); % The denominator is sqrt(3) for Ht = 0.08 mSv and
Ht = 0.09 mSv, and sqrt(6) for Ht = 3 mSv.
%output uncertainty
U=sqrt((Ucontr(1))^2+(Ucontr(2))^2+(Ucontr(3))^2+(Ucontr(4))^2+(Ucontr(5))^2+U
hm^2);
Urel=(U/hp)*100;
Uexpand=U*1.96;
RangeLow=hp-Uexpand;
RangeUp=hp+Uexpand;RespRangeLow=hp/RangeUp;RespRangeUp=hp/RangeLow;
% Values displayed in command window
U
Urel
hp
Uexpand
RangeLow
RangeUp
RespRangeLow
RespRangeUp
```

Uhm